332.8
P567

U.S. DEPT. OF AGRICULTURE
LIBRARY
SEP 12 1962
CURRENT SERIAL RECORDS

SPSE

Photographic

SCIENCE AND ENGINEERING

Effect of Developer Composition on the Structure of Photographic Images
J. H. Altman and R. W. Henn 129

Xerography for Close-Access Recording of Continuous-Tone Line-Scan Cathode-Ray Tube Presentations • *J. T. Bickmore and A. H. Ett* 136

The Relation of Quantum Efficiency to Energy- and Contrast-Detectivity for Photographic Materials • *H. J. Zweig* 142

The Capillary Chamber Process for Ultrarapid Negative Processing
K.-H. Lohse and M. B. Skolnik 149

Characteristics of Physical Development with Developer Solutions Containing Thiosulfate–Silver Complex Ions • *R. M. Cole and R. B. Pontius* 154

A High-Resolution Exposure Determinant for Aerial Films • *Marilyn Levy* 159

Selection of Film and Process for a High-Acuity Photographic System
Malor Wright, R. G. Polk, and Paul Fedelchak 166

A Design Approach to Rapid High-Acuity Processing
Malor Wright, Ernest Thompson, and Irving Spiegel 171

The Printing of Underexposed Photographs by Means of "Optical Contrasters" • *Michel Cloupeau* 175

Discussion and Evaluation: Equivalent Dyes for Color Films with Incorporated Colored Couplers • *A. J. Sant* 181

Book and Journal Reviews 185

New Products and Developments • *Frank Smith* 190

Coming Technical and Scientific Meetings 165

NOTE on "The Effect of the Variables of a Photographic System on Detail Rendition with Special Reference to Camera Motion," by *R. N. Wolfe and S. A. Tuccio* 135

Volume 5 • Number 3

MAY-JUNE • 1961

Editorial Policy

Photographic Science and Engineering is dedicated to the advancement of the knowledge and application of photography and other directly related sciences. Its pages are open to all who wish to report on new studies dealing with the theory of photosensitive systems, the design of photographic instruments and apparatus useful in the treatment of photographic materials, photographic optics and illuminants, the use of photography for scientific or engineering measurement or recording, and photographic instrumentation and data recording. Only original papers should be submitted except on special invitation.

Manuscripts should be typed double-spaced on white bond paper with 1¼-inch margins all around. Literature references should be exact, and should include titles of journals, names of authors, numbers of volumes and pages, and year of publication. Book references should include title of volume, names of authors, publisher, number of edition, year of publication, and chapter and pages cited.

Graphs, charts, and other line illustrations should conform to good usage such as given in the American Standards Association Document Y-15, "A Guide for Preparing Technical Illustrations for Publication and Projection." Continuous-tone photographs should be made on 8 by 10-inch glossy paper and should show pertinent image detail sufficiently clearly to permit reduction to fit a 3-inch column in this journal. All illustrations should be numbered in soft blue pencil on the back to correspond with captions typed on a separate page. Tables should also be submitted on separate pages appropriately identified. An abstract should accompany each manuscript.

Papers intended for publication (two copies) and books for review should be submitted to the editor, T. H. James, Research Laboratories, Eastman Kodak Co., Rochester 4, N.Y. Correspondence regarding proofs and reprints should be directed to Jennie H. Allen, 94 Hastings Ave., Croton-on-Hudson, N.Y. All papers submitted for publication will be reviewed by members of the Editorial Review Board and if not accepted will be returned to the author. Published papers become the property of the Society and are protected by appropriate copyrights. Each author receives one copy of the issue in which his contribution appears. Authors may order reprints of their papers at the time they return the galley proofs. The Society does not assume responsibility for material in transit, nor guarantee publication of unsolicited material.

Photographic
SCIENCE AND ENGINEERING

official publication of the
Society of Photographic Scientists and Engineers

MAY–JUNE 1961
Volume 5, Number 3

EDITORIAL STAFF

T. H. James, *Editor*
Jennie H. Allen, *Managing Editor*
H. F. Nitka, *Associate Editor*
Norman A. Exley, *Assistant Editor*
S. C. Goddard, *Feature Editor*
Frank Smith, *Feature Editor*

EDITORIAL REVIEW BOARD

J. H. Altman	K. G. Leistner
R. S. Barrows	Marilyn Levy
Richard L. Bent	C. S. McCamy
Fordyce M. Brown	J. A. Maurer
B. R. Harriman	F. W. H. Mueller
John H. Jacobs	W. S. Shoemaker
R. Clark Jones	Thos. D. Smith
Peter Krause	William West
John H. Ladd	Deane R. White

Photographic Science and Engineering is published six times a year by the Society of Photographic Scientists and Engineers.

• Address remittances, orders for subscriptions and for single copies, claims for missing numbers, and notices of change of address to the Society at Box 1609, Main Post Office, Washington, D. C. Subscription to nonmembers of the Society, $12.00 per year; subscription cost to members included in $10.00 annual dues; single copies, $2.00 each.

• The publication office is at 20th and Northampton Streets, Easton, Pa. Second-class mail privileges authorized at Easton, Pa. This publication is authorized to be mailed at the special rates of postage prescribed by Section 132.122.

• The Society is not responsible for the accuracy of statements made by authors and does not necessarily subscribe to their views.

© Copyright 1961 by the Society of Photographic Scientists and Engineers, Inc. Permission to reprint any part of the contents, except in reviews and abstracts, must be obtained in writing from the Editorial Vice President.

RING
of the
aphic
neers
1961
ber 3
Editor
Editor
Editor
Editor
Editor
Editor
ARD
istner
Levy
Camy
laurer
ueller
maker
Smith
West
White
ering is
by the
its and
or sub-
claims
ces of
at Box
hington,
bers of
bscrip-
$10.00
0 each.
ith and
. Sec-
zed at
horized
ates of
32.122.
for the
authors
ribe to
iety of
ers, Inc.
of the
stracts,
om the

PHOTOGRAPHIC SCIENCE AND ENGINEERING
Volume 5, Number 3, May-June 1961

Effect of Developer Composition on the Structure of Photographic Images

J. H. ALTMAN AND R. W. HENN, *Research Laboratories, Eastman Kodak Company, Rochester, N.Y.*

Two microstructure properties of the photographic image — acutance and granularity — were examined as functions of developer composition for three black-and-white 35mm films. Systematic variations in developer composition were made to explore the effects of the concentration of sulfite and of *p*-methylaminophenol independently. The resulting changes in sharpness and graininess were found to depend on the particular emulsion involved. The effects of simultaneous changes in these two quantities were estimated on two different bases to find optimum film–developer combinations both for general photography and from the standpoint of informational sensitivity.

It is well known that the graininess of photographic materials is affected by the composition of the developer in which they are processed, and since the advent of the miniature camera, many studies of fine-grain development and developers have appeared in the literature. Although it was noted[1,2] more than fifteen years ago that the sharpness of the photographic image is sometimes reduced by fine-grain development, this aspect of development seems to have attracted little attention until comparatively recently.

The great expansion of miniature photography and the increasing capabilities of modern lenses and emulsions, however, have caused renewed interest in the possibilities of developing for improved sharpness, and a number of formulas giving such improvement have been devised and marketed in recent years. These mostly appear to be of the type described by Beutler,[3] which contain *p*-methylaminophenol developing agent and sulfite in low concentrations.

But practical experience with special-purpose developers has shown that they often work at cross purposes; a gain in one emulsion characteristic is accompanied by losses in other characteristics which are also of interest. The loss in sharpness, just cited, that sometimes occurs as a result of fine-grain development is an example. Conversely, the use of high-sharpness developers generally results in increased graininess. Since, of course, it is desirable to improve both qualities simultaneously, it seemed useful to investigate the properties of both fine-grain and high-sharpness developers. Furthermore, where incompatibility between desirable properties occurred, it seemed desirable to investigate methods of choosing the best compromise. Accordingly, two series of experiments were arranged, using developers in which one property was varied systematically while others were held (as far as possible) constant.

The first series of developers was a "fine-grain" group. One common method of producing a fine-grain developer is to add a silver halide solvent to the solution; this was the method chosen for these experiments. The solvent used was sodium sulfite. The second series was a group of high-sharpness formulas. Such developers act by producing increased adjacency effects; one way to achieve this is merely to reduce the concentration of the developing agent, which in the present study was Kodak Elon* Developing Agent, and this was done progressively through the series.

The image-structure properties selected for study were the graininess and sharpness of the various samples processed to matched gammas in the various developers. Previous work carried out in these Laboratories had shown that the comparative effects of two developers were not the same for all emulsions, which means that it is not possible to generalize with respect to such results. Therefore, tests were carried out on the three Kodak black-and-white emulsions then available for 35mm amateur photography: Kodak Panatomic-X Film, Kodak Plus-X Film, and Kodak Tri-X Film.†

Communication No. 2138 from the Kodak Research Laboratories. Presented at the National Conference, Chicago, 28 October 1959. Received 7 December 1960.

1. R. W. Henn and J. I. Crabtree, *J. Phot. Soc. Am.*, **10**: 727 (1944).
2. H. Harvey, "Development and Developers," in *The Complete Photographer* (W. D. Morgan, ed.), **4**: 1267 (1942).
3. W. Beutler, *Leica Photographie* (English ed.), Sept.-Oct. 1953, p. 182.

* Kodak Elon Developing Agent is the Eastman Kodak Company trade name for *p*-methylaminophenol sulfate.

† The data presented in this paper are representative of the emulsions manufactured at the time the experiments were made. However, it must be recognized that the characteristics of products of the same name may vary within manufacturing tolerances and may change significantly as improvements are effected.

Experimental Details

Developer Formulas. The first step in the experiment was to formulate the appropriate series of developers. This was done by the sensitometric testing of preliminary formulas with the aim of establishing reasonably uniform activity levels and development times. The first section of Table I shows the composition of the fine-grain series (Series I).

TABLE I. Constituents of Developers

Series	Formula No.	Kodak Elon (g/l)	Sodium sulfite (anhydr.) (g/l)	Sodium bisulfite (g/l)	Total sulfite (*M*/l)	Kodalk (g/l)
I (fine-grain)	AH-1	7.50	10	0	0.08	4
	AH-2	7.50	30	5	0.29	0
	AH-3	7.50	100	15	0.95	0
	AH-4	7.50	200	20	1.80	0
II (high-sharpness)	AH-15	2.50	10	0	0.08	4
	AH-16	1.00	10	0	.08	6
	AH-17	0.50	10	0	.08	20
	AH-18	0.25	10	0	.08	20

The central formula in this series, AH-3, is essentially Kodak Developer D-25.[4] It is a true fine-grain developer, giving grain reduction at the expense of reduced emulsion speed. The solvent action has been lowered in the AH-1 and AH-2 formulas by decreasing the sulfite content. Since this reduction would lower the pH and the activity as well, most of the bisulfite was removed in AH-2 and Kodalk Balanced Alkali was added in AH-1. Formula AH-4 contains more than the usual amount of bisulfite. This maintenance of approximately constant activity was considered essential since Henn and Crabtree[1] have shown that graininess is affected by both activity and sulfite content.

The solvent action is obtained from the combined effect of the sulfite and bisulfite, and these are totaled as moles of sulfite ion in the table.

The composition of the second series of developers is given in the second section of the table. These developers are of the "high-sharpness" type, characterized by low sulfite content and decreasing Elon content. The AH-16 developer, containing 1 gram of Elon per liter, is similar to the Beutler high-sharpness developer, which contains 0.83 gram of Elon per liter of diluted developer; both AH-16 and Beutler's formula have low sulfite content and moderate alkalinity. The Elon contents of the AH-1, 15, 17, and 18 developers bracket this, varying from 7.5 to 0.25 grams/liter. They all contain 10 grams of sodium sulfite per liter and the proper amount of alkali to equalize the activity. Full compensation of activity was not possible in the case of AH-18, containing the least amount of Elon, but the others are matched reasonably well.

Procedure. Once the final formulas had been established, complete time–gamma studies were made, and times of development at 68°F for a gamma of 0.65 for all emulsion–developer combinations were chosen. Acutance, granularity, and sensitometric-control strips were then exposed and processed for the times indicated by these studies. Processing was in the sensitometric machine of Jones, Russell, and Beacham,[5] which gives strong and uniform agitation. The resultant strips were evaluated in accordance with standard practices described in the literature. The speeds which will be cited later in the paper are 0.3*G* speeds measured according to the familiar ASA criterion. Granularity was measured in terms of the root-mean-square of the granularity fluctuations.[6] The diameter of the scanning aperture was 24 μ and the sample density was unity. Acutance was measured as described by Perrin;[7] the sample density was also unity. Since the curve shapes were similar, a single number at a constant density is a reasonable indication of the behavior of the developers.

Results

The results are summarized in Tables II–IV, which give the results for Panatomic-X, Plus-X, and Tri-X Films, respectively. Kodak Developer D-76 is included for comparison[4] and is taken arbitrarily as 100%. The sulfite concentration is given in grams per liter. The data for AH-1 in Series I are repeated in connection with Series II because, in a sense, this developer also forms a part of the latter series.

Speed, Acutance, and Granularity. The results for the fine-grain series, AH-1 to AH-4, are shown in Fig. 1, where they are plotted on the basis of 100% for AH-1. The abscissas are in terms of moles of sulfite ion per liter. As the sulfite concentration is increased, the speed and the granularity (top and bottom graphs) of all three emulsions diminish to a minimum at about 1.0 mole/liter and then rise again. The broken line shows the rate of solution of silver as determined by Lee and James,[8] and this exhibits a maximum at about 0.6 mole/liter. Although the data are not sufficient to locate the minima for speed and granularity precisely, these minima fall near the maximum rate of solution, and the proximity may be regarded as more than accidental. (The speed curve for Tri-X Film as drawn does not show a minimum, but the data are insufficient to determine whether there may be a minimum between 1.0 and 1.8 moles/liter.) The curves of acutance

4. *Processing Chemicals and Formulas*, Eastman Kodak Company, Rochester, N.Y., 5th ed., 1954, p. 39.

5. L. A. Jones, M. E. Russell, and H. R. Beacham, *Jour. SMPE*, **28**: 73 (1937).

6. G. C. Higgins and K. F. Stultz, *J. Opt. Soc. Am.*, **49**: 925 (1959).

7. F. H. Perrin, *Jour. SMPTE*, **69**: 151 (1960).

8. W. E. Lee and T. H. James, private communication

TABLE II. Speed, Acutance, and Granularity of Kodak Panatomic-X Film

	Formula No.	Kodak Elon	Sulfite (g/l)	Dev. time (min)	γ	Speed	%	Acutance	%	Granularity	%
Series I (fine-grain)	AH-1[a]	7.50	10	9	0.62	130	113	2340	106	0.027	123
	AH-2	7.50	30	8	.63	125	108	2200	100	.019	86
	AH-3	7.50	100	8¼	.63	82	71	2200	100	.011	50
	AH-4	7.50	200	11	.63	96	83	1850	84	.012	55
Series II (high-sharpness)	AH-1*	7.50	10	9	0.62	130	113	2340	106	0.027	123
	AH-15	2.50	10	4	.61	107	93	2500	113	.034	155
	AH-16	1.00	10	5	.61	117	102	2550	116	.036	164
	AH-17	0.50	10	7	.69	129	112	2750	125	.036	164
	AH-18	0.25	10	13	.64	150	130	3100	141	.034	155
Kodak Developer D-76 (1:1)[b]				6½	0.62	115	100	2200	100	0.022	100

All data from single runs except for:
a. average of 5 runs; b. average of 2 runs.

* Data repeated for convenience.

TABLE III. Speed, Acutance, and Granularity of Kodak Plus-X Pan Film

	Formula No.	Kodak Elon	Sulfite (g/l)	Dev. time (min)	γ	Speed	%	Acutance	%	Granularity	%
Series I (fine-grain)	AH-1[a]	7.50	10	12	0.68	340	128	1820	96	0.044	147
	AH-2	7.50	30	9½	.62	224	84	1500	79	.027	90
	AH-3	7.50	100	8½	.63	120	45	1400	74	.014	47
	AH-4	7.50	200	12½	.62	219	82	1300	68	.019	63
Series (II (high-sharpness)	AH-1*	7.50	10	12	0.68	340	128	1820	96	0.044	147
	AH-15	2.50	10	10	.64	316	119	1850	97	.047	157
	AH-16	1.00	10	11	.62	288	108	2000	105	.048	160
	AH-17	0.50	10	12	.63	347	130	2250	118	.050	167
	AH-18	0.25	10	20	.64	363	136	2300	121	.051	170
Kodak Developer D-76 (1:1)[b]				7	0.66	266	100	1900	100	0.030	100

All data from single runs except for:
a. average of 5 runs; b. average of 2 runs.

* Data repeated for convenience.

TABLE IV. Speed, Acutance, and Granularity of Kodak Tri-X Film

	Formula No.	Kodak Elon	Sulfite (g/l)	Dev. time (min)	γ	Speed	%	Acutance	%	Granularity	%
Series I (fine-grain)	AH-1[a]	7.50	10	22	0.62	1090	128	950	79	0.074	132
	AH-2	7.50	30	20	.67	910	107	1150	96	.064	114
	AH-3	7.50	100	16	.65	590	70	700	58	.050	89
	AH-4	7.50	200	20	.64	525	62	500	42	.050	89
Series II (high-sharpness)	AH-1*	7.50	10	22	0.62	1090	128	950	79	0.074	132
	AH-15	2.50	10	11	.62	852	100	900	75	.082	147
	AH-16	1.00	10	11½	.62	795	94	900	75	.084	150
	AH-17	0.50	10	26	.67	795	94	1050	88	.086	154
	AH-18	0.25	10	35	.62	742	87	1150	96	.090	161
Kodak Developer D-76[b]				8½	0.63	850	100	1200	100	0.056	100

All data from single runs except for:
a. average of 5 runs; b. average of 2 runs.

* Data repeated for convenience.

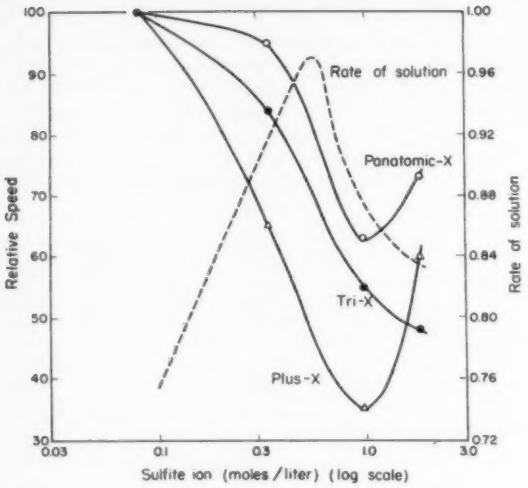

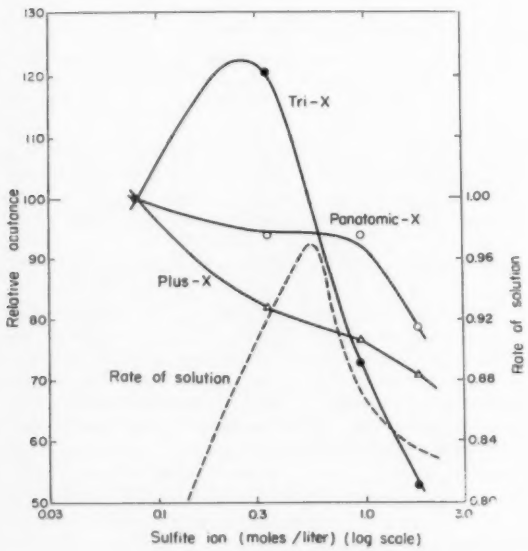

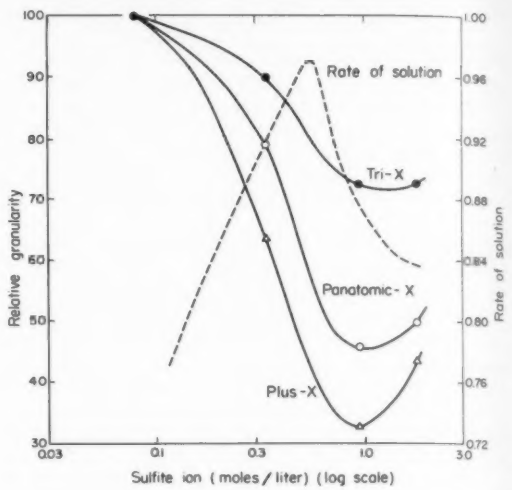

Fig. 1. Effect on three Kodak films of varying the sulfite concentration in the fine-grain series of developers. Abscissas, total sulfite ion, moles per liter (log scale); ordinates, relative values of indicated characteristics (arithmetic scale), with values for Developer AH-1 taken as 100%. Broken curves, relative rate of solution of silver (right-hand ordinate scale) according to Lee and James.

(middle graph), on the other hand, except for Tri-X Film, drop rather steadily with increasing sulfite concentration between 0.1 and 0.5 mole/liter. Plus-X Film is affected the most in speed and granularity and Tri-X the least by a change in sulfite concentration.

Figure 2 shows the results for the high-sharpness series of developers (Series II), with the values for AH-1 being again taken as 100%. Here the abscissas are in terms of Elon concentration in grams per liter. Speaking generally, reducing the Elon concentration does increase acutance without seriously reducing the speed except for Tri-X Film. However, it also increases granularity, especially of Panatomic-X Film.

Microstructure

Since, broadly speaking, fine-grain development and high-sharpness development have been found to be incompatible in these series of developers, we come next to the question of making the best choice between these competing qualities. Obviously a formula may be chosen to fit a specific use—for example, to emphasize speed or to minimize grain. But is it possible to relate the speed, grain, and acutance curves moving in different directions, and what is the relative importance of the three parameters? Although not much information is available on this problem, some recent work of Wolfe and Tuccio[9] does suggest one approach to it.

9. R. N. Wolfe and S. A. Tuccio, *Phot. Sci. & Eng.*, **4**: 330 (1960).

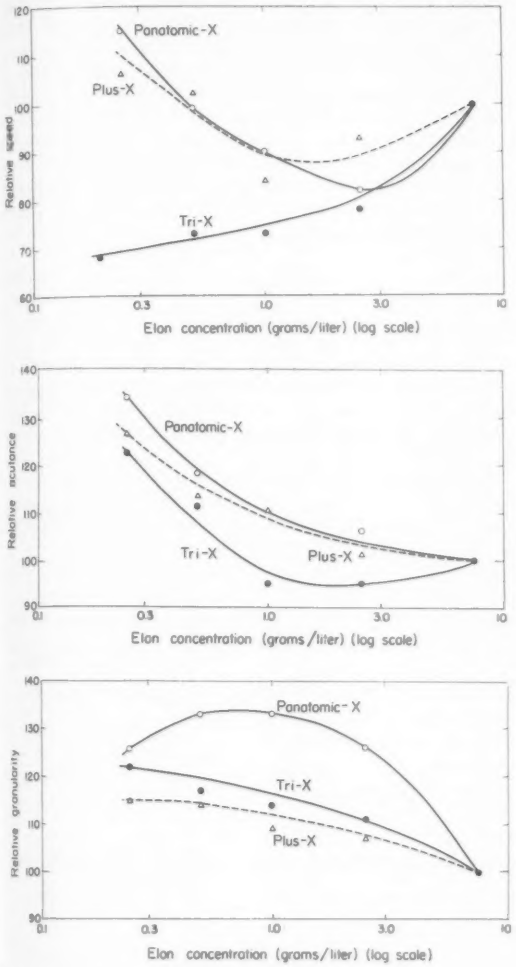

Fig. 2. Effect on three Kodak films of varying the Elon concentration in the high-sharpness series of developers. Abscissas, Elon concentration, grams per liter (log scale); ordinates, relative values of indicated characteristics (arithmetic scale), with values for Developer AH-1 taken as 100%.

In a study of the definition of aerial photographs—"definition" being specified as the characteristic that relates to the clarity with which detail is reproduced—these authors evaluated a series of pictures in terms of the quantity $(\sigma_B \cdot \sigma_G)^{-1}$ and found that this agreed well with the subjective judgments of definition made by a jury of observers on the pictures.

The factor $\sigma(_G)$ in this expression is the granularity of the emulsion and is expressed as the root-mean-square variation from average density indicated by a microdensitometer scanning a uniformly exposed and processed sample. The quantity σ_B was essentially the width of the composite spread-function for the entire photographic system, which in this case, involved a camera lens, the negative material, and the effects of image motion. Now it can be shown that the distribution of energy in a knife-edge exposure is given by the integral of the spread function between its end points, so that the width of the spread function and the width of the edge are much the same. Furthermore, when the shapes of the edge distributions are similar and gamma is held constant—as in the present experiment—we may say that acutance is roughly inversely proportional to the width of the edge trace. In others words, when we consider film and developer alone, the reciprocal of the σ_B of Wolfe and Tuccio is approximately proportional to acutance.

Since σ_G is the granularity of the emulsion, it seems reasonable in the present state of our knowledge to appraise the simultaneous variations of granularity and acutance in terms of the simple fraction, acutance/granularity. This ratio gives us a value for the microstructure properties of the image, and a high ratio shows good over-all microstructure properties.

It is also conceivable that increases in speed could lead to improvements in the over-all definition of the final picture, since such increases permit the use of smaller apertures or higher shutter speeds. However, we do not know quantitatively how increased depth of field or reduced subject movement is reflected in over-all picture quality.

We have therefore evaluated the simple ratio, acutance/granularity, at a density of unity for the various emulsion–developer combinations considered here, and these are given in Table V. The values are relative, with D-76 being taken as 100% to show the changes with developer variations. A value of over 100% indicates an improvement in the acutance/granularity ratio with respect to D-76.

Inspection of this table shows that, in these experiments, variations in Elon and sulfite concentrations have resulted in very much greater changes in granularity than in acutance. This is why the fine-grain developers (Series I) in general appear to be advantageous on a combined basis; the improvement in granularity is proportionately so much greater than the loss in acutance. For the same reason, the high-sharpness developer formulas (Series II) in general are evaluated at less than 100%—one has paid a disproportionate price in granularity for a moderate gain in acutance.

Of course, as reference to Tables II–IV shows, the improvement in the microstructure ratio in Series I is accompanied by the expected loss in speed, so that under some circumstances this gain may not be realized in practice. Likewise, the losses exhibited by the emulsions in the Series II developers may be offset to some degree by increases in speed.

Informational Sensitivity

The acutance/granularity ratio appears at present to be a reasonable way to appraise simultaneous changes of graininess and sharpness in general pho-

tography. Recently there has also been described in the literature[10] a more specialized concept—informational sensitivity. Informational sensitivity is based on considerations of the minimum energy-increment detectable by a given photographic emulsion, and its relation to the granularity, spread function, and sensitometric characteristics of that emulsion. One application of this concept is in the design of complete photographic systems, that is, in the choice of optimum lens–film combinations. If the conditions are imposed that the physical size of the lens aperture be fixed but that lens focal length may be varied to use each film and developer combination to its best advantage, the informational-sensitivity value indicates the combination that will record a star in the shortest exposure time.

The expression given by Zweig, Higgins, and MacAdam for informational sensitivity at any given density is

$$IS = g/a \cdot \sigma_D,$$

where g is the slope of the density-exposure (*not* D-log E) curve at this given density, a is the area of the emulsion spread-function, and σ_D is the rms-granularity of the emulsion at that density for a scanning aperture of area a. It can be shown that, when the same emulsion is processed to a constant gamma in a series of developers, g is proportional to the reciprocal of E_D, the exposure required to produce the reference density. Also, since acutance Ac is inversely proportional to r, the radius of the spread function, it turns out that

$$IS \sim \frac{1}{E_D} \cdot \frac{Ac}{G}$$

where G is Selwyn granularity, $\sigma\sqrt{a}$.

It will be noted that this approximate conversion of the informational-sensitivity expression is similar to the Ac/σ_D quantity already employed, with the addition of a special type of speed term for this special application.

The informational sensitivity of the three emulsions used with the three developers was computed, since this may be of interest in some applications of

10. H. J. Zweig, G. C. Higgins, and D. L. MacAdam, *J. Opt. Soc. Am.*, **48**: 926 (1958).

TABLE V. Relative Acutance/Granularity Ratio at Unit Net Density

	Formula No.	Kodak Elon (g/l)	Sulfite (g/l)	Kodak Panatomic-X Film	Kodak Plus-X Film	Kodak Tri-X Film
Series I (fine-grain)	AH-1	7.50	10	88	69	60
	AH-2	7.50	30	117	92	76
	AH-3	7.50	100	204	162	65
	AH-4	7.50	200	156	114	47
Series II (high-sharpness)	AH-1*	7.50	10	88	69	60
	AH-15	2.50	10	75	65	51
	AH-16	1.00	10	73	70	50
	AH-17	0.50	10	79	76	57
	AH-18	0.25	10	93	76	59
Kodak Developer D-76 (1:1)				100	100	100

* Data repeated for convenience.

TABLE VI. Relative Informational Sensitivity

	Formula No.	Kodak Elon (g/l)	Sulfite (g/l)	Kodak Panatomic-X Film	Kodak Plus-X Film	Kodak Tri-X Film
Series I (fine-grain)	AH-1	7.50	10	89	52	64
	AH-2	7.50	30	117	55	100
	AH-3	7.50	100	135	31	36
	AH-4	7.50	200	133	36	22
Series II (high-sharpness)	AH-1*	7.50	10	89	52	64
	AH-15	2.50	10	65	84	36
	AH-16	1.00	10	82	73	27
	AH-17	0.50	10	135	89	52
	AH-18	0.25	10	165	79	32
Kodak Developer D-76 (1:1)				100	100	100

* Data repeated for convenience.

photography. Table VI summarizes the results, with D-76 again being taken as 100%.

It should be noted that these values are given for a density of unity, that is, for a point moderately well up on the characteristic curve. Because of this, the $1/E_D$ term is rather sensitive to mismatches of gamma and to slight changes in curve shape, and this is reflected in some instances in the tabulated values. (For instance, we have observed that Plus-X Film, when processed in low-Elon developers, exhibits a distinct tendency to an upward concavity of the characteristic curve. This, of course, could be an advantage for some applications.) It may also be remarked that informational sensitivity is generally at its maximum at very low densities (see Ref. 10, Fig. 8).

At any rate, Table VI shows the manner in which informational sensitivity varies throughout these series of developers. It is apparent that useful gains over D-76 result, in these series of formulas, only with Panatomic-X Film.

Summary and Conclusions

A number of simple Elon–alkali developers were formulated, grouped into two series. In the first series, the silver-solvent (sulfite) content of the developer was systematically varied. In the second series, acutance was varied by systematic variations in Elon concentration.

In general, the first series of developers showed that large amounts of sulfite in connection with a high and constant Elon concentration resulted in decreases in acutance as well as decreases in granularity and speed. When sulfite concentrations in excess of about 1 mole/liter are used, the action reverses and granularity starts to increase again; acutance, however, continues to drop.

In the second series of developers, where the sulfite concentration is low and constant, moderate improvements in acutance result from lowering the Elon concentration. In all cases in this series, however, the granularity was found to be excessive for the resulting speed of the materials. Acutance continued to increase to the lowest concentration of Elon which was tried—0.25 gram/liter.

An attempt was made to appraise the combined effect of changes in both acutance and granularity (microstructure) on the over-all photographic definition of the negative in terms of the simple ratio of acutance to granularity, in accordance with the work of Wolfe and Tuccio. In general, because the variations in granularity produced by developer changes are much greater than the variations in acutance, fine-grain development appears to offer an advantage.

A simple approximate conversion of the Zweig-Higgins-MacAdam expression for informational sensitivity was introduced, and the various emulsion–developer combinations were evaluated with reference to this.

NOTE on "The Effect of the Variables of a Photographic System on Detail Rendition, with Special Reference to Camera Motion," by Robert N. Wolfe and Sam A. Tuccio, *Photographic Science and Engineering*, 4: 330 (1960).

Through an unfortunate oversight on the part of the authors, proper recognition was not given to the work described in the paper entitled "Contrast Rendition as a Design Tool," by Roderic M. Scott, in *Photographic Science and Engineering*, 3: 201–209 (1959). This earlier paper describes a method of calculating the sine-wave response or transfer function of an optical system in terms of the transfer functions of its elements. An analogous calculation in terms of spread function was given by the present authors, who also extended the calculation to include the effects of photographic granularity and presented pictures to demonstrate their conclusions.

PHOTOGRAPHIC SCIENCE AND ENGINEERING
Volume 5, Number 3, May-June 1961

Xerography for Close-Access Recording of Continuous-Tone Line-Scan Cathode-Ray Tube Presentations

JOHN T. BICKMORE, *Research and Development Division, Haloid Xerox Inc., Rochester, N.Y.*, AND ALLEN H. ETT, *Research Division, Philco Division, Philadelphia, Pa.*

An experimental device has been developed to demonstrate the use of xerographic techniques for displaying and recording continuous-tone information with very short delay. Incoming continuous-tone signals generate a line scan on a high-intensity high-resolution cathode-ray tube. This scan line is focused on the surface of a rotating selenium-coated xerographic drum, previously charged to a uniform potential. Subsequent scan lines overlap, thus creating a two-dimensional electrostatic image. This image is developed by an electrostatically charged black powder suspended in an aerosol. The powder image is transferred to a continuous paper web, so that the scan lines are integrated to create an unbroken continuous-tone record of the incoming information. For the processor, not including CRT or optics, resolution is 14 line-pairs/mm and the density range is 1.5. The peripheral speed of the drum is continuously adjustable between 0.3 and 0.03 in./sec; the lengths of the development zone and the transfer zone are approximately 1.5 in. each. Thus, the elapsed time between exposure and the completion of development is 5 sec at the highest speed; an additional 5 sec elapse before the print can be viewed. Details concerning the cathode-ray tube input, the optical system, the xerographic processor, and the test results are included.

The Philco Corporation and Haloid Xerox Inc. jointly engaged in a program to develop a system that included an experimental close-access strip-display recorder using the xerographic process. This was a first attempt to combine continuous-tone xerography with cathode-ray tube inputs, as well as a first attempt to use xerography for close-access recording.

The term "close-access" is used to describe this device because it emphasizes an inherent problem in the design of equipment of this type. The object is to produce a visible record as soon as possible after reception of the input signal. The actual velocity of the record may be relatively low because of the necessity for producing an orthogonal image. The only way to minimize the delay is to minimize the total length of the processing elements in the direction of record travel. The central problem is thus to design a device which processes the image in the shortest distance along the direction of record motion.

This paper describes the xerographic recorder that was developed. Such a device might find application in vehicles or ground installations with inputs from flying spot scanners and other line-scan sensors. This particular device was constructed so that it could be airborne. Included is information on the cathode-ray tube input and on the electronic signal simulator used for testing.

Presented at the SPSE Rapid Processing Symposium, Washington, D.C., 14 October 1960. Received 10 November 1960; revised 7 March 1961. The work described here was performed under AF33(616)-5325, which is sponsored by Wright Air Development Division, Air Research and Development Command, United States Air Force.

General Description

The functional elements of the processors are shown schematically in Fig. 1. Incoming electrical signals intensity-modulate a line scan on a high-resolution recording cathode-ray tube. This image is focused on a synchronously rotating selenium-coated metal cylinder, the xerographic surface, which serves as a photoreceptor. The motion of the selenium drum provides the orthogonal scan. Broadly speaking, the xerographic process steps are conventional, as follows:

The selenium drum rotates near a corona charging unit which uniformly charges it. The charged selenium surface is then exposed to the focused image of the line scan on the face of the cathode-ray tube. The light pattern selectively discharges areas of the selenium drum to give an electrostatic pattern corresponding to the pattern of light intensity. This electrostatic image next passes into a development zone where a charged black powder carried in an aerosol is deposited on the selenium, the quantity deposited increasing with the charge density on the selenium. The resulting powder image then revolves against a paper web to which the powder image is transferred. This paper-supported image can be viewed as soon as it emerges from the transfer roller.

At this stage, the powder image is not fixed to the paper, but is satisfactory for viewing provided it is not touched. To form a permanent image, a plastic-coated paper is used. The application of heat softens the plastic coating, into which the powder becomes embedded. The heat is applied

by a heated platen located just past the viewing position. The paper is then rolled up to provide a permanent record.

A small fraction of the powder image on the selenium drum is not transferred to the paper. This residual developer powder is removed by a pair of rapidly-revolving fur brushes. A discharge lamp, installed between these brushes and the corona charging unit, removes any residual charges from the selenium surface before it is reused.

These process elements are discussed in more detail in the next section.

Process Elements

The peripheral speed of the selenium drum is continuously variable from 0.03 to 0.3 in./sec. The corona charging unit deposits positive ions on the selenium. The charging unit contains two independent sets of parallel wires held parallel to the axis of the selenium drum. A positive d-c potential of several thousand volts, applied to one set of wires, produces a corona discharge, while the other set of wires, located between the corona wires and the selenium drum, controls the charging current by virtue of the potential applied to it. Higher potentials lead to higher charging currents.

The potential applied to the control wires is determined by a special feed-back circuit which monitors the charging current flow from the selenium drum to the negative terminal of the corona power supply. This circuit regulates charging current against variations of line voltage or atmospheric pressure. By means of a bias potential determined by the selenium-drum speed control, the circuit also adjusts the charging current for changes in drum speed.

The 5-in. cathode-ray tube is of the high-brightness flat-face variety. Several tube types were tested in the equipment, including special designs fabricated by the Landsdale Tube Division of Philco. The CRT receives its input from several video circuits which provide wide-band amplification and video processing to control exposure and contrast.

The doubly folded optical system consists of two front-surface mirrors and a special $f/2.5$ lens of 5-in. focal length, color corrected for the P-11 spectrum. Magnification is 2:1.

Complete discharge of the selenium drum could be obtained under the conditions listed in Table I.

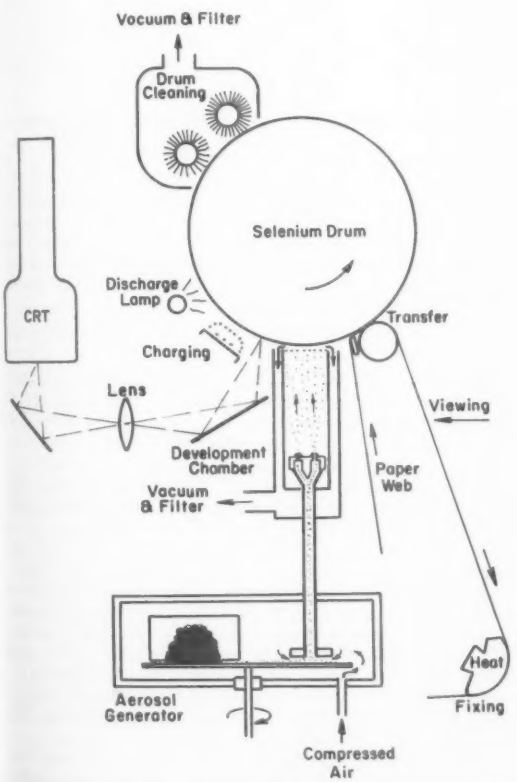

Fig. 1. Schematic drawing of functional elements of the processor, illustrating operational sequence: electrostatic charging of selenium surface; exposure to scan line of cathode-ray tube; development; transfer of developed image to paper web; removal of residual powder from drum; and removal of stray charges.

TABLE I. Conditions for Complete Discharge of Selenium Drum

Initial potential of selenium drum	300 v
Thickness of selenium layer	50 μ
Magnification, M	2:1
Sweep length, l	3.6 in.
Lens aperture, f	$f/3$
Peripheral drum speed, V	0.3 in./sec
CRT accelerating potential, E	10 kv
CRT beam current, i	15 μA
Duty cycle, θ	0.25

It is interesting to calculate the cathode-ray beam energy which must be dissipated to discharge completely a unit area of the photoconductor. Neglecting light losses in the lens, and multiplying by the ratio of cathode-ray tube brightness to the intensity of illumination of the photoconductor, it can be shown that:

$$\text{Beam energy to discharge unit area of the photoconductor} = \frac{\pi E i \theta}{4f^2 (M+1)^2 MlV}$$

where the symbols are those defined in Table I. The beam energy per unit area to obtain complete discharge of the photoconductor is 1700 ergs/sq in., calculated from the numerical values of Table I.

The operation of the aerosol development device can be understood by referring to Fig. 1. An aerosol consisting of charged black powder particles, suspended in air, is produced in the aerosol generator. This is an airtight vessel, capable of withstanding internal air pressures, in which rotates a turntable. A thin layer of powder is spread on the turntable by means of two fixed blades. The only outlet from this vessel is a powder take-off head located approximately 0.15 in. above the turntable. Air rushing between the outlet head and the turntable raises the developer powder, mixes it with the pressurized air, and carries it to the development chamber.

The short-access aerosol development unit presents a serious design challenge. For the purposes to be served by the equipment, the length of the unit along the circumference of the selenium drum must be as small as possible,

and yet enough developer powder must be presented to the charged selenium surface to develop high densities. Higher aerosol concentrations can compensate for shorter development times, but there is a limit to the degree of compensation.

As is shown below, at high aerosol concentrations, development rate increases only very slowly as aerosol concentration is increased. In addition, the developer must be presented at a low velocity normal to the photoconductor. High velocities cause a large fraction of the developer powder to impact against the selenium and stick by electrostatic image forces or intermolecular forces, thus causing high minimum densities.

Still another requirement is that the aerosol must develop uniformly across the full image width, in this case about 9.5 in. It might be presumed that this and the requirement for high developing rate could be eased by producing smaller images and utilizing lower peripheral drum speeds. However, the fact that the image moves more slowly means that the length of the development zone must be proportionally decreased if access time is to remain constant, so that there is little, if any, advantage.

Finally, as explained below, to achieve continuous-tone response it is necessary to utilize a conductive electrode as a development zone boundary. This restricts the manner in which the aerosol can be caused to flow past the photoconductor.

The development chamber shown in Fig. 2 represents a workable solution to the above problems. The operation of this unit can be understood by referring to Fig. 1.

Aerosol entering the development chamber is divided, half going to each of two rows of jets which spread the aerosol uniformly, parallel to the axis of the selenium drum. The aerosol then passes through a fine wire screen located at the end of the development chamber and emerges into the narrow space between the screen and the selenium drum, where development takes place.

Aerosol that is not utilized in development passes into vacuum slots located on each side of, and parallel to, the screen. The total length of the chamber along the circumference of the selenium drum is 1.5 in.

The wire screen serves as a unipotential plane situated close enough to the surface of the selenium drum to cause a fraction of the lines of force emanating from the charge on the selenium to terminate on the screen. The necessity for this can be understood by referring to Fig. 3.

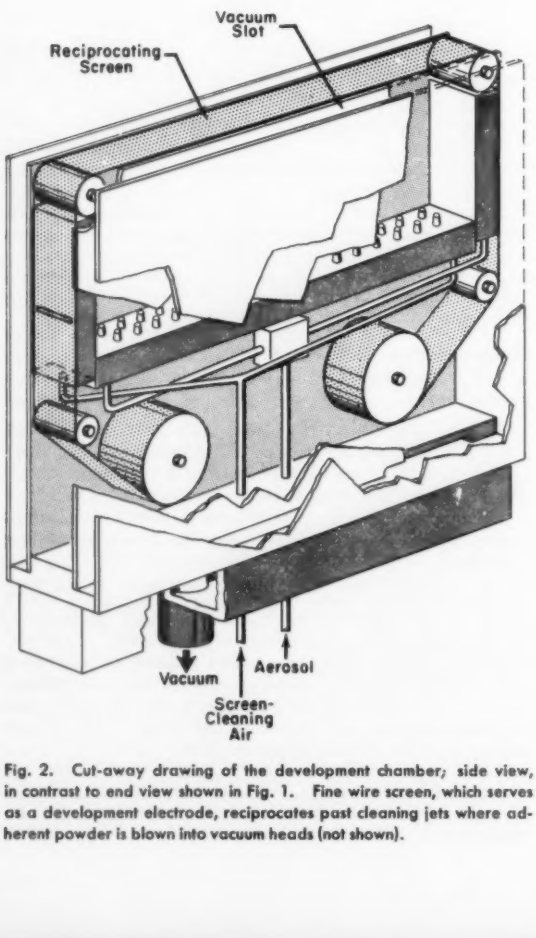

Fig. 2. Cut-away drawing of the development chamber; side view, in contrast to end view shown in Fig. 1. Fine wire screen, which serves as a development electrode, reciprocates past cleaning jets where adherent powder is blown into vacuum heads (not shown).

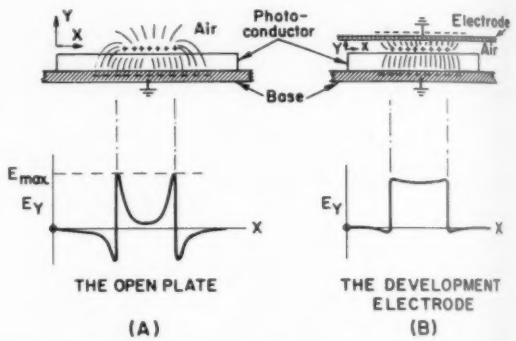

Fig. 3. Effect of the development electrode. The normal component of the electrostatic field above a photoconductor is strongest at the edges of a charged area and weakest at the center (A). A conductive plane situated near and parallel to the photoconductor and electrically connected to the base (B) increases the relative intensity of the interior fields as compared with the edge fields.

When a selenium plate is removed from surrounding conductors, most of the field from charges situated on the selenium passes through the selenium layer to the conductive base (A, Fig. 3). However, fields of considerable magnitude loop through the space above the selenium surface near charge gradients. Under these conditions, introducing charged developer powder above the selenium surface leads to development of the gradients; large charged areas are only slightly developed except at the edges.

In order to develop in direct relation to the *quantity* of charge, instead of to the *gradient* of charge, a closely-spaced conductor is situated parallel to the selenium surface and electrically connected to the conductive substrate (B, Fig. 3). This increases the field above the selenium at the expense of the internal field, and results in uniform development of uniformly charged areas. The fine wire screen performs this function.

The minimum quantity of developer pigment that must be presented to the selenium drum is that which would be capable of giving a uniform layer of the maximum reflection density. In addition, roughly one-third of the developer particles are of a polarity opposite to that being utilized in development; and finally, only a fraction of the correctly charged powder is utilized, even

when developing a uniform black. For these reasons, more developer powder must be presented to the selenium surface than is actually deposited.

The fraction of the developer powder in the aerosol which can contribute to the development of the image depends upon the peripheral speed of the selenium drum. This fraction can be defined as the mass per unit area of developer powder on the print required to give unit optical density, divided by the mass of powder which must be delivered to the development chamber to develop the same area to the same optical density.

The fraction of powder utilized decreases at higher drum speeds, as shown in Fig. 4. The reason for the decrease is evidently related to the increased aerosol concentration required to develop in a shorter time. Previous studies[1] have revealed similar effects when changing the aerosol concentration.

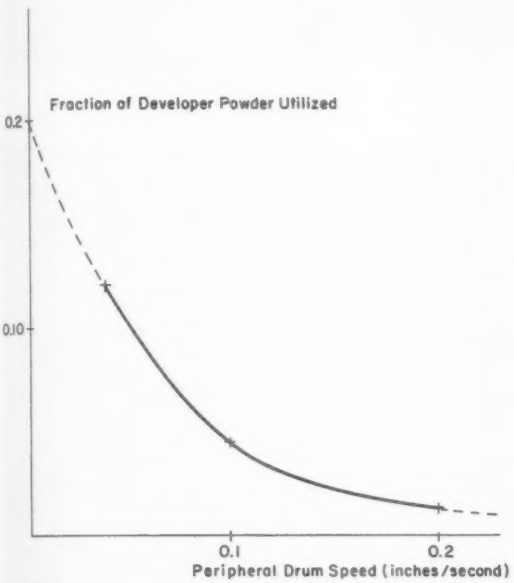

Fig. 4. Fraction of developer powder utilized, as a function of peripheral drum speed. As drum speed is increased, the mass of powder which must be delivered to the development chamber to obtain a given print density increases more rapidly than the area developed per unit of time.

The concentration of the aerosol in the subject processor is not particularly high in comparison with other aerosol devices for xerography (0.03 grams of powder per liter at 0.1 in./sec); but the particular geometry of, and flow rates in, the development zone evidently cause a loss in the fraction of toner utilized at this level of concentration.

Developer powder tends to deposit in parts of the development chamber, the most rapid deposition occurring on the screen electrode. To prevent build-up of developer powder, this screen reciprocates past air knives and vacuum slots located outside the development zone, thus keeping the most vulnerable element clean.

The next most vulnerable element is the inside of the development chamber itself. The present unit can be operated for approximately 25 min at a peripheral drum speed of 0.1 in./sec before sufficient deposition occurs to interfere with operation. At this time, agglomerates of powder may break off deposition points and be carried by the air stream through the screen and against the selenium drum with sufficient force to cause blotted areas on the image. The development chamber must be cleaned with a large volume of compressed air before satisfactory operation can be resumed.

Transfer of the powder image from the selenium drum to paper is effected electrically. An electrically conductive rubber roller (Fig. 1) 0.625 in. in diameter presses the plastic-coated side of the paper against the pigment image on the selenium drum. A potential of 1500-v ac applied between the roller and the selenium drum base causes most of the pigment to transfer to the paper. The mechanism of electrostatic transfer of the slightly conductive powder used with this device is different from the transfer of insulating powders. In this case, the powder is evidently charged by induction and caused to transfer by the applied field. The polarity of this field has only a minor effect upon the completeness of transfer.

Special tensioning devices maintain constant tension on the paper web, with a slight excess of force in the direction of selenium drum rotation so that the paper web is pulled through the transfer zone by the selenium drum. This avoids smudging due to differences in drum and paper speeds.

A metal bar over which the paper passes before it reaches the transfer roller serves to prevent transfer of powder from the selenium drum to the paper prior to intimate contact of the two surfaces.

Results

Operation of the processor was evaluated with several optical inputs. Direct optical exposure was generally accomplished by inserting a positive transparency in the location normally occupied by the face of the cathode-ray tube. The optical path in the processor is designed to allow projection of a line on the selenium drum, but there is insufficient clearance to allow exposure along an arc of more than $^1/_4$ in. To create a continuous image, a $^1/_4$-in. strip was repeatedly exposed by periodically illuminating the transparency with a strobotron. Such exposures permitted determination of processor characteristics exclusive of the cathode-ray tube.

Under these conditions, optimum picture quality was obtained when the aerosol concentration was set to give maximum reflection densities on the print in the range from 1.3 to 1.6. The accompanying minimum reflection density was roughly 0.1 above the paper density, and resolution was 14 line-pairs/mm. Exposure range was essentially independent of aerosol powder concentration. Exposure through a density step wedge with 0.15 density steps yielded a print with seven clearly differentiated densities, corresponding to an exposure range of about 1.0 log unit.

These images, composed of repetitive $^1/_4$-in.-wide strips, are difficult to evaluate as pictures. Wider images, which are easier to evaluate, were produced in a prototype processor in which the development chamber and the corona charging unit were sep-

1. J. T. Bickmore, M. Levy, and J. Hall, *Phot. Sci. & Eng.*, 4: 37 (1960).

Fig. 5. Reproduction of xerographic print produced in the prototype processor. Selenium drum was exposed directly to a positive transparency illuminated by a strobotron. Peripheral selenium drum speed, 0.25 in./sec. Development chamber was essentially identical with that in the final processor.

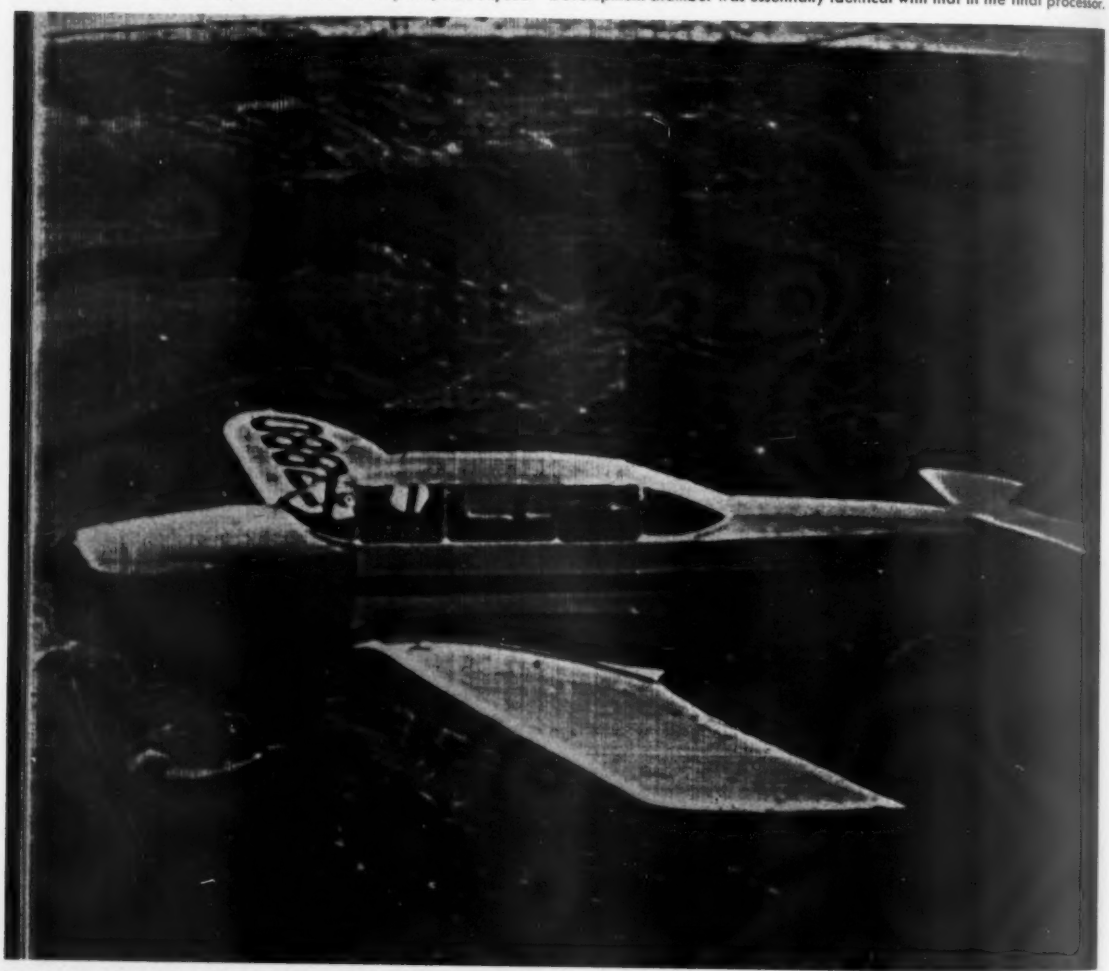

Fig. 6. Reproduction of xerographic print produced in the processor. A positive transparency was scanned by a flying spot scanner, the output of which modulated the processor CRT. Peripheral selenium drum speed, 0.1 in./sec. Vertical striations are caused by nonuniform light output from processor CRT along the scan line (phosphor noise). Horizontal striations are caused by nonuniform motion of the selenium drum.

arated sufficiently to allow exposure along a much longer arc. The length of these images along the arc was limited, but to a lesser degree, by the distortion resulting from exposure onto the cylindrical drum surface.

Figure 5 is a reproduction of a xerographic print produced in the prototype processor, using a development unit essentially identical to that employed in the final processor. The peripheral drum speed was 0.25 in./sec.

Tests of the entire processor, including the cathode-ray tube, were performed using input signals derived from either an electronic function generator or a special flying spot scanner signal simulator. This scanner uses a CRT identical with the recorder, but with a P-16 phosphor. The CRT is scanned with a raster scan consisting of a line scan and a very slow orthogonal scan with a rate of speed corresponding to the strip recorder velocity. The chassis, the lens system, and many of the circuits in each equipment are identical. The simulator is designed to work with 3 by 4-in. glass plates or 35mm film strips and is adaptable to the use of 3-in. film strips. Figure 6 is a reproduction of a xerographic print produced in this manner.

The internal test equipment generates an electronic step wedge or gray scale and a resolution pattern to check sine-wave response of the over-all equipment. With a sine-wave modulating the intensity of the cathode-ray tube beam, a line pattern is clearly visible up to frequencies corresponding to 3 line-pairs/mm on the finished print, which corresponds to approximately 6 line-pairs/mm (150 line-pairs/in.) on the cathode-ray tube. The difference between this figure and that previously given of 14 line-pairs/mm is that this is for the xerographic process alone, while the other is limited by all further elements in the system.

Many problems encountered in integrating the processor and electronic equipment are of interest. One of the major problems, the appearance of longitudinal streaks in the picture, was traced to an uneven distribution of the phosphor in the CRT. Special CRT's with ultrafine screens were fabricated to reduce this disturbance, but even the finest screens did not completely clear up the difficulty. It is anticipated that future strip-recording equipment may employ evaporated phosphors to eliminate this streaking problem.

Conclusions

Although the processor has a resolution over twice that of the cathode-ray tube and adequate print characteristics, it is felt that this unit does not begin to show the limits of the xerographic process for this application. In particular, the running time before a cleaning operation is required must be substantially lengthened; the requirements for associated air pressure and vacuum cleaning units must be reduced or eliminated; and the access length must be shortened. There are good prospects that such improvements can be made.

Acknowledgments

The writers wish to acknowledge the many contributions by others to this work both in the laboratory and on advisory levels. These include H. Bogdonoff, W. J. Burris, H. E. Clark, J. J. Codichini, J. H. Dessauer, C. L. Huber, R. T. Kimbrough, and others at Haloid Xerox Inc., and J. Angeloni, R. B. Goldman, and R. A. Schaphorst at the Philco Corporation. Finally, the authors acknowledge the support and guidance of the USAF.

PHOTOGRAPHIC SCIENCE AND ENGINEERING
Volume 5, Number 3, May-June 1961

The Relation of Quantum Efficiency to Energy- and Contrast-Detectivity for Photographic Materials

H. J. ZWEIG, *Research Laboratories, Eastman Kodak Company, Rochester, N.Y.*

The roles of quantum efficiency, noise-equivalent energy, noise-equivalent contrast, and informational sensitivity in the detecting ability of photographic materials are studied. Curves are derived from which it should be possible to determine the number of quanta required for the detector to respond.

In a recent paper,[1] a theoretical study of idealized photographic detectors was presented and some conclusions as to the limiting quantum efficiency were deduced. The present paper shows how the quantum efficiency of a photographic material reflects upon its ability to detect signals and gives some empirical verifications of the relations involved. The relations between quantum efficiency η^2, noise-equivalent energy $\Delta\mu_{ne}$, and noise-equivalent contrast C_{ne} for idealized photographic detectors are first developed, an experimental device for examining the relations between these last two quantities and the corresponding observable quantities (i.e., minimum detectable energy and minimum detectable contrast) is then described, and finally some preliminary experimental results are presented.

Quantum Efficiency, Noise-Equivalent Energy, and Contrast-Detectivity—Interrelations and Magnitude for Idealized Photographic Detectors

As in the aforementioned work,[1] the following notation will be used:

- E = background exposure in photons per square micron
- λ = exposure in photons per grain area
- $f(\lambda)$ = output (usually in fractional number of developed grains) at the exposure level λ
- A = area of a "cell"
- A_s = area of spread function
- n = number of developed grains in a cell
- N = maximum number of developed grains in a cell
- $\bar{n}(\lambda)$ = average number of developed grains in a cell
- R = number of photons required by a grain for developability
- μ = $AE = N\lambda$ = number of photons incident on a cell area A
- η = increment detectivity
- η^2 = quantum efficiency
- σ = standard deviation

To these we now add:

- $\Delta\mu_{ne}$ = noise-equivalent energy
- C_{ne} = noise-equivalent contrast
- $\sigma_A(D)$ = standard deviation in density measured with scanning aperture of area A

The defining relations are:

$$\Delta\mu_{ne} = \frac{\sigma(n)}{df(\lambda)/d\lambda} = \frac{N\sigma(n/N)}{d(n/N)/d\lambda} = \frac{A\sigma_A(D)}{dD/dE} \quad (1)$$

$$C_{ne} = \Delta\mu_{ne}/\mu \quad (2)$$

$$\eta^2 = \mu/(\Delta\mu_{ne})^2 \quad (3)$$

Therefore:

$$\Delta\mu_{ne} = (\mu/\eta^2)^{1/2} = A^{1/2}(E/\eta^2)^{+1/2} \quad (4)$$

$$C_{ne} = (\mu\eta^2)^{-1/2} = A^{-1/2}(E\eta^2)^{-1/2} \quad (5)$$

Written in this manner, the formulas show clearly that both the noise-equivalent energy and the noise-equivalent contrast depend not only on the magnitude of the quantum efficiency η^2, but on the exposure level E at which this quantum efficiency is achieved and the area A of the detecting surface or cell.

For idealized photographic detectors, we can compute η^2 from a knowledge of the number of photons R required for developability, the equations being (Eq. (17), Ref. 1)

$$\eta^2 = \lambda[f'_R(\lambda)]^2/f_R(\lambda)\cdot[1 - f_R(\lambda)] \quad (6)$$

with

$$f_R(\lambda) = 1 - e^{-\lambda}[1 + \lambda + \ldots + \lambda^{R-1}/(R-1)!] \quad (7)$$

The resulting curves for $R = 1, 2, 3, 4$, and 10 are shown by the solid lines in Fig. 1. The noise-equivalent energy and noise-equivalent contrast corresponding to these values of R are shown in Figs. 2 and 3, respectively. In making the calculations, the cell area A was taken to be unity, i.e., one grain area.

It is apparent from Fig. 2 that for all values of R of 3 or greater, the noise-equivalent energy is di-

Communication No. 2151 from the Kodak Research Laboratories. Received 8 February 1961.

1. H. J. Zweig, *J. Opt. Soc. Am.*, **51**: 310 (1961).

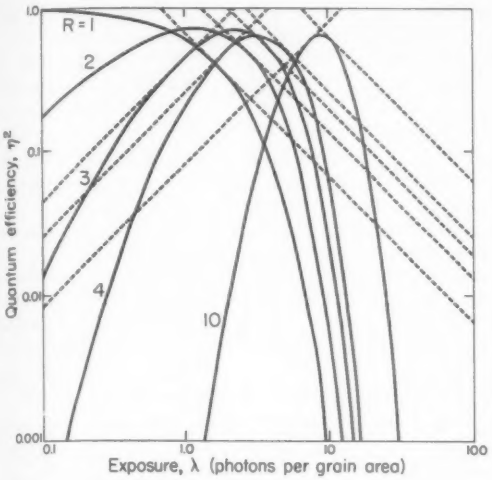

Fig. 1. Quantum efficiency as a function of exposure for detectors requiring R (shown on curves) photons for developability. The broken curves are straight lines having slopes of $+1$ or -1.

minished by a certain pre-exposure. This means that the minimum energy detectable with a given detector is achieved by using a pre-exposure. In fact, to determine the optimum pre-exposure, i.e., the point on the curve where $d\Delta\mu_{ne}/d\lambda = 0$, we can use Eq. (4) and by differentiation obtain:

$$0 = \frac{d\,\Delta\mu_{ne}}{d\lambda} \approx \frac{d}{d\lambda}\left[\frac{\lambda}{\eta^2(\lambda)}\right]^{1/2}$$

$$= \frac{1}{2}\left[\frac{\lambda}{\eta^2(\lambda)}\right]^{-1/2}\left[\frac{1}{\eta^2(\lambda)} - \frac{\lambda}{[\eta^2(\lambda)]^2}\cdot\frac{d\eta^2}{d\lambda}\right] \quad (8)$$

so that

$$\frac{d\eta^2}{d\lambda} = \frac{\eta^2}{\lambda} \quad (9)$$

or

$$\frac{d\,\log\,\eta^2}{d\,\log\,\lambda} = +1. \quad (10)$$

Thus the minimum detectable increment occurs at the pre-exposure at which the tangent to a curve of Fig. 1 has a slope of $+1$. This result was obtained also by R. C. Jones,[2] using a somewhat indirect geometrical argument. A similar argument using Eq. (5) shows that the minimum detectable contrast is obtained for

$$\frac{d\,\log\,\eta^2}{d\,\log\,\lambda} = -1. \quad (11)$$

It is clear from Figs. 1 and 3 that, to detect the minimum contrast, a pre-exposure is necessary, even when $R = 1$ or $R = 2$. However, it is not usually necessary to use pre-exposure to increase contrast detectivity. Because C_{ne} is inversely proportional to the square root of the detecting area A, it is only necessary to increase the image size in order to reduce the detectable contrast to any desired value. On the other hand, $\Delta\mu_{ne}$ is directly proportional to $A^{1/2}$, so that it is necessary to shrink the image area as far as possible to achieve the optimum energy detectivity. Since there is a limit to this shrinkage, imposed by the spread function of the detector or the detecting system, the value of $\Delta\mu_{ne}$ cannot be made arbitrarily small but has a minimum corresponding

2. R. C. Jones, in *Advances in Electronics and Electron Physics*, L. Marton, ed. (Academic Press, Inc., New York, 1959), Vol. XI, pp. 87 ff.

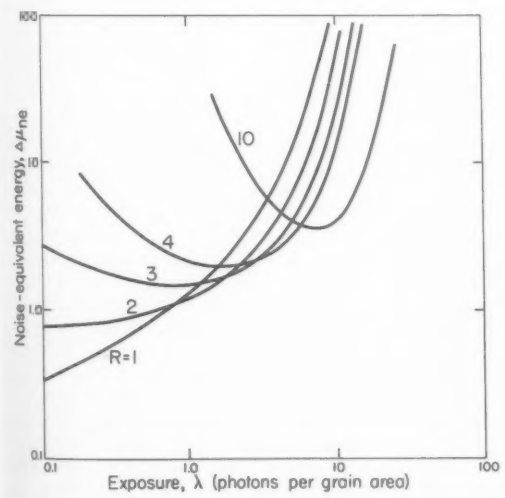

Fig. 2. Noise-equivalent energy as a function of exposure for detectors requiring R (shown on curves) photons for developability.

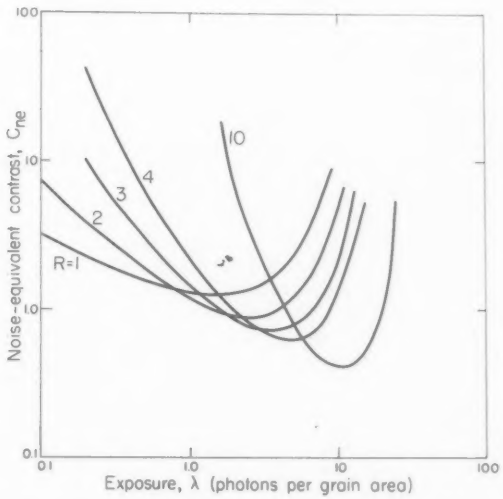

Fig. 3. Noise-equivalent contrast as a function of exposure for detectors requiring R (shown on curves) photons for developability.

to A_s, the spread-function area. The term "informational sensitivity," I, has been introduced[3] to denote the quantity

$$I = 1/\Delta_{ne}(\min) = A_s^{-1/2}[E/\eta^2]^{-1/2} \qquad (12)$$

and to serve as a measure for comparing the detecting ability of photographic emulsions.

Pictorial photography demands a compromise among mutually inconsistent requirements. These are:

1. A latitude of at least 100:1 in exposure must be provided so that detail will be visible in both shadow and highlight regions.
2. The detectable contrast should be as small as possible for a given detail size and should be uniform throughout the region of background illumination.
3. The exposure time required to lead to the detectivity of a given contrast at the minimum background exposure should be a minimum.

Using Eq. (5) with C_{ne} constant and taking the logarithm, we find

$$\log C_{ne} = -1/2 \log \mu - 1/2 \log \eta^2 \qquad (13)$$

or

$$\log \eta^2 = -\log \lambda + \text{const.} \qquad (14)$$

Using this equation in the differential equation (6), together with boundary conditions $\lambda_{min} = 0.5$, $\lambda_{max} = 50$ arising from the latitude requirements, and solving the differential equation, we obtain the results shown in Fig. 4. As is also apparent from Eq. (14), the given requirements lead to a linear curve of log η^2 vs. log λ which has a slope of -1. Equation (11) shows that such a curve shape gives the minimum possible uniform noise-equivalent contrast, which, under the conditions specified, is $\sqrt{2}$ when A is equal to one grain area. The noise-equivalent energy increment $\Delta\mu_{ne}$ that is detectable in the range between $\lambda_{min} = 0.5$ and $\lambda_{max} = 50$ is shown as a broken line. Its minimum value for $A = 1$ is $1/\sqrt{2}$ at $\lambda = 0.5$ or about 35 photons in a square cell, 50 grain diameters on a side.

These figures are obtained merely from the defining relations (5) and (6) and do not include the effects of the statistical fluctuations of the number of grains per unit area, nor of their sizes and their quantum requirements R. From Fig. 2 it is apparent that not even a one-photon detector has a noise-equivalent energy as low as $1/\sqrt{2}$ at $\lambda = 0.5$ nor (as can be seen from Fig. 3) can a one-photon detector maintain a noise-equivalent contrast detectivity of $\sqrt{2}$ over a latitude of more than 4:1. It follows that the curve shapes and the magnitude of Fig. 4 are not obtainable by even an ideal photographic type of detector. To achieve a latitude of 100, along with a quantum-efficiency curve as in Fig. 4, one could select a judicious proportion of R-photon grains to match the curve in the region of $\lambda = 5$ to $\lambda = 500$. This would lead to a maximum achievable quantum efficiency of between 5% and 10% at $\lambda = 5.0$ and a curve having the shape sketched in Fig. 5.

Results on Some Experimental Emulsions

In order to determine the effect of various chemical sensitizers on the quantum efficiency of a wide range of black-and-white emulsions, some special emulsion coatings were prepared in which each of four different sensitizers was used with each of four emulsions of different grain sizes. The complete experiment also involved mixtures of these as well as develop-

3. H. J. Zweig, G. C. Higgins, and D. L. MacAdam, *J. Opt. Soc. Am.*, **48**: 926 (1958).

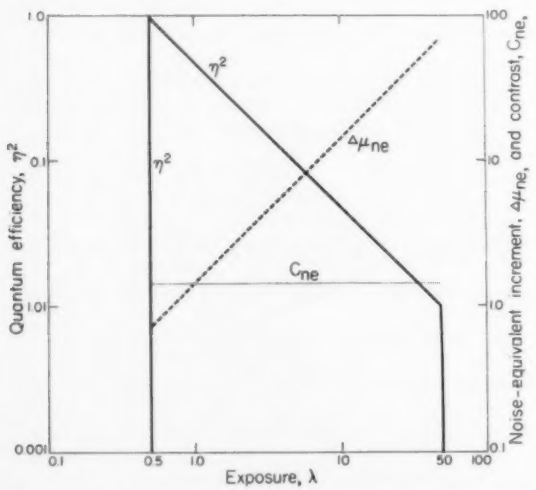

Fig. 4. Ideal curve of nonphotographic detector for a latitude of 100.

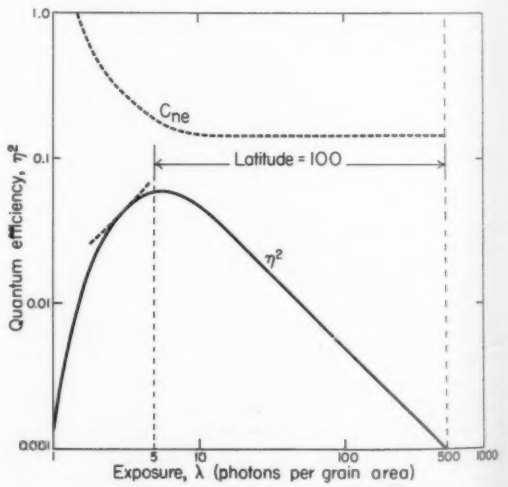

Fig. 5. Ideal curves of photographic detector for a latitude of 100 when $A = 1$.

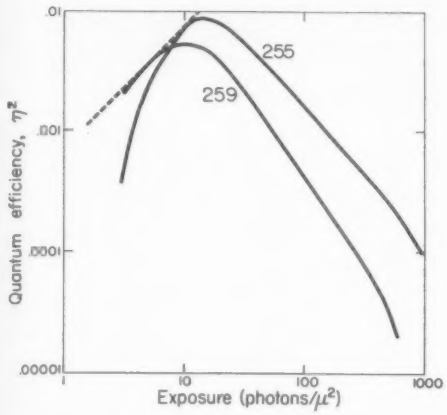

Fig. 6. Quantum efficiency as a function of exposure for two experimental emulsions differing in grain size when the wavelength of the exposing light is 430 mμ.

ment in two developers for two development times. Only the results of using the best sensitization on the two largest-grained emulsions with development for 8 min in Kodak Developer SD-28 will be described here.

The emulsions were exposed through a narrow-band filter (Kodak Wratten Filters No. 36 + 47B) to approximately monochromatic light of 430-mμ wavelength. The exposure time was $^1/_5$ sec, which is near the optimum with respect to reciprocity failure, so that no correction for this factor appeared to be necessary. Development was for 8 min in Kodak Developer SD-28. The characteristic curves were obtained in absolute energy units. Granularity values were obtained by scanning steps of different density with an aperture 24 μ in diameter.

The quantum-efficiency curves for these two emulsions are plotted in smoothed form in Fig. 6. It can be seen that, although the finer-grained emulsion (255) has a higher quantum efficiency than the coarser-grained emulsion (259), the curves are located so that a single line of slope +1 can be laid down tangent to both curves. Since the minimum energy detectivity is determined by the location of such lines, the single line shown by these two emulsions indicates that they should be capable of detecting the same amount of energy *at their respective optimum pre-exposure levels*. For a spread function having a diameter of 15 μ, the minimum noise-equivalent energy for the coarser emulsion turns out to be about 400 photons. For the same size of spread function, the minimum noise-equivalent energy of the idealized emulsions shown in Fig. 5 is about 150 photons. From these facts, it can be concluded that improvements in actual emulsions should be sought either by decreasing the spread function or shortening the required latitude. An increase in informational sensitivity by a factor of only about 3 is to be had for the factor of 10 increase in η^2 that is still available. (The factor is 3 rather than 10 because all the quantities I, $\Delta\mu_{ne}$, and C_{ne} are proportional to the first power of the increment detectivity η and not to the square, which is the quantity appearing in the graphs.)

Figure 6 contains other interesting implications. A comparison of the curve for Emulsion 259 with the curves in Fig. 1 shows that this curve corresponds to the curve for $R = 4$ in the latter figure with respect to the steepness of the left-hand portion. Since the left-hand portions of the curves in Fig. 6 are generated by the most sensitive grains in these composite emulsions, that is, the grains for which R has the lowest value, we can infer that Emulsion 259 acts as though it were a composite of R = 4-, 5-, . . . photon detectors. Similarly, the curve for Emulsion 255 approximately corresponds to the curve of $R = 10$ in Fig. 1, from which we infer that this emulsion acts as though it were a composite of R = 10-, 11-, . . . photon detectors. Since Emulsion 255 has a higher quantum efficiency than the other, we may further infer that it contains a larger proportion of $R = 10$ grains than the other emulsion does of $R = 4$ grains.

In general, it should be possible to infer whether an arbitrary detector is a one-, two-, or three-, etc., quantum device by matching the left-hand portion of its quantum-efficiency curve to one of those in Fig. 1. Rose[4] has presented corresponding data for the eye. A comparison of his Fig. 6 with the curve of our Fig. 1 for $R = 1$ would lead to the conclusion that, after allowing for absorption, the underlying phenomenon in the case of the eye is that of a one-photon sensitive device.

Relation of Noise-Equivalent Energy and Contrast to Minimum Detectable Energy and Contrast

In order to determine the relationship between the abstract quantities $\Delta\mu_{ne}$ and C_{ne} and the amount of energy that is required to produce a detectable density difference, as well as to test the validity of the dependence of $\Delta\mu_{ne}$ and C_{ne} on detection area, the following experiment was devised:

A test object was prepared consisting optically of a square matrix of transparent circular disks on an opaque background. (Physically, it consisted of a plate in which holes were drilled.) The disks in a given column had the same diameter, the diameters in successive columns ranging from 65 μ to 5850 μ. The ratio between the diameters of the disks in successive columns was $\sqrt{2}$, the ratio between areas thus being 2. The arrangement can be seen from Fig. 7. Over this matrix were placed two neutral step tablets at right angles to each other so that the density increased by 0.3 (transmittance I decreased by 2×) in successive columns (where the disks in any one row increased in size) and by 0.15 in successive rows (where the disks in any one column had a constant size). By this means a test object was produced in which the total number of photons per second through each disk in a given row was the same and the number for successive rows increased

4. A. Rose, in *Advances in Electronics and Electron Physics*, L. Marton, ed. (Academic Press, Inc., New York, 1948), Vol. I, pp. 146 ff.

$\sqrt{\text{area}}$ (μ) =	175	250	350	500	700	1000	1400...
Relative area =	1	2	4	8	16	32	64....
Relative trans. =	1	1/2	1/4	1/8	1/16	1/32	1/64...

Relative trans.	Total photons						
1	350 °	○					
$\sqrt{2}$	500 °	○	○				
2	700 °	○	○	○			
$2\sqrt{2}$	1,000 °	○	○	○	○		
4	1,400 °	○	○	○	○	○	
$4\sqrt{2}$	2,000 °	○	○	○	○	○	○
⋮	⋮						

Fig. 7. Scheme of experimental test of theory.

by $\sqrt{2}$. This means that the total number of photons per square micron per second along 45° diagonals *increased* by $\sqrt{2}$ while $\sqrt{A}$ *decreased* by $\sqrt{2}$. Therefore, by Eq. (12), if $\Delta\mu_{ne}$ is directly proportional to $\sqrt{A}$, then the visibility contour of the imaged test pattern should be along the 45° diagonal. For example, if there are 2000 photons through each of the holes in the sixth row, 1400 through each hole in the fifth row, 1000 through each hole in the fourth row, etc., and if 2000 photons produce a detectable image when incident on a hole

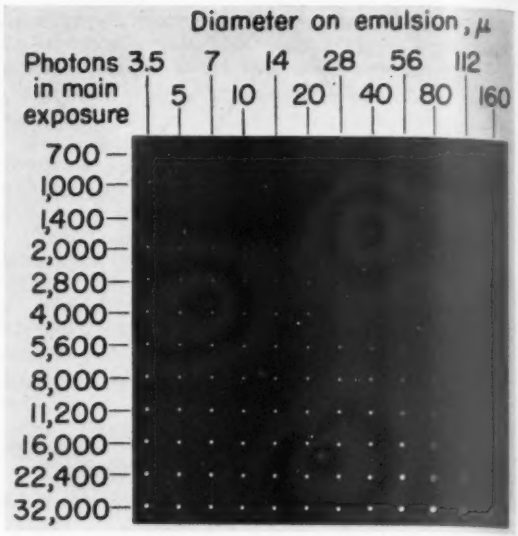

Fig. 9. Experimental results with Emulsion 259. Pre-exposure, 10 photons/μ^2.

(No. 7, say) with a relative area of 64, then according to the theory, 1400 photons should be detectable when incident on a hole (No. 6) whose relative area is 32 and 1000 photons when incident on a hole (No. 5) of area 16, etc. The limit is set by the spread function of the system, and if this has, say, a relative area of 4, then the hole in this column that is in the row containing three dots should be the last one visible since in any further rows there would only be

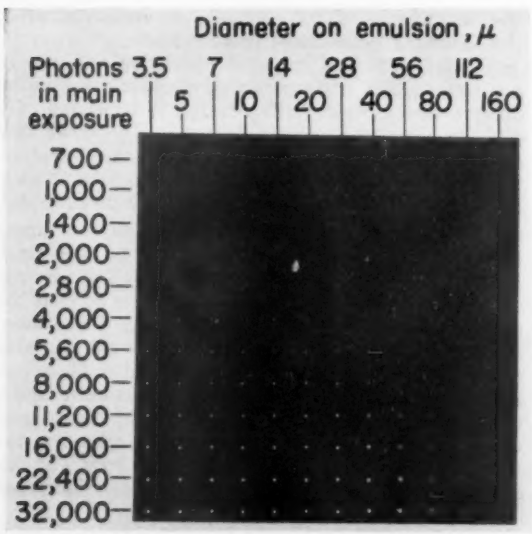

Fig. 8. Experimental results with Emulsion 259 (coarser-grained). Pre-exposure, 1.0 photon/μ^2.

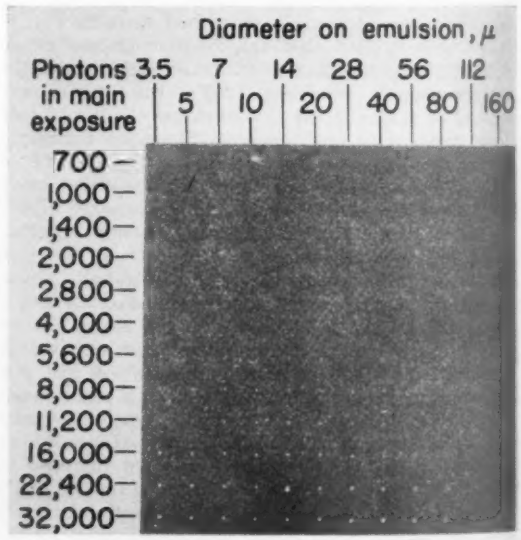

Fig. 10. Experimental results with Emulsion 259. Pre-exposure, 100 photons/μ^2.

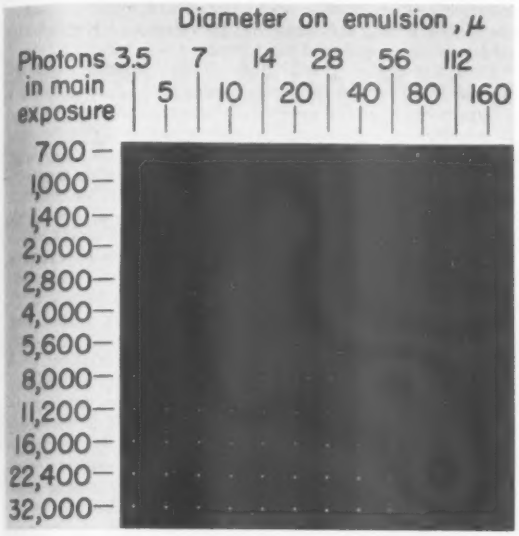

Fig. 11. Experimental results with Emulsion 255. Pre-exposure, 1.0 photon/μ^2.

sufficient energy to make visible the holes of area less than 4.

Figures 8–13 show the results of photographing the test object just described on the two emulsions for which data were presented in the previous section. Again filters were used to produce radiation at 430 mμ. Development was in SD-28 at 68°F for 8 min. The test object was photographed at 20× reduction and the negative was enlarged 20× in printing. Figures 8–10 show the results on the emulsion with the larger grain size and pre-exposures of 1.0, 10, and 100 photons/μ^2, respectively.

In the original prints, 9, 10, and 7 rows of dots were visible, representing approximately 2000, 1400, and 4000 photons respectively. These are the minimum numbers of photons (at 430 mμ) producing a *visible* signal on one of the fastest emulsions available today.

Figures 11–13 show similar results for the emulsion with a somewhat smaller grain size. In this case, the numbers of rows visible with 1.0, 10, and 100 photons/μ^2 pre-exposure are respectively 10, 11, and 9, representing 1400, 1000, and 2000 photons. These results are in accordance with those obtained from the quantum-efficiency curves of these emulsions since these show that in the region beyond a pre-exposure of 10 photons/μ^2 the finer-grained emulsion should be the better energy detector. Below this pre-exposure, the shape of the curves is too uncertain to allow any accurate inference to be drawn.

Conclusions

The results of this investigation can be interpreted as indicating that the concepts of quantum efficiency, noise-equivalent energy, noise-equivalent contrast, and informational sensitivity all play important roles in appraising the detecting ability of photographic materials and that these concepts can be directly related to what can be detected by a human observer.

The conclusions that can be drawn from this experiment are:

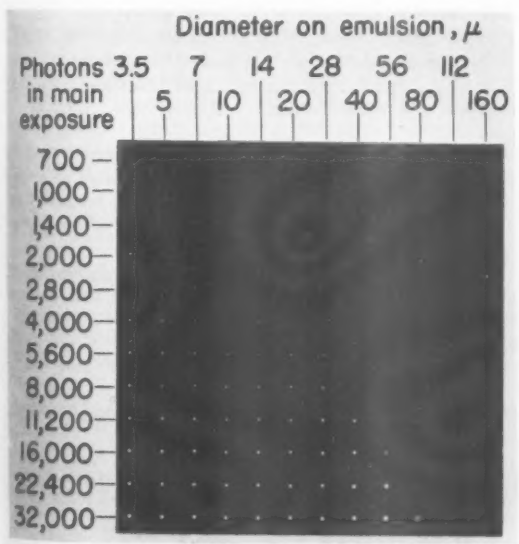

Fig. 12. Experimental results with Emulsion 255. Pre-exposure, 10 photons/μ^2.

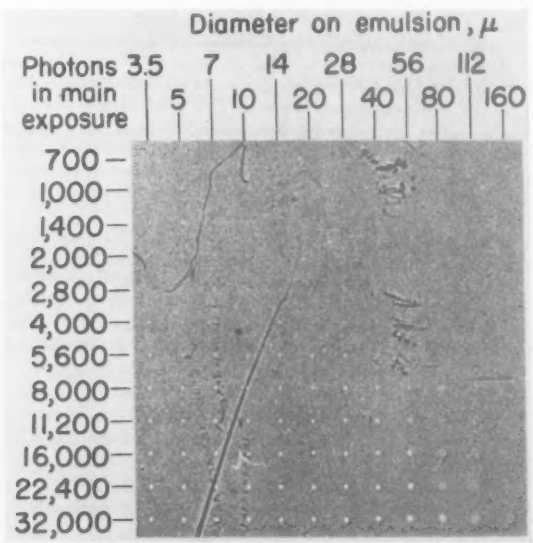

Fig. 13. Experimental results with Emulsion 255. Pre-exposure, 100 photons/μ^2.

1. The ratio of minimum-detectable energy to noise-equivalent energy is of the order of 4 or 5 when $\Delta\mu_{ne}$ is computed at optimum pre-exposure for a circular area having a diameter of 15 μ (see *Appendix*, below).
2. The diameter of the spread function of the coarser emulsion used (including that of the imaging system) is about 14 μ (corresponding to the fifth column of the test object) and that of the finer about 10 μ (corresponding to the fourth column).
3. The dependence of detecting ability on the area of the target is confirmed by the fact that disappearance contours are approximately on a 45° diagonal (for spot sizes smaller than about 80 μ in diameter).
4. By comparing the quantum-efficiency curves of a composite emulsion with the corresponding theoretical curves of emulsions requiring a uniform number of quanta per grain for developability, it is possible to estimate the number of quanta required for developability by the most sensitive component of the composite emulsion.

APPENDIX

It is often assumed that a signal is present if the observed density (or other measurement made) differs from the average or expected value of $\pm 2\sigma$. The assumption is that, for a normal distribution of readings about an average value, the probability is about 5% that by chance a single reading will fall outside the limits of $\pm 2\sigma$. If only an increase in density above the background is to be called a signal, there is thus about a 2.5% probability that a reading of $\overline{D} + 2\sigma$ is due to chance. If only one observation is taken, it would seem reasonable, therefore, to call such an observation real and to assume that a signal of this order of magnitude should be detectable.

In the case of a photographic film, however, this is unfortunately not the way that information is extracted. Usually we look at a considerable area of the film and try to pick out a place at which a signal might be present. If the signal covers an area of, say, 2500 μ^2 and we scrutinize a film 1 cm sq, we are in effect measuring about 4×10^4 distinct signal areas. The probability that in one or more of these the density will exceed $\overline{D} + 2\sigma$ is close to unity. In fact, on the average, we expect that there will be about 10 such areas by chance. We should not, therefore, expect to detect a signal of this order of magnitude in such a case.

What is really wanted in such a case is a level $\overline{D} + k\sigma$ at which there is only a 2.5% probability that *any* of the 400 observations will exceed this level by chance. If we choose a probability level of $2.5/4 \times 10^4 \approx 6 \times 10^{-4}\%$, we shall have such a point (approximately). This corresponds to a value of k of about 5. It should be noted, however, that a slight departure from normality can exert a strong influence on this value, and it should be used only as an order of magnitude.

That the value of k is difficult to determine exactly can be seen from the following argument:

Supposing that the presence or absence of a signal is to be inferred by inspecting three different areas in each of which the signal could be present. Suppose further that the magnitude of the density increment decided upon to announce the presence of a signal is such that 10% of the time it would occur by chance in any one location. This means that the probability that one or more of the three areas will give a spurious indication of the presence of a signal is one minus the probability that *none* of them will give such an indication, that is, it is $1 - (0.90)^3 = 0.27$. If instead of three areas we looked at six areas, this probability would increase to about 0.50; that is to say, we would infer the presence of a signal in 50% of such experiments when actually there was no signal present. As the number of areas examined increases to beyond 100, it becomes virtually certain that we shall erroneously conclude that some area contains a signal according to the above criterion. Only by tightening our requirements on the increment required shall we avoid such error. For 500 areas, the following probabilities of erroneous signals in isolated areas will result in the over-all levels of error tabulated:

Probability of spurious signal	Probability of deciding that a signal is present when in fact there is none (in 500 independent areas)
0.01	0.9938
.001	.394
.0001	.050
.00001	.005

If the random noise is normally distributed into the "tails" of the normal probability density function (and that this would happen is certainly questionable), these levels of probability correspond to the following values of k:

Probability	k
0.01	2.58
.001	3.29
.0001	3.89
.00001	4.41

These values of k need to be increased considerably if the distribution is heavy in the tails. On this basis a value of $k = 5$ ought perhaps to be considered the minimum required for near error-free detection.

PHOTOGRAPHIC SCIENCE AND ENGINEERING
Volume 5, Number 3, May-June 1961

The Capillary Chamber Process for Ultrarapid Negative Processing

KARL-HEINZ LOHSE AND MARVIN B. SKOLNIK, *Aeronutronic, A Division of Ford Motor Company, Newport Beach, California*

The special requirements of a rapid access display system led to the development of an ultrarapid negative processing technique. The design of the capillary chamber process is described and the high image quality obtainable by this method is discussed. The method uses minimum volumes of solutions for single-frame development of 35mm black-and-white films within 5-sec processing and drying time. Various applications are described to illustrate the flexibility of the system. Since the technique is insensitive to gravity and attitude, it is useful in space applications.

The capillary chamber process was designed to meet the unusual quality requirements of a particular rapid access optical display system. Its development was initiated after other techniques failed to produce the desired image characteristics in the short processing time available.

The display system called for a technique capable of producing fully processed line images within 5 sec. The lines had to appear on an exceptionally clear background of less than 0.06 density. The required density difference was 1.5 to 2.0, and the image resolution had to be at least 35 lines/mm.

The capillary chamber process produces such high quality with economic liquid consumption. Other features of the process are that it is a low-pressure system and that the liquid consumption is not dependent on processing time. Since nothing but the processing solutions and air contact the image area, images are completely free from scratches.

Although considerable work has been reported on thin chamber processes, it is felt that the capillary chamber provides significant advances and advantages in this field.[1-4] It is the purpose of this paper to describe the basic process and to report on the solutions to associated problems.

The Capillary Chamber

The heart of the process is the capillary processing chamber which permits the contact of small amounts of processing liquids with the emulsion of the film. Figure 1 illustrates the capillary chamber. A narrow space is provided between the film emulsion and the processing platen. After the film is located over the sealing frame it is held tightly against the seal by means of a pressure plate. Through the center bore of the processing platen metered volumes of processing solutions are brought into the capillary chamber. The liquid could freely overflow the platen but is held within the chamber by capillary forces.

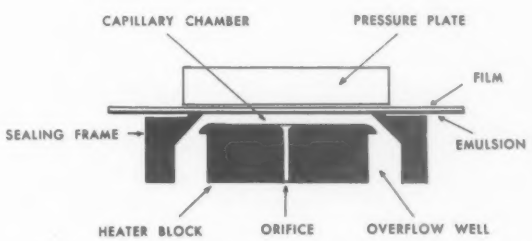

Fig. 1. Cross-section diagram of capillary chamber.

For reasons which we shall discuss later, the chamber dimensions are critical and must be optimized. Good processing results have been obtained using a chamber depth from 0.010 to 0.030 in. At present, a nearly square frame of 1.16 by 1.06 in. is in use; however, equal success has been attained with a more rectangular frame of 1.16 by 0.92 in.

The volume of processing liquid required to fill the chamber ranges from 0.3 to 0.5 cc, depending on the frame size. The figures given apply to the processing of a 35mm double frame. Since the processing solutions contact the emulsion side of the film only, this process is well suited to ultrarapid processing.

Because of the necessity for maintaining an extremely precise parallel separation between the film and the processing platen, a sealing frame made of noncompressible material was used.

Presented at the SPSE Rapid Processing Symposium, Washington, D.C., 14 October 1960. Received 16 November 1960.

1. F. M. Brown, L. L. Blackmer, and C. J. Kunz, *J. Franklin Inst.*, **242:** 203 (1946).
2. C. M. Tuttle and C. J. Kunz, U.S. Patent 2,472,007, July 12, 1949.
3. C. M. Tuttle and P. H. Stafford, U.S. Patent 2,582,182, Jan. 8, 1952.
4. E. J. Mainwald, Jr., U.S. Patent 2,587,350, Feb. 26, 1952.

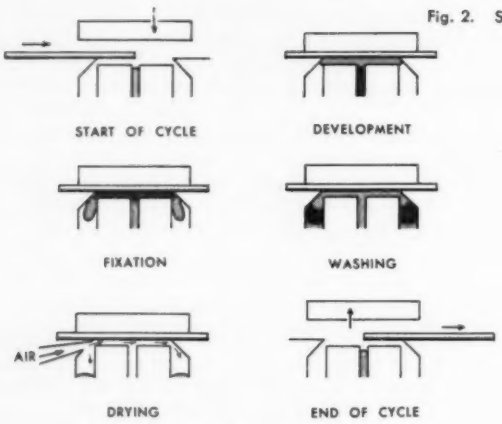

Fig. 2. Schematic diagram of processing cycle.

A typical processing cycle is shown schematically in Fig. 2. After the development is completed, the fixing solution is introduced into the capillary chamber through the center bore. This pushes the developer into the overflow and then into the waste container. Any intermixture of the two liquids is counteracted by the strength of the fixing solution, which not only rapidly stops the development but also completes the fixation of the image in the presence of traces of the developing solution. A wash solution follows the fixing solution after fixation is completed. Four to eight times the chamber volume will yield sufficient washing. The processing cycle is completed by drying the emulsion with a hot,

Fig. 3 (below). Example of image processed in chamber (full frame shown).

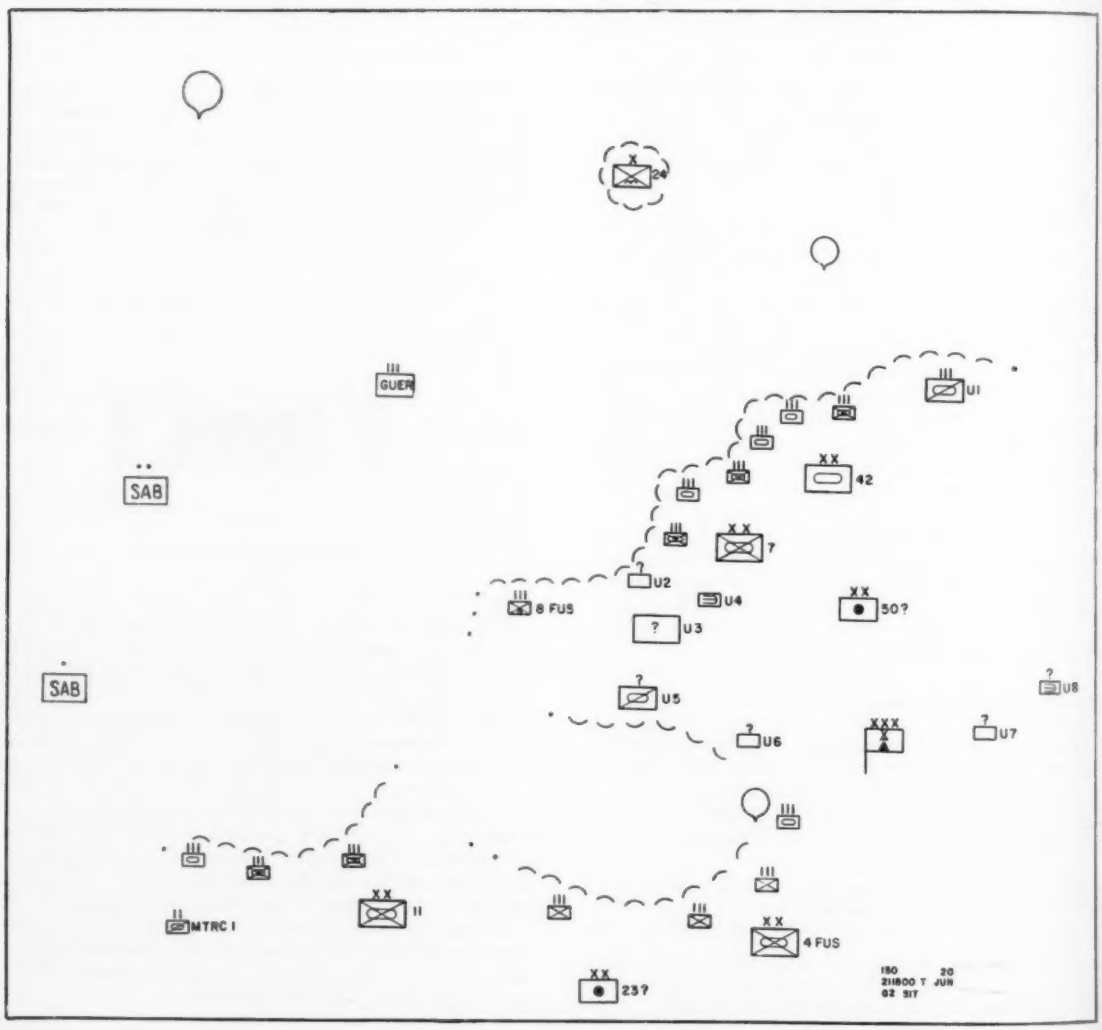

high-velocity airstream which enters the chamber from the side and is directed evenly over the film surface. The drying air, which escapes through the waste spacing into the vented waste container, cleans and dries the chamber as well as the film.

Processing

The emulsion of the film and the desired image characteristics determine the selection of processing solutions. The capillary chamber process permits great flexibility in this area, for any wet process can be used with this technique. Monobath processing yields acceptable results, although in certain applications, such as the one mentioned above where image requirements of high contrast combined with low fog level were desired, better results are attainable if development and fixation are separated.

While this processing technique is not limited to the use of certain types of emulsions, it has been noted that for ultrarapid processing those emulsions especially designed by the manufacturers for rapid processing applications give superior results. For rapid cathode-ray image transfer in conjunction with this process, Ansco Hyscan, Ilford BY, and Kodak Types 264 and 265 films are recommended.

The capability of the capillary chamber process may be illustrated by the following typical processing cycle:

Process	Time (sec)
Development	1.5
Fixation	0.5
Washing	1.0
Drying	2.0

Figure 3 shows an example of an image obtained using this program. The corresponding characteristic curve is given in Fig. 4.

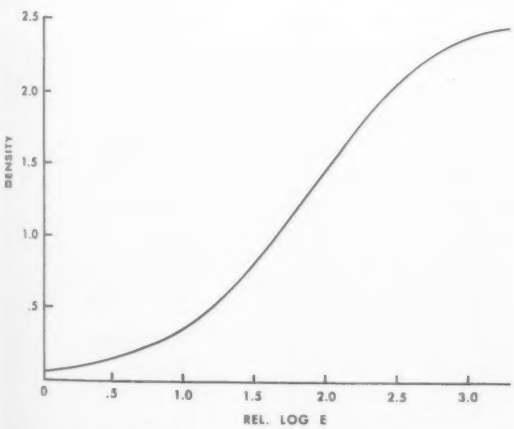

Fig. 4. Characteristic curve of Ilford BY processed in capillary chamber.

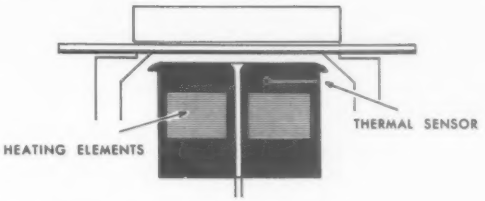

Fig. 5. Cross-section diagram of heater block.

Temperature Control

The processing platen, which is part of the heater block (Fig. 5), contains heating elements and a temperature sensing probe. The preselected processing temperature is automatically controlled and is maintained within $\pm 0.5°F$. The processing temperature can be set for any point from ambient to 130°F. Although high-temperature processing is not necessarily needed for ultrarapid processing, it has been found that, at varying ambient conditions, elevated processing temperatures can be maintained more easily.

Because of the relatively large mass of the heater block in proportion to the small liquid volumes, the maintaining of uniform temperature presents no problem. Each processing volume of the liquids is preheated inside the block prior to entering the capillary chamber, and therefore neither the storage containers nor the connecting tubings require preheating.

The drying air is preheated in a storage container or by means of a duct heater. Air temperatures up to 250°F are practical for ultrarapid drying. The permissible temperature depends on the selected film material and the flow pattern of the air.

Liquid Metering and Valving

Several different arrangements of liquid metering and valving have been designed. The final choice of

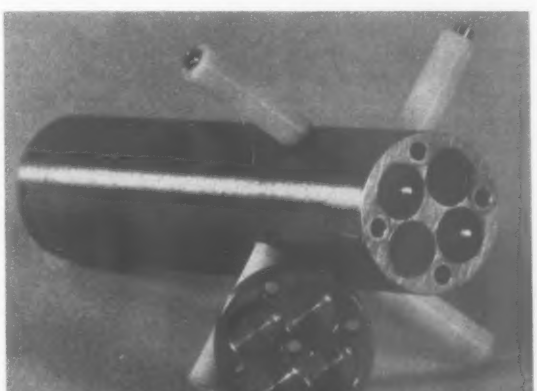

Fig. 6. Four-solution valve.

preferred method depends on the application. While all the methods described are equally adaptable to the process, there are certain features of each method which make it more suitable to a specific equipment requirement.

For multibath processing, contamination of the developer must be prevented. This is accomplished by installing a suitable valve near the liquid entrance of the capillary chamber. Figure 6 shows one such valve which can handle four different solutions. Each of the liquids is pumped into a separate compartment and is contained there by a spring-loaded check valve, to prevent its contamination by any of the other solutions, prior to its being channelled into the center orifice of the chamber.

Also acceptable is a rotating valve (Fig. 7) which has a conical shape in order to function properly at

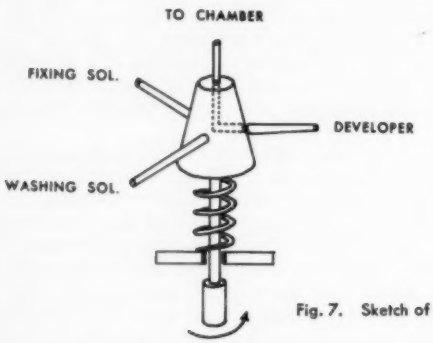

Fig. 7. Sketch of conical valve.

varied processing temperatures. The bores of the valve are slightly enlarged to insure the flow of liquids when the cone is displaced due to thermal expansion of the heater block. Spring loading of the valve prevents leakage. The rotating valve requires a solenoid or mechanical drive, whereas the four-solution valve functions without external control.

Since the capillary chamber permits free overflow of the liquids, accurate metering of the processing solutions is not critical as long as the minimum amount required to fill the chamber is provided. For certain applications it is, therefore, sufficient to open and close solenoid-operated valves for a given duration. However, if the liquid consumption is critical, a more precise method of metering may be achieved with cam-operated adjustable metering pumps. Depending on the arrangement of the various equipment components, one may choose between gravity liquid feed or low-pressurized storage containers.

Image Quality

Since image quality is a relative matter, depending solely on the desired result, we confine our statements concerning this topic to specific observations. The results of numerous tests have shown that the image quality of films processed in the capillary chamber is equivalent to the quality obtained using conventional processing techniques. Losses of film resolution were not noted. Fine-line resolution in excess of 60 lines/mm was measured. This does not imply that this is the attainable limit. The indicated resolution was well beyond the requirements of a specific application, and further studies were discontinued.

As mentioned above, the capillary chamber process is particularly adaptable to high-contrast line processing. Preliminary tests have indicated that continuous-tone processing is also feasible. The technique will permit reversal processing if modifications are made in the metering and valving components. Images processed by this method can withstand immediately after processing prolonged exposure to highly actinic light sources, and the permanency of the images is estimated to be about one year. Samples kept in the laboratory for five months have shown no signs of staining, image deterioration, or increase of fog level.

The pressure plate contains vacuum grooves which assure the flatness of the film during processing. This vacuum technique prevents dimensional distortion of the film.

Critical Design Variables

A breadboard (Fig. 8) permitting various mechanical adjustments was used to define critical variables of this technique.

One of the major difficulties of the design phase was air entrapment in the capillary space, but extensive tests proved that after adjusting the chamber size and/or altering the viscosity of the developer, air entrapment could be avoided. Furthermore, extension of the capillary space beyond the frame line prevented the air from collecting within the image area. It was also noted that the flow rate of the liquids entering the capillary chamber had to be optimized, for any sudden injection of the liquids led to the formation of air bubbles and caused serious image defects at the center of the frame. A gentle

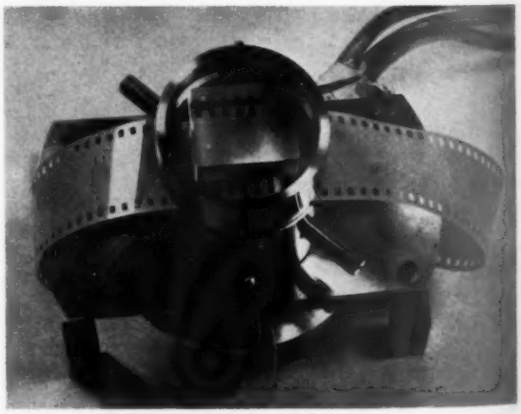

Fig. 8. Experimental breadboard.

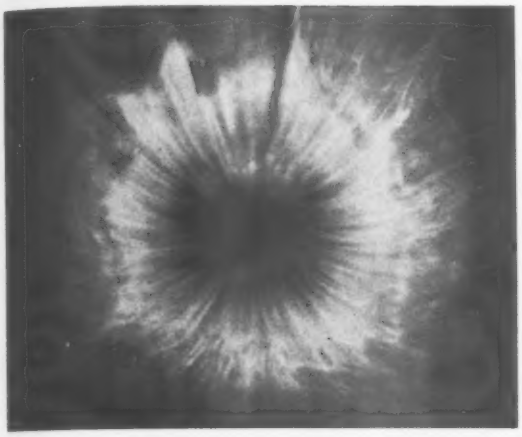

Fig. 9. Image defect due to extreme agitation above center orifice of processing platen (full frame shown).

introduction of the solutions, somewhat simulating the normal rate of liquid flow in the capillary, prevented such disturbances. A slight overpressure to speed up the filling of the chamber could be tolerated.

The displacement of the developer by the fixing solution presented another problem. At the interface, the two liquids intermixed and caused localized fog in the emulsion. If not properly counteracted, such mixture would raise the fog level, but experimentation showed that this effect could be avoided by adjusting the flow rate of the fixing solution.

Since all processing solutions enter the chamber at the same center bore, uniform processing times prevail over the image area. The image, therefore, shows no evidence of uneven development due to time variation.

Uneven development did result, however, from the extreme agitation which occurred at the center of our capillary chamber (see Fig. 9). Image defects of this type can be avoided by adjusting the activity of the developing solution, adjusting the flow rate, and/or using one of several means of agitation. In the particular rapid access optical display system on which we were working, agitation was not necessarily required. This was found to be an unexpected feature of the capillary chamber process.

The highly corrosive processing solutions demand the use of corrosion-resistant materials for all exposed parts, and materials must be carefully chosen for other system components which may be exposed to vapors.

Design Variations

Some design variations which extend the range of applications for this processing technique include the method described below. This method yields uniform development for continuous tone.

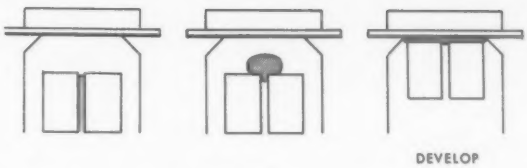

Fig. 10. Schematic diagram of moving processing platen.

One alternate method is based on a movable processing platen. Figure 10 illustrates the development phase. A metered volume of developer is introduced into the capillary chamber while the processing platen is in the low position. (Since the drop of developer must remain at the center of the platen, this technique requires leveling the processor.) When the platen is raised, thus compressing the chamber to capillary size, a uniform liquid contact is established with the emulsion. It may be necessary to increase the surface tension of certain developers by adding a thickening agent.

Applications

The capillary chamber process is flexible and is adaptable to a variety of applications although foremost in importance are the rapid access display systems.

The process is well suited to compact design. The principles of liquid displacement and the utilization of capillary forces permit the use of the technique in a gravitation-free environment. Since the processing technique is not influenced by gravity, two capillary chambers facing each other can be used to process radiographic film which is coated on both sides.

Although the basic design was optimized for "one-frame-at-a-time" processing of film chips, the technique can be adapted to "frame-by-frame" processing of continuous lengths of film. The arrangement of several capillary chambers at the periphery of a processing wheel permits such processing. The maximum framing rate under these conditions is presently limited to about 1 frame/sec.

Acknowledgments

The capillary chamber process was developed under Government Contract No. DA-36-039-SC-75084 with the U.S. Army Signal Research and Development Laboratory, Fort Monmouth, N.J.

We wish to express our thanks to the many members of the Ford-Aeronutronic Display Department who have made valuable suggestions, especially H. Weiss, who encouraged this project from its inception, E. Moeckel, R. Robinson, and H. Schendel, who solved many of the mechanical problems, and to the members of the staff of the Model Shop who fabricated the precision parts.

PHOTOGRAPHIC SCIENCE AND ENGINEERING
Volume 5, Number 3, May-June 1961

Characteristics of Physical Development with Developer Solutions Containing Thiosulfate–Silver Complex Ions

R. M. Cole and R. B. Pontius, *Research Laboratories, Eastman Kodak Company, Rochester, N.Y.*

Effectively stable physical developers containing silver ion supplied by dissociation of a thiosulfate–silver complex have been used to study the kinetics of pure physical development onto colloidal silver nuclei dispersed in a plain gelatin coating. A comparison of physical development rates of two *p*-phenylenediamine-type developers with *p*-phenylenediamine itself and with a Metol–hydroquinone developer has been made. The effects of pH, silver-ion concentration, developer concentration, and the effect of buffer ion on the rate of physical development have been measured.

In order to investigate factors which affect physical development, particularly in regard to the kind and surface of nuclei, it is desirable first of all to make a preliminary study of the effects of "external" factors such as silver-ion concentration, pH, developer concentration, and buffer on the kinetics of physical development.

Many aspects of physical development have been studied in the past,[1–12]* and, in a previous paper,[13] measurements of the activation energy of physical development for a *p*-phenylenediamine-type developer were reported. Described in the present paper are some details of the effects of "external" factors on physical development by the color-developing agent CD-2 (the commercial designation of Kodak Color Developing Agent, 4-amino-N,N-diethyl-3-methylaniline monohydrochloride) and CD-3 (the commercial designation of Kodak Developing Agent, 4-amino-3-methyl-N-ethyl-N-(β-methylsulfonamidoethyl)aniline sesquisulfate monohydrate). It is desirable also to compare these two developers with each other, with simple *p*-phenylenediamine, and with a Metol–hydroquinone (MQ) developer so as to show the relative strength of each, both when used as pure physical developers and when their relative solvent actions for silver halide come into play.

Method

Physical developer solutions are characteristically unstable. The tendency towards spontaneous precipitation of silver is increased by increase in developer potential, itself a function of pH, and by increase in the silver-ion concentration.[2] In the study of the kinetics of physical development under conditions where the concentration of silver ion must be known, physical developer solutions ought to be stable over a period of several hours.§ Physical developers which are stable over a period of 2 hr may be prepared by use of the thiosulfate–silver complex ion, $Ag(S_2O_3)_2^{---}$. The stability constant for this complex has been determined by Chateau, Hervier, and Pouradier[16] as a function of temperature. In direct physical development, the silver ion is the species reduced, not the silver complex.[3,13] The concentration of silver ion can be fixed by adjusting the concentration of excess thiosulfate in equilibrium with the silver ion and the complex. The complex provides a reserve of silver ion by dissociation. The method of preparing the developer solutions was described in the previous paper.[13]

The materials used for the physical-development experiments were plain gelatin coatings containing 15 mg of Carey-Lea-type colloidal silver per square foot. Development was carried out with nitrogen-burst agitation in thermostated glass cylinders at 25°C. After development and washing, the samples were analyzed for silver content. The silver-ion concentrations in the developers were varied from 10^{-14} mole/liter to 10^{-12} mole/liter. One liter of a typical developer having 4×10^{-13} mole of silver ion in equilibrium with the complex was composed of: developing agent, 0.00516 mole; tribasic potassium phosphate, 0.13 mole; and 0.00359 mole of silver chloride which was dissolved first in a solution containing 0.025 mole of sodium thiosulfate. The pH was adjusted to 12.0 with a few drops of sulfuric acid.

In comparing the solvent action of developers, a coating was used containing 15 mg of Carey-Lea-type colloidal silver per square foot, dispersed in a fine-grain unhardened positive-type emulsion, similar to the type employed by James and Vanselow.[5] One liter of developer contained: 0.00516 mole of developing agent; 0.13 mole of tribasic potassium phosphate; 0.0084 mole of potassium bromide; and acid or base, as necessary, to give a pH of 12.0 at 25°C. Development was carried out without exposure at 25°C.

Comparison of Developing Agents

Three developers, CD-2, CD-3, and *p*-phenylenediamine, were compared as pure physical developers

Communication No. 2149 from the Kodak Research Laboratories. Presented at the Annual Conference, Binghamton, N.Y., 26 May 1961. Received 13 February 1961.

* References are listed at the end of the paper.

§ This problem of developer stability does not arise in the case of solution physical development, in which the nuclei are incorporated within the emulsion layer,[5] and in the case of diffusion transfer, in which the nuclei are incorporated in a layer adjacent to an emulsion layer,[4,14,15] since the silver ion results from solution of the halide and does not appear in the solution phase until development commences.

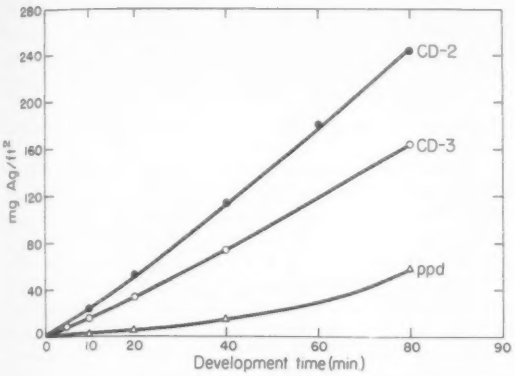

Fig. 1. Comparison of developing agents as pure physical developers at pH 12. Developer concentration, 0.00516 M. Silver-ion concentration, 4×10^{-13} M. ●, CD-2 as developing agent; ○, CD-3 as developing agent; and △, *p*-phenylenediamine as developing agent.

at equal molar concentrations, a pH of 12, and silver-ion concentration of 4×10^{-13} *M*. The rates of development of silver ion by these three developers are shown in Fig. 1, from which it appears, as was to be expected from the polarographic half-wave potentials,[17] that *p*-phenylenediamine is much the weakest of the three. An equivalent developer containing a mixture of Metol and hydroquinone developing agents could not be used at such a high pH and silver-ion concentration, since the conditions of developer stability were exceeded by the use of this more powerful developer combination. A comparison, however, was made with CD-3 developing agent at the milder condition of pH 11.0 and silver-ion concentration of 1×10^{-13} *M*, as shown in Fig. 2. The combination of Metol and hydroquinone gives a pure physical developer very much more powerful than that given by any of the three *p*-phenylenediamines used here.

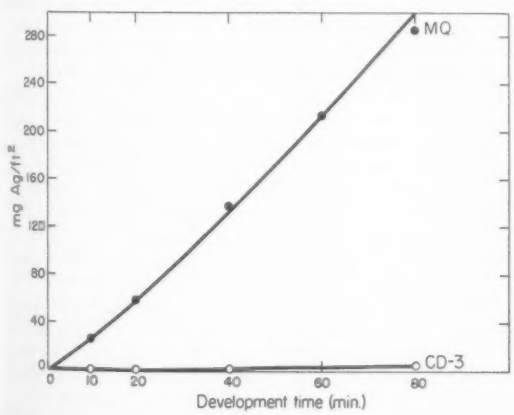

Fig. 2. Comparison of developing agents as pure physical developers at pH 11. Developer concentration, 0.00516 M. Silver-ion concentration, 1×10^{-13} M. ●, Metol-hydroquinone in equimolar combination as developing agents; ○, CD-3 as developing agent.

The rate of development by solution physical developers depends upon two factors, the solubilizing action of the developer on the silver halide and the activity of the developer in reducing silver ion. The results of this comparison are shown in Fig. 3. It is now seen that, although *p*-phenylenediamine is the weakest of the four as a pure physical developer, it is nearly the best when it acts simultaneously as a solvent. It is due to this solvent action that *p*-phenylenediamine has long had a reputation as a good physical developer.[11] The MQ developer, in spite of its powerful action in directly reducing silver ion, is not greatly better than *p*-phenylenediamine in solution physical development, from which one must conclude that it possesses very little solvent action. In the case illustrated in Fig. 3, the silver ion reduced by the MQ developer is probably provided by the solvent action of the 1 gram/liter of potassium bromide present. The substituted *p*-phenylenediamine CD-3, a weaker physical developer than CD-2, is a better solvent for silver halide than CD-2.

Kinetics of Physical Development

The rate of physical development by CD-2 and CD-3 in these experiments was found to vary as the $^1/_5$ power of the silver reduced,† when Carey-Lea-type colloidal silver was used as the source of nuclei. Essentially identical behavior was also found, however, in independent experiments with latent-image nuclei (postfixation physical development), and with filamentary silver used as nuclei (developed and fixed samples). The development-rate constant can be obtained conveniently by plotting $y^{4/5}$ against time,

† This behavior is not generally true for all *p*-phenylenediamine-type developing agents. When simple *p*-phenylenediamine was used in place of CD-2 or CD-3 in equivalent concentration, the rate of physical development was found to vary as the $^1/_2$ power of the silver reduced. It has been shown, however, that *p*-phenylenediamine behaves quite differently from CD-2 and CD-3 in regard to adsorption to silver.[18] This adsorptive behavior may, however, have no bearing on the case, since the MQ developers were found to follow the same kinetics as CD-2 and CD-3, and yet hydroquinone does not adsorb to silver.

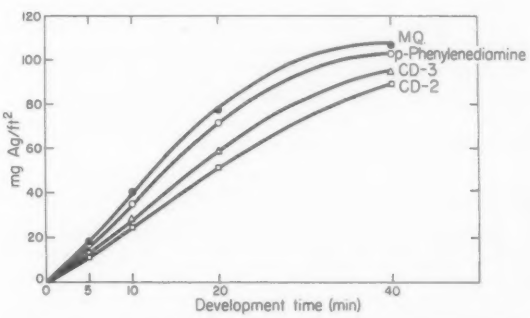

Fig. 3. Comparison of developing agents as solution-physical developers at pH 12. Developer concentration, 0.00516 M. Potassium bromide concentration, 0.0084 M. ●, Metol-hydroquinone in equimolar combination as developing agents; ○, *p*-phenylenediamine as developing agent; △, CD-3 as developing agent; and □, CD-2 as developing agent.

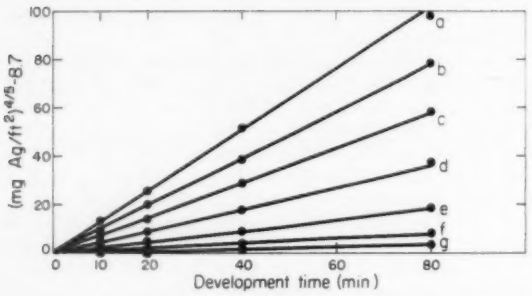

Fig. 4. Effect of silver-ion concentration on pure physical developmen by CD-3 developer at pH 12. Silver-ion concentration: (a) 1.6×10^{-12} M; (b) 8×10^{-13} M; (c) 4×10^{-13} M; (d) 2×10^{-13} M; (e) 1×10^{-13} M; (f) 5×10^{-14} M; and (g) 2.5×10^{-14} M.

where y is the analyzed silver in milligrams per square foot, after correction for the mass of silver initially present as nuclei.‡ This behavior is illustrated in Fig. 4, which shows the variation in rate of physical development by CD-3 as a function of silver-ion concentration in the developer.

The variation of development rate as the $^1/_3$ power of the silver developed has a weaker dependence upon nuclei surface than would be anticipated if the catalytic surface were critical to the process (variation as the $^2/_3$ power of the silver reduced). Microscope sections of samples used for pure physical development showed more development near the surface than in the interior of the colloidal silver–gelatin layers. The silver ion from the developer diffusing into the gelatin coating that contains a homogeneous dispersion of silver nuclei encounters the surface nuclei first, and is rapidly reduced to silver, while the supply of silver ion in the solution penetrating into the interior of the layer is depleted. This "stripping-off" of the silver ion can also be inferred from the fact that two coatings of colloidal silver—one half the thickness of the other—gave essentially identical amounts of silver developed. It seems certain, therefore, that only a portion of the total colloidal silver is being utilized here for the physical development. At the silver-ion concentrations used, at which the stable developer solutions can be prepared, the catalytic nuclei are "starved" for silver ion and a strong dependence of development rate on silver surface is not likely to be observed unless much higher ion concentrations are employed.

Effect of Silver-Ion Concentration

The rate of pure physical development varies as the logarithm of the silver-ion concentration. Figure 5 shows the variation, which is linear over most of the range of silver ion, for CD-2 and CD-3. In these experiments, the pH is maintained constant at 12.0,

‡ The rate equation, $dy/dt = ky^{1/3}$, has as solution $y^{4/3} = {}^4/_3 kt +$ constant. At time zero, y is the amount of silver, 15 mg/sq ft, present as nuclei; the constant in the equation is, therefore, 8.7, and the rate constant is equal to the slope of the line obtained by plotting $y^{4/3} - 8.7$ against time, as in Fig. 4.

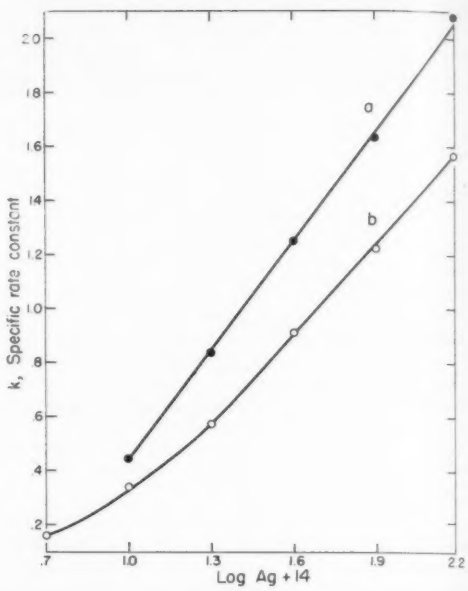

Fig. 5. Dependence of rate of pure physical development upon silver-ion concentration at pH 12 and developer concentration of 0.00516 M; ●, CD-2 as developer; ○, CD-3 as developer.

the developer concentration is held at 0.00516 mole/liter, and the silver ion is adjusted by varying the excess of complexing agent. A similar variation in rate with logarithm of the silver ion was found for *p*-phenylenediamine, and for the MQ developer (at pH 11).

Effect of pH

The electrochemical potential of a developer increases with the negative logarithm of the hydrogen-ion concentration (since hydrogen ions are lost in the oxidation of the developer). It would be expected, therefore, that developer potential and development rate would increase linearly with the pH. This be-

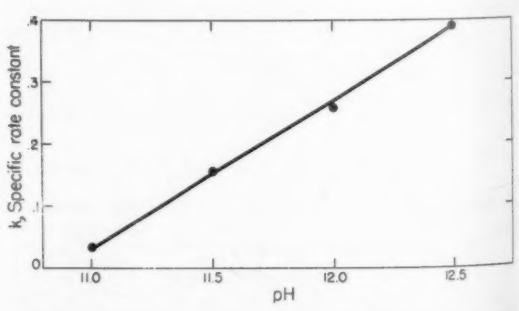

Fig. 6. Dependence of rate of pure physical development by CD-3 developer upon pH. Developer concentration, 0.00516 M. Silver-ion concentration, 1×10^{-13} M.

havior was found for CD-2, CD-3, MQ, and *p*-phenylenediamine. An example of the linear dependence of rate upon pH from 11 to 12.5 for CD-3 is shown in Fig. 6.

Effect of Developer Concentration

The effect of developer concentration upon the rate of pure physical development was investigated for CD-3. With a pH of 12.0, the developer concentration was varied from 0.00129 *M* to 0.0206 *M*, the silver-ion concentration being held constant at 2×10^{-13} *M*. In Fig. 7, the development rate constant is plotted against the logarithm of the developer concentration. The variation in rate of physical development with the logarithm of the developer concentration is consistent with the Nernst equation

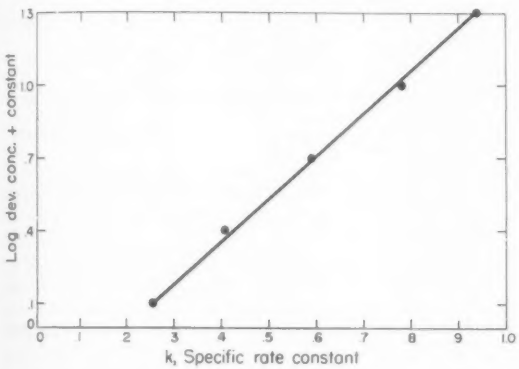

Fig. 7. Dependence of rate of pure physical development by CD-3 developer upon the logarithm of the developer concentration, at pH 12 and silver-ion concentration of 2×10^{-13} M.

for the electrochemical potential of the system, provided the concentration of the oxidized developer remains constant. This interpretation may be questioned, however, if the effective concentration of developer is the concentration in the adsorbed phase rather than the concentration in the solution phase.[19] In a previous publication, the concentration of developer necessary to secure equilibrium adsorption to a clean silver surface was determined.[18] By means of these adsorption isotherms, and from a knowledge of the surface of the colloidal silver nuclei,[20] it is possible to estimate in the present experiments the developer concentrations necessary to secure equilibrium adsorption to the colloidal silver nuclei. The actual developer concentrations used are considerably greater than those necessary to give complete surface coverage of the nuclei. It would seem inadmissible, therefore, to attribute an increase in rate with increasing developer concentration to an increase in concentration adsorbed unless the rate of adsorption of developer were an important factor, or unless competition for adsorption sites existed between the developer and other material present, such as gelatin, silver ion, or thiosulfate. Under such circumstances, the actual amount of developer adsorbed might be less than the amount estimated from the adsorption isotherms. In this connection it should be mentioned that Stevens and Block have measured a strong adsorption between labeled thiosulfate and silver,[20] and competitive adsorption of the thiosulfate to the silver could be a factor in the dependence of rate upon developer concentration.

Effect of Buffer Ion on Physical Development

In the course of the present investigation, it was observed that the buffer ion employed had an effect on the rate of physical development. This effect of buffer cation and anion in pure physical development onto colloidal silver nuclei was investigated with the thiosulfate–silver complex with silver-ion concentration of 4×10^{-13} mole/liter. In each case, the pH was adjusted to 12 with the same alkali hydroxide as the cation used in the buffer. The pH measurements were all made with a Beckman Model G pH meter with blue glass electrode, and the small correction for sodium ion was applied when sodium ion was present. The buffers used were all at approximately the same ionic strength. The results for potassium carbonate, potassium phosphate, sodium carbonate, and sodium phosphate are shown in Fig. 8. The sodium salts give higher rates of physical development than the potassium salts, while the phosphate anions give higher rates than the carbonate anions. Measurement of pAg made in the two extreme cases showed no difference in silver-ion concentration, so the effect cannot be due to any depression of silver ion by the potassium carbonate buffer.

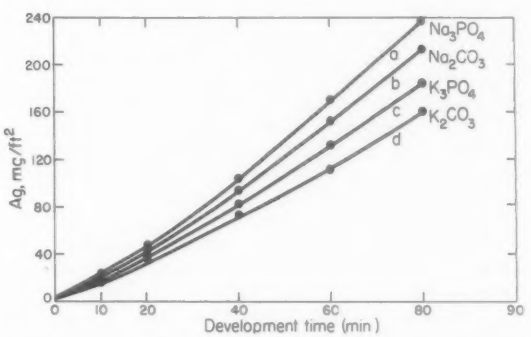

Fig. 8. Effects of buffer cation and anion upon pure physical development by CD-3 developer at pH 12. Developer concentration, 0.00516M. Silver-ion concentration, 4×10^{-13} M (a) tribasic sodium phosphate; (b) sodium carbonate; (c) tribasic potassium phosphate; and (d) potassium carbonate.

The differences in physical development rates resulting from the use of different buffer anions and cations may be the result of a salt effect on the protective colloid action of the gelatin, as suggested by

James,[21] who observed such an effect with the aromatic amine developers. However, it has been shown that the diffusion of dye anions within gelatin is strongly affected by added electrolyte,[22] and the effects of buffer ions on physical development rate may possibly represent an influence on the diffusion into gelatin of the developer components.

Conclusion

The experiments described on pure physical development have been confined to cases of effectively stable developer solutions under conditions which make possible a knowledge of the silver-ion concentration. Although these special conditions of physical development are not usually the same as those met with in practical photography, as in diffusion-transfer processes, or as a component in the ordinary development of silver halide emulsion, the latter conditions are usually so complex as to make impossible a knowledge of the silver ion present. The type of experiment described here is suitable for studying physical development in its simplest aspects. The ability of developing agents to reduce silver ion, catalyzed by a substrate, can be seen, independent of other effects, such as halide solvent action, which occur in ordinary development. It is thus possible to demonstrate the relative development potentials of different developing agents. The linear dependence of development rate upon the logarithm of the silver-ion concentration over a large range, and upon the pH, is in agreement with the theoretical influence of silver and hydrogen ions upon the oxidation potential. The dependence of development rate upon developer concentration is, however, not so readily interpreted because of uncertainty of the part which adsorption plays in the process. The dependence of development rate upon the buffer is by no means a minor effect and needs to be taken into account in further studies of physical development. Further work also is required to elucidate the influence of the adsorption of developer components on the silver nuclei under conditions in which the surface coverage as well as the concentration of substances in the solution phase, such as silver ion, are known.

References

1. H. Arens and J. Eggert, *Z. Elektrochem.*, **35:** 728 (1929).
2. W. Reinders and M. C. F. Beukers, *Trans. Faraday Soc.*, **34:** 912 (1938).
3. T. H. James, *J. Am. Chem. Soc.*, **61:** 648 (1939); *ibid.*, **61:** 2379 (1939); *ibid.*, **62:** 3411 (1940); *J. Phys. Chem.*, **45:** 223 (1941).
4. A. Rott, *Sci. et inds. phot.*, (2) **13:** 151 (1942); *ibid.*, (2) **19:** 324 (1948).
5. J. Eggert, *Helv. Chim. Acta*, **30:** 2114 (1947); *Sci. et inds. phot.*, (2) **19:** 321 (1948).
6. T. H. James, W. Vanselow, and R. F. Quirk, *PSA Journal*, **14:** 349 (1948).
7. A. Kuster, *Z. wiss. Phot.*, **43:** 191 (1949).
8. T. H. James and W. Vanselow, *Phot. Sci. and Tech.*, [II], **2:** 135 (1955); *J. Phys. Chem.*, **62:** 1189 (1958).
9. G. P. Faerman and E. D. Voeikova, *Uspekhi Nauch. Fot.*, **3:** 174 (1955); **4:** 150 (1955).
10. G. P. Faerman and I. I. Shishkina, *Uspekhi Nauch. Fot.*, **4:** 164 (1955).
11. T. H. James and W. Vanselow, *Phot. Eng.*, **7:** 90 (1956); *Phot. Sci. and Eng.*, **1:** 104 (1958).
12. R. B. Pontius and J. S. Thompson, *Phot. Sci. and Eng.*, **1:** 45 (1957).
13. R. B. Pontius, R. M. Cole, and R. J. Newmiller, *Phot. Sci. and Eng.*, **4:** 23 (1960).
14. E. H. Land, *J. Opt. Soc. Am.*, **37:** 61 (1947).
15. L. E. Varden, *J. Phot. Soc. Am.*, **13:** 551 (1947).
16. H. Chateau, B. Hervier, and J. Pouradier, *J. chim. phys.*, **54:** 246 (1957).
17. W. R. Ruby, private communication.
18. R. J. Newmiller and R. B. Pontius, *J. Phys. Chem.*, **64:** 584 (1960).
19. G. I. P. Levenson and T. H. James, *J. Phot. Sci.*, **2:** 172 (1954).
20. G. W. W. Stevens and P. Block, *J. Phot. Sci.*, **7:** 111 (1959).
21. T. H. James, personal communication, and *J. Phys. Chem.*, **45:** 232 (1941).
22. R. B. Pontius, M. L. Kaplan, and R. M. Husney, *J. Phys. Chem.*, **60:** 9 (1956).

PHOTOGRAPHIC SCIENCE AND ENGINEERING
Volume 5, Number 3, May-June 1961

A High-Resolution Exposure Determinant for Aerial Films

MARILYN LEVY, *U.S. Army Signal Research and Development Laboratory, Fort Monmouth, N.J.*

The procedures commonly used for determining aerial camera exposure are ambiguous and depend largely on the experience and skill of the aerial photographer. Since the recording of fine detail is the primary function of aerial photography, it is essential that the exposure of aerial films be controlled so as to insure their use at maximum resolution capacity. A simplified system, whereby the exposure yielding maximum detail can be determined from any sensitometric H&D curve, was developed after analyzing the resolution vs. exposure curves of representative aerial films at varying development times. The exposure required for maximum resolution for these films was found to be the same as the exposure required to yield a density of 0.85 above fog. Actual camera exposures based on this exposure criterion were determined and applied successfully on aerial photographic missions. This exposure determinant system can also be modified to obtain the exposure required for 0.9 maximum resolution. The use of the 0.6 gamma speed criterion is also discussed.

The recording of fine detail is the primary function of aerial reconnaissance photography. It is essential, therefore, that the exposure of aerial films be controlled so as to insure their use at maximum resolution capacity. In spite of this requirement, we still continue with hit-or-miss techniques for selecting aerial camera exposures that are based for the most part on empirical standards. For example, many manufacturers rate aerial films with a spurious ASA number or index which is often confused with the ASA index proposed by Jones.[1] His system evolved from a statistical study of the tone-reproduction characteristics of a large number of emulsions used for aesthetic pictorial photography, and it depends on a subject with a log brightness range of 1.5 and a development gamma of approximately 0.8.

Since aerial photography emphasizes detail rather than tone reproduction and is concerned with subjects of low log brightness range requiring high development gammas the ASA system is not applicable. Nevertheless, this rating is used by the aerial photographer as an exposure meter setting for determining aerial camera exposures. Since the photographer cannot always rely on his meter reading, he also employs nebulous correction factors, which he has gleaned from trial-and-error experience, to produce his final camera setting. This ambiguous procedure would not seriously hamper the quality of pictorial photographs, but in aerial photography a poor estimate of camera exposure may result in a marked loss in detail and an ineffectual photographic flight mission.

Presented at the Annual Conference, Binghamton, N.Y., 24 May 1961. Received 27 February 1961.

1. L. A. Jones, *J. Franklin Inst.*, **227:** 297, 497 (1939).

Howlett[2] recognized the importance of accurate exposure determination and proposed a speed system utilizing a speed point at the exposure required for 0.9 maximum resolution. This speed rating is actually a means for selecting the exposure point for good detail and cannot be used as a basis for comparison of speed of individual films. His system of determining exposure is certainly valid, but it probably has not gained popularity because of the necessity for tedious resolution measurements for all aerial films at all conditions of development.

There have been indications in the literature that there is a well-defined image density which gives optimum resolution. If such a point could be determined for aerial films, it would be relatively simple to derive the exposure for maximum resolution from any sensitometric H&D curve. Unfortunately there is a conflict of opinion in the literature concerning this optimum image density. Jackson[3] reports a density of 0.3 above fog for maximum resolution of aerial films, while Brock[4] and Istomin[5] recommend a density above fog of approximately 1.0. Kardas[6] investigated all types of emulsions and found the best detail reproduction at densities of 0.6–0.8. We decided, therefore, to evaluate the resolution vs. exposure data of representative aerial films in order to ascertain whether there is an average density that could be used for the practical determination of exposure.

2. L. E. Howlett, *Can. J. Research*, **24A:** 1 (1946).
3. K. B. Jackson, *Can. Surveyor*, **114:** 454 (1959).
4. G. C. Brock, *Physical Aspects of Air Photography*, Longmans, Green and Co., 1952.
5. G. A. Istomin, *Uspekhi Nauch. Foto. Akad. Nauk SSSR*, **4:** 17 (1955).
6. R. S. Kardas, *Phot. Eng.*, **6:** 190 (1955).

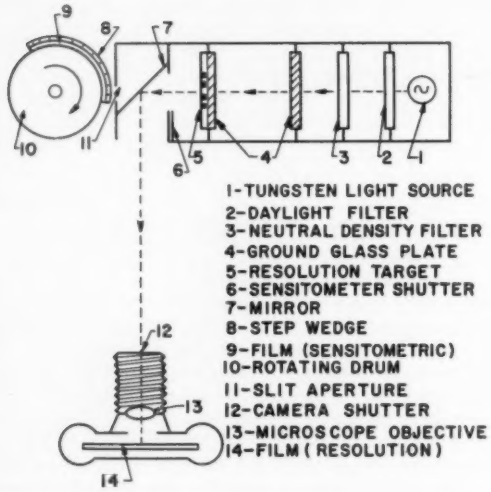

Fig. 1. Apparatus for resolution and sensitometric measurement.

Laboratory Procedure

The optimum average density of maximum resolution was obtained utilizing the modified sensitometric apparatus* shown in Fig. 1. A USAF 1951 high-contrast resolution target, illuminated by a standard light source (6100°K), was imaged onto the film from a mirror arrangement through an achromat 32mm microscopic objective. Although we realize that high-contrast targets do not simulate aerial subject contrast, we felt that better comparative data would be obtained using the higher resolution figures produced by high-contrast subjects. Moreover, the resolution curves published by Kardas,[5] which show varying target contrasts, seem to indicate that there is no appreciable variation of exposure for maximum resolution with varying target contrast. In order to have a range of intensity-modulated exposures through the target, neutral density filters ranging in densities from 0.15 to 1.75 in 0.20 increments were placed between the light source and the target. After exposure of the resolution target, the apparatus was utilized as a sensitometer by removing the resolution target and mirror assembly so that the film pack, consisting of an optical wedge backed by a test strip, could be exposed. Since the sensitometric strip and the resolution image were developed together, the exact exposures in meter-candle-seconds impinging on the film in the resolution camera could be determined. Unfortunately, diffuse density readings could not be obtained directly from the resolution image since the target area was smaller than the scanning aperture of our densitometer. Therefore, the densities of the largest exposed area of the resolution target (approximately 0.25 sq mm) and the step wedge were read on the Jarrell-Ash Microphotometer (JA-203), which measures specular densities. The diffuse densities of the step wedge, which corresponded to these specular densities, were then determined on the Western Electric Densitometer (RA-1100-B). An example of the information obtained using this procedure is illustrated in Fig. 2, which shows the specular and diffuse characteristic curves with the corresponding resolution curve of Kodak Plus-X Aerecon Film developed for 5 min in D-19 at 68°F.

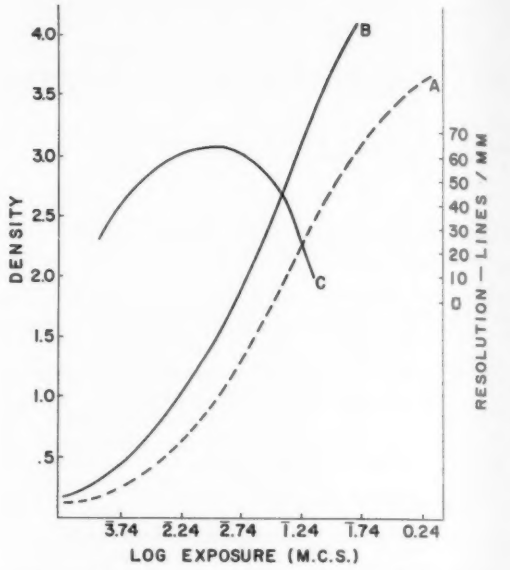

Fig. 2. Resolution and characteristic curves, Plus-X Aerecon Film developed in D-19 at 68°F for 5 min. A, diffuse density H&D curve; B, specular density H&D curve; C, resolution curve.

Experimental Results

The data obtained from these measurements are given in Table I. (Kodak Plus-X Panchromatic Negative Film, although not an aerial film, was included to introduce the characteristics of a different developer and film type.) The diffuse density above fog ($D_{\#}$) for maximum resolution was determined for the four films tested at varying developing times and temperatures. An average diffuse density of 0.85 above fog was obtained from these tests. We then compared the experimentally determined log exposure required for maximum resolution (log E_1) with the corresponding log exposure required to give a density of 0.85 above fog (log E_2). The differences are shown in the last column. The average of the absolute values of these differences is only 0.06, indicating a very close correlation with the experimental values. Even the extreme difference of 0.25, shown by Plus-X Aerecon developed in D-19 for $2^1/_2$ min at 68° F, represents a variation of only one stop in camera exposure (one stop is equivalent to a difference in log exposure of 0.30). These results seem to corroborate our selection of a definite density point on the characteristic curve, namely 0.85 above fog,† as an exposure determinant for aerial films.

* Intensity Scale Sensitometer Model 21, Type 2, developed by Ansco under Signal Corps Contract DA-36-039 sc-557.

† The USSR speed criterion for aerial films according to GOST Standard 2817-50 is at a density of 0.85 above fog (see I. A. Tschernij, *Bild und Ton*, **13**: 330 (1960)).

TABLE I. Determination of Exposure for Maximum Resolution

Film	Developer	Temperature	Time, min	$\gamma^{\parallel}$	$\gamma^{\#}$	$D^{\parallel}$ at maximum resolution	$D^{\#}$ at maximum resolution	Log E_1	Log E_2	Log $\lvert E_2/E_1 \rvert$
Plux-X Aerecon	D-19	68°F	2½	1.65	1.50	1.04	0.54	$\bar{2}.79$	$\bar{1}.04$	0.25
			5	2.10	1.85	1.26	0.78	$\bar{2}.50$	$\bar{2}.58$	0.08
			10	2.45	2.00	1.46	0.96	$\bar{2}.35$	$\bar{2}.30$	0.05
		77°F	2	2.10	1.50	1.12	0.76	$\bar{2}.66$	$\bar{2}.72$	0.06
			4	2.00	1.90	1.38	0.92	$\bar{2}.45$	$\bar{2}.42$	0.03
			8	2.50	2.10	1.57	1.08	$\bar{2}.35$	$\bar{2}.20$	0.15
Tri-X Aerecon	D-19	68°F	2½	1.00	0.70	1.30	0.84	$\bar{1}.27$	$\bar{1}.30$	0.03
			5	1.50	1.00	1.33	0.86	$\bar{2}.58$	$\bar{2}.58$	0.00
			10	1.70	1.30	1.40	0.94	$\bar{2}.07$	$\bar{2}.00$	0.07
		74°F	8	1.80	1.25	1.40	0.92	$\bar{2}.16$	$\bar{2}.12$	0.04
Plus-X Pan. Neg.	DK-60A	73°F	4	1.70	1.15	1.37	0.93	$\bar{2}.39$	$\bar{2}.31$	0.08
			8	1.60	1.20	1.36	0.94	$\bar{2}.20$	$\bar{2}.16$	0.04
Ilford Aerial N	D-19	80°F	2	0.95	0.75	1.15	0.84	$\bar{2}.08$	$\bar{2}.12$	0.04
			4	1.50	1.15	1.41	0.92	$\bar{3}.79$	$\bar{3}.75$	0.04
			8	1.35	1.10	1.18	0.84	$\bar{3}.70$	$\bar{3}.72$	0.02
Average						1.30	0.85			0.06

E_1 = Exposure in meter-candle-seconds required for maximum resolution.
E_2 = Exposure in meter-candle-seconds required to give a diffuse density of 0.85 above fog.

$\gamma^{\parallel}$ = Gamma of specular density vs. log E curve.
$\gamma^{\#}$ = Gamma of diffuse density vs. log E curve.
$D^{\parallel}$ = Specular density above fog
$D^{\#}$ = Diffuse density above fog.

Camera Exposures Using Determinant $D^{\#} = 0.85$

In order to compute the actual camera exposure, the time, t, required for properly exposing a scene, whose average luminance is measured in foot-lamberts, was determined for the different films and processing conditions.

The camera exposure time

$$t = E_2 \times 4K^2/B_0TC$$

where

E_2 = exposure in meter-candle-seconds required to give a density of 0.85 above fog
K = f-number of the lens
B_0 = luminance of the scene
T = transmission of the lens
C = conversion factor

If E_2 is measured in meter-candle-seconds and B_0 is measured in foot-lamberts (equivalent lumens/sq ft), then $C = 10.76$

Assuming a lens aperture of $f/8$ and a lens transmittance of 80%

$$4K^2/TC = C' = 29.7$$

Then $$t = E_2 \times 29.7/B_0$$

The results of these determinations for a scene luminance of 100 ft-L are shown in Table II. The exposures indicated in the table were tried successfully with Plus-X Aerecon and Tri-X Aerecon on actual photographic missions at varying altitudes and weather conditions. The Spectra Brightness Meter was used to measure the brightness of object points estimated as representing the average luminance of the scene in foot-lamberts.

It should be noted that the exposure point selected is on the straight-line portion of the curve and is therefore dependent on development gamma.

TABLE II. Camera Exposures Using Determinant $D^{\#} = 0.85$

Film, developed in D-19	Temperature	Time, min	E_2	t	γ
Plus-X Aerecon	68°F	2½	0.1096	33	1.50
		5	0.0380	11	1.85
		10	0.0199	6	2.00
	77°F	2	0.0525	16	1.50
		4	0.0263	8	1.90
		8	0.0158	5	2.10
Tri-X Aerecon	68°F	2½	0.1995	59	0.70
		5	0.0380	11	1.00
		10	0.0100	3	1.30
	74°F	8	0.0132	4	1.25
Ilford Aerial N	80°F	2	0.0132	4	0.75
		4	0.0056	2	1.15
		8	0.0053	2	1.10

E_2 = Exposure in meter-candle-seconds required to give a density of 0.85 above fog.
t = Exposure time in milliseconds when scene brightness is 100 ft-L and aperture is set at $f/8$.

An examination of exposures required for Tri-X Aerecon developed to gammas of 0.70 to 1.30 (Table II) shows that the film developed to a gamma of 0.7 requires a $4^1/_2$-stop increase in exposure over the same film developed to a gamma of 1.3. The difference is not so marked for Plus-X Aerecon, where an approximate $2^1/_2$-stop increase in exposure is required for development from a gamma of 2.0 to a gamma of 1.5. It is obvious that the final development gammas must be considered when the aerial photographer makes his camera exposure.

Practical Test of Exposure Determinant System

As a practical test, the exposure determinant system was applied to several aerial films whose resolution curves had not previously been determined. Eastman Kodak SO-220, Du Pont 931, and Du Pont Type 140 films were exposed with a 1.5 neutral density filter on the Edgerton Sensitometer (Mark VI) at 1/100 sec and developed in D-19 for 5 min at 68° F. The sensitometric curves and corresponding exposure determinants at 0.85 above fog are shown in Fig. 3. Camera exposures were then determined, using the formulations just described. For a scene of 200 ft-L average luminance, the following camera settings were required, according to our calculations:

For Du Pont 931 and Type 140 — $^1/_{200}$ sec at $f/8$
For Kodak SO-220 — $^1/_{50}$ sec at $f/8$

A range of exposures under and above these figures were then used to photograph a laboratory model of an aerial scene scaled so that the image on the film would be the same size as an aerial scene photographed at 1500 ft with a 6-in. lens. The negatives were then enlarged 15 times and examined for detail. In every case, the calculated correct exposure produced the sharpest picture.

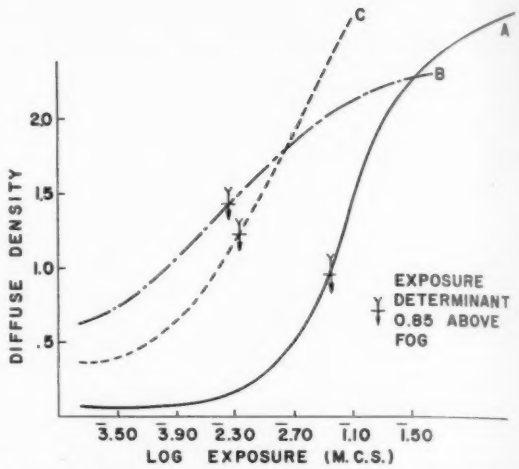

Fig. 3. Characteristic curves of aerial films developed in D-19 at 68°F for 5 min. A, Eastman Kodak SO-220; B, Du Pont 931; C, Du Pont Type 140.

Comparison of Exposure Determinant System with Proposed Aerial Speed Systems

The point on the curve where the gradient is 0.6 gamma has been proposed by photographic scientists as a possible speed criterion for aerial films. A comparison (log E_2/E_3) of the 0.85 exposure determinant and the 0.6 gamma exposure determinant is shown in Table III. It can be

TABLE III. Comparison of Exposure Determinant System with Proposed Aerial Speed Systems

Film	Developer	Temperature	Time, min	Log E_2	Log E_3	Log E_2/E_3	Log E_4	Log E_5	Log E_5/E_4
Plus-X Aerecon	D-19	68°F	$2^1/_2$	$\bar{1}.04$	$\bar{2}.66$	+0.38	$\bar{2}.35$	$\bar{2}.59$	+0.24
			5	$\bar{2}.58$	$\bar{2}.50$	+0.08	$\bar{2}.10$	$\bar{2}.13$	+0.03
			10	$\bar{2}.30$	$\bar{2}.04$	+0.26	$\bar{3}.95$	$\bar{3}.85$	+0.10
		77°F	2	$\bar{2}.72$	$\bar{2}.40$	+0.32	$\bar{2}.20$	$\bar{2}.27$	+0.07
			4	$\bar{2}.42$	$\bar{2}.10$	+0.32	$\bar{2}.04$	$\bar{3}.97$	−0.07
			8	$\bar{2}.20$	$\bar{3}.92$	+0.33	$\bar{2}.04$	$\bar{3}.75$	−0.29
Tri-X Aerecon	D-19	68°F	$2^1/_2$	$\bar{1}.30$	$\bar{2}.29$	+1.01	$\bar{2}.94$	$\bar{2}.85$	−0.09
			5	$\bar{2}.58$	$\bar{2}.00$	+0.58	$\bar{2}.16$	$\bar{2}.13$	−0.03
			10	$\bar{2}.00$	$\bar{3}.54$	+0.46	$\bar{3}.70$	$\bar{3}.55$	−0.15
		74°F	8	$\bar{2}.12$	$\bar{3}.42$	+0.70	$\bar{3}.75$	$\bar{3}.67$	−0.08
Plus-X Pan. Neg.	DK-60A	73°F	4	$\bar{2}.31$	$\bar{3}.40$	+0.91	$\bar{2}.04$	$\bar{3}.86$	−0.18
			8	$\bar{2}.16$	$\bar{3}.30$	+0.86	$\bar{3}.72$	$\bar{3}.71$	−0.01
Ilford Aerial N	D-19	80°F	2	$\bar{2}.12$	$\bar{3}.04$	+1.08	$\bar{3}.66$	$\bar{3}.67$	+0.01
			4	$\bar{3}.75$	$\bar{3}.04$	+0.71	$\bar{3}.50$	$\bar{3}.30$	−0.20
			8	$\bar{3}.72$	$\bar{3}.00$	+0.72	$\bar{3}.35$	$\bar{3}.27$	−0.08

Log E_2 = Log exposure required to give a diffuse density of 0.85 above fog.
Log E_3 = Log exposure at the point where the gradient is 0.6 of gamma.
Log E_4 = Log exposure required for 0.9 maximum resolution.
Log E_5 = Log $(E_3/0.45)$.

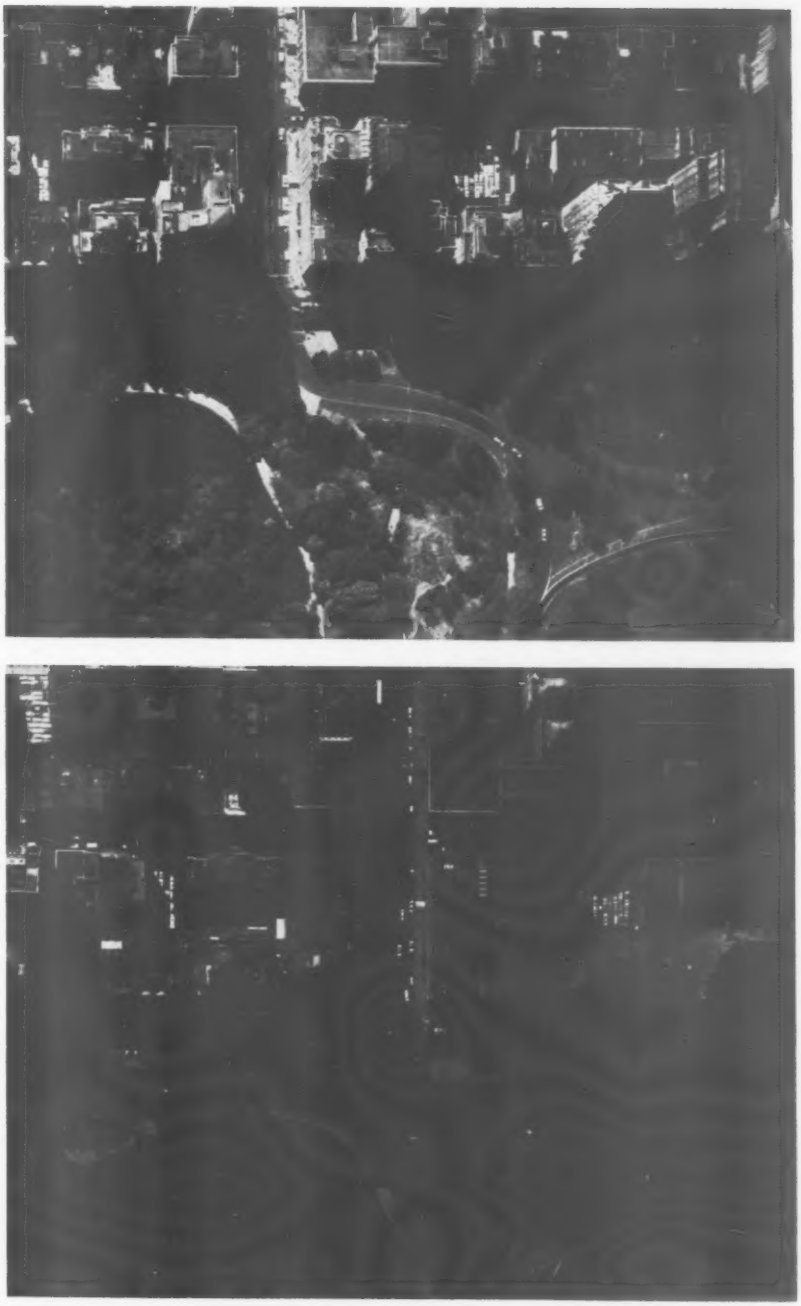

Fig. 4. Effect of underexposure on image quality. Top, reproduction of negative exposed at 0.9 maximum resolution; bottom, reproduction of negative exposed one stop below exposure for 0.9 maximum resolution.

seen that in some cases there would be a two or three stop underexposure of the film if the 0.6 gamma speed system were used. These underexposed negatives would be severely deficient in sharp detail and unserviceable from the photointerpretation or mapping viewpoint. There does not seem to be any correspondence between the 0.6 gamma speed criterion and the 0.85 exposure determinant.

In many cases, especially where the light level is low, rapid shutter speeds and small diaphragm diameters are essential to eliminate the destructive

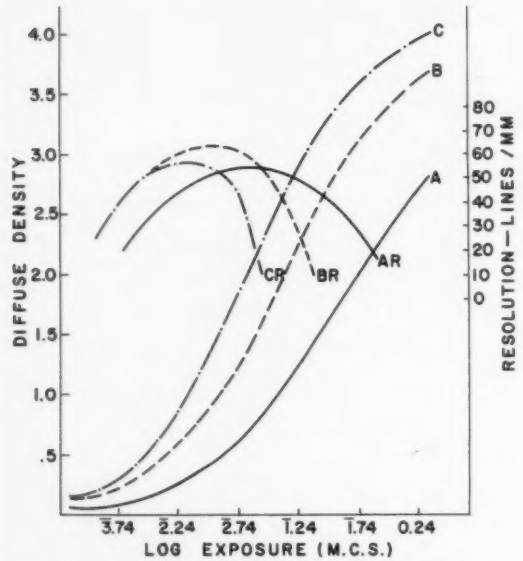

Fig. 5. Resolution and characteristic curves, Plus-X Aerecon Film developed in D-19 at 68°F. H&D curves at various development times: A, 2½ min; B, 5 min; C, 10 min. Resolution curves at various development times: AR, 2½ min; BR, 5 min; CR, 10 min.

effects of image motion. Then, of course, we must forego the luxury of exposure at maximum resolution and select the compromise exposure which minimizes image motion effects. As indicated in Table III, if 0.45 is subtracted from the log exposure required for a density of 0.85, an exposure (log E_5) is obtained that corresponds very well with the experimentally determined exposure (log E_4) for 0.9 maximum resolution. Therefore, a $1^1/_2$ stop underexposure from the determined value would not represent a severe loss in detail characteristics. However, the resolution curve is such that any exposure below this point results in severe resolution deficiencies. This degradation is shown in Fig. 4, which compares an actual aerial photograph on Plus-X Aerecon exposed at approximately the 0.9 maximum resolution point with the same scene exposed one stop below this exposure.

Conclusion

The use of the ASA exposure index nomenclature for aerial films has led to the erroneous belief that these figures can be used as a basis of exposure comparison. We are likely to assume, for example, that Tri-X Aerecon (with a manufacturer's index of 200) is $2^1/_2$ times as fast as Plus-X Aerecon (with a manufacturer's index of 80). Certainly, this assumption would be confirmed by a comparison of the respective threshold speeds derived from the sensitometric curves of the films. It would seem logical, therefore, to choose Tri-X Aerecon as the more desirable film for aerial photography at low light levels. However, Plus-X Aerecon exposed at the extreme toe region (log E 3.74) and developed for 5 min in D-19 gives a slightly higher resolution than Tri-X Aerecon exposed at the same point and developed for 10 min in the same developer. This is illustrated in Figs. 5 and 6, which show the characteristic and resolution curves of Plus-X Aerecon and Tri-X Aerecon at varying development times. A comparison of these curves with the curves for Ilford Aerial N, shown in Fig. 7, indicates that Aerial N can be exposed at much lower light levels before image detail is completely lost. Kardas[4] did extensive work on this subject and proved that there is no correlation between the ASA speed cri-

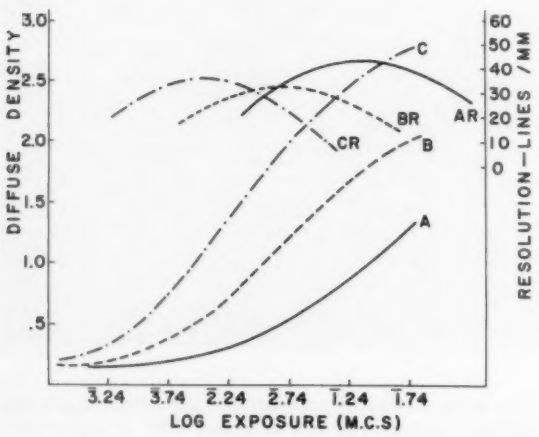

Fig. 6. Resolution and characteristic curves, Tri-X Aerecon Film developed in D-19 at 68°F. H&D curves at various development times: A, 2½ min; B, 5 min; C, 10 min. Resolution curves at various development times: AR, 2½ min; BR, 5 min; CR, 10 min.

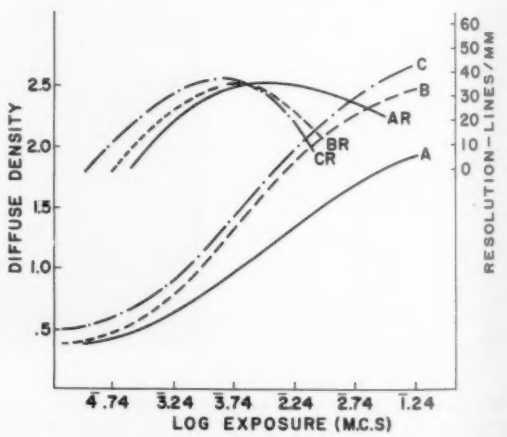

Fig. 7. Resolution and characteristic curves, Ilford Aerial N Film developed in D-19 at 80°F. H&D curves at various development times: A, 2 min; B, 4 min; C, 8 min. Resolution curves at various development times: AR, 2 min; BR, 4 min; CR, 8 min.

teria and the information capacity of a specific film. Once the correct film has been selected on the basis of its informational capacity, we can guard against poor quality by using an exposure that retains the optimum efficiency of the chosen film. The 0.85 exposure determinant system is presented as a practical and simple means for performing this task.

Acknowledgments

The author is indebted to Karl G. Leistner, Dieter P. Paris, and L. D. Goldfarb for their valuable advice and assistance. She would also like to express her appreciation to Sp/4 Robert Degree, Jr., for his assistance in performing the laboratory experiments discussed in this paper.

• Coming Technical and Scientific Meetings

Joint Automatic Control Conference, American Institute of Chemical Engineers, American Institute of Electrical Engineers, American Society of Mechanical Engineers, Institute of Radio Engineers, Instrumentation Society of America, June 28–30, University of Colorado, Boulder, Colo.

International Union of Pure and Applied Physics, International Commission for Optics, July 5–8, Paris, France

International Optical Congress, July 5–10, London, England

Color Photographic Association of Canada, July 9–11, Sheraton-Connaught Hotel, Hamilton, Ont.

International Conference on Optical Instruments and Techniques, July 10–14, London, England

National Audio-Visual Association, Annual Convention, July 22–25, Hotel Morrison, Chicago, Ill.

Professional Photographers of America, Annual Exposition of Professional Photography, July 30–August 4, Statler-Hilton, New York

American Rocket Society, Guidance and Control Conference, August 7–9, Stanford University, Stanford, Calif.

Society of Photographic Instrumentation Engineers, Annual Technical Symposium, August 7–11, Ambassador Hotel, Los Angeles, Calif.

Biological Photographic Association, Inc., August 21–24, Chicago, Ill.

International Conference on Photoconductivity, August 21–24, Cornell University, Ithaca, N.Y.

Electron Microscopy Society, August 25–September 5, Philadelphia, Pa.

International Congress of Radiology, August 26–September 1, Montreal, Que.

American Chemical Society, 6th International Conference on Coordination Chemistry, August 27–September 1, Wayne State University, Detroit, Mich.

Inter-American Congress of Radiology, September 3–10, São Paulo, Brazil

Institute of Radio Engineers, PGIT, International Symposium on Transmission and Processing of Information, September 6–8, Massachusetts Institute of Technology, Cambridge, Mass.

International Congress for Scientific Photography, September 11–17, Zürich, Switzerland

American Roentgen Ray Society, September 26–29, Deauville Hotel, Miami Beach, Fla.

90th Semiannual Convention, Society of Motion Picture and Television Engineers, October 2–6, Lake Placid, N.Y. Papers Chairman, C. Loren Graham, Research Laboratories, Eastman Kodak Co., Rochester 4, N.Y.

American Photoengravers Association, October 8–10, Penn-Sheraton, Pittsburgh, Pa.

Optical Society of America, October 18–20, Biltmore Hotel, Los Angeles, Calif.

International Symposium on Photoelasticity, October 29–31, Chicago, Ill.

Society of Reproduction Engineers, Visual Communications Congress, December 1–4, Hotel Biltmore, Los Angeles, Calif.

91st Semiannual Convention, SMPTE, April 30–May 4, 1962, Ambassador Hotel, Los Angeles, Calif.

1962 Annual Conference, SPSE, May 7–11, Somerset Hotel, Boston, Mass.

92nd Semiannual Convention, SMPTE, October 22–26, 1962, Drake Hotel, Chicago, Ill.

PHOTOGRAPHIC SCIENCE AND ENGINEERING
Volume 5, Number 3, May-June 1961

Selection of Film and Process for a High-Acuity Photographic System

MALOR WRIGHT, ROBERT G. POLK, AND PAUL FEDELCHAK, *Information Technology Laboratories, Itek Corporation, Lexington, Mass.*

A film and processing chemistry were selected for use in information-handling equipment for a special aerial reconnaissance system. The equipment was required to reproduce on a single film sheet both high-resolution continuous-tone photography and digital (graphic) information. Additional requirements were for a total dry-to-dry time of 30 sec, commercial keeping quality, high processing uniformity, low fog level, maximum density of at least 2.5, and a gamma of 1.5. Factors such as film speed, color sensitivity, amenability to "low" contrast rapid processing, physical durability, drying rate, curl, resolution, and sinewave response were studied. As a result of this investigation, Eastman Kodak 57-1 Film was chosen, and a process was achieved which meets the requirements stated above.

A study was conducted of film and processing requirements in connection with the design of ground-handling equipment for a special aerial reconnaissance system. The equipment was required to reproduce on a single film sheet both high-resolution continuous-tone photography and digital information. The input photography had fine detail over a range of 1.8 log E units and, in addition, included high-contrast digital records. Rapid reproduction of the photographs at approximately 100 lines/-mm was required; a dry-to-dry processing time of 30 sec was desired. Additional requirements were: commercial keeping quality, high processing uniformity, and low fog level.

An extremely fine-grained film was deemed essential because of its high resolution. Since such films have a high contrast, the lowest gamma believed to be consistent with the uniformity required was 1.5. The maximum density needed was estimated to be 2.5, since, because of the limited intensity of the viewing illumination, densities higher than 2.5 would bring virtually no advantage.

It was apparent that some of the input information would be recorded on the toe and shoulder of the characteristic curve. From tone control sketches, it appeared advisable to place the negative exposures well up on the shoulder of the curve and the positive exposures well down on the toe. This technique would place more of the nonlinear information on the toe of the viewing curve where light intensity and thus visual acuity is higher.

The major problem in the design of the processing chemistry was to achieve a consistent uniform gamma well below the norm for the class of emulsions used and, at the same time, maintain a neutral image color[1] and low fog. It was estimated that contrast should be held constant to ± 0.1 gamma unit to eliminate erratic compression of information in either the highlight or shadow areas. To eliminate halation, a gray-base film having a density of 0.2 was necessary. Since the images were to be viewed by projection, a very low fog was indicated, and it was desirable that the development fog not exceed 0.05 $\pm$ 0.01, yielding a total gross fog density of 0.25. To maintain consistent reproduction, replenishment of the developer was necessary.[2]

Approach

This problem was approached from three considerations—equipment design, film, and chemistry. The equipment design is reported separately.[3] It was planned to select a film using an approximate processing formula, then, having selected the film, to design an optimum formula to suit the requirements.

The high-resolution films[4] were rated on the following points:

1. Compatibility with high-temperature processing.
2. Gamma and other photometric characteristics we expected to achieve.
3. Estimated resolution capability of the film at a gamma of 1.5.
4. Estimated batch-to-batch variations in photometric character.

Presented at the SPSE Rapid Processing Symposium, Washington, D.C., 15 October 1960. Received 14 November 1960; revised 28 February 1961.

1. J. H. Altman and R. L. Lamberts, *Phot. Sci. and Eng.*, **2**: 160 (1958).
2. A. J. Axford and J. D. Kendall, *Phot. Eng.*, **6**: 50 (1955).
3. M. Wright, E. Thompson, and I. Spiegel, *Phot. Sci. & Eng.*, **5**: 171 (1961).
4. W. M. Drumm *Phot. Sci. & Eng.*, **1**: 147 (1958).

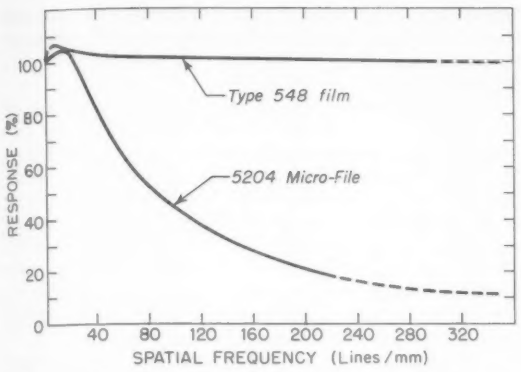

Fig. 1. Micro-File curve (supplied through the courtesy of Eastman Kodak Co.), indicating characteristics of a particular sample of the material (5204), and curve for Type 548 Film, replotted to the same scale as the Micro-File curve to permit comparison. The 548 film was processed in DK-50, 1:10, for 10 min, and exposed through a Wratten 61 filter.

5. Photographic speed under conditions of exposure to blue-green light with a maximum allowable exposure time of 1–5 sec.
6. Availability.

The three Eastman Kodak films—Micro-File B, Type 548, and SO-1181—were tested. Type 548 and SO-1181 are similar films, so when a question of the availability of the latter arose, the film search was reduced to two —Micro-File B and Type 548.

The frequency response of the Micro-File Film (Fig. 1) shows a serious reduction in contrast at 100 lines/mm. A frequency response curve of Type 548 Film is also shown in Fig. 1.[5] Comparison of the curves indicates that more fine-detail information will be retained on Type 548 Film.

Since the gamma of the selected film will be reduced to a level of 1.5 from the 4 to 5 at which the frequency response data was taken, it is apparent that the image-to-object contrast at the 100-line/mm frequency of the Micro-File will not be adequate; Type 548 is definitely superior.

A test object was provided at such a resolution level that when photographed at the appropriate reduction ratio, the image quality matched that which the system was required to reproduce. Test exposures were made and processed on both films. In addition, microdensitometer traces of knife-edge exposures were made. Both testing methods indicated that, when processed to a 1.5 gamma, Type 548 Film was superior for this purpose. These resolution target and knife-edge tests indicated that reproduction of the input information on the nonlinear portion of the characteristic curve of Type 548 Film would be less deleterious than reproduction on the straight-line portion of the characteristic curve of a coarser emulsion. This confirmed the observations made during the tone-control study.

The Eastman Kodak Experimental Test Film 57-1 used in the tests described below is a Type-548 emulsion, coated on 0.00525-in. gray base. It is primarily a modified Lippmann-type emulsion and yields a gamma of 7 when processed in D-8 for 2 min at 68° F. In a less energetic developer, such as D-19, very high gammas still result. Thus, some overexposure and considerable underdevelopment are necessary to achieve our required "low" gamma, and this inevitably introduces problems of non-uniform development, which are further exaggerated by the requirement for rapid processing

Developing and fixing baths was selected, rather than monobath, to permit adjustment of the photometric response, to compensate for both film and exposure variations, and to adjust for batch-to-batch emulsion variances. A developer with reasonable storage life and good exhaustion characteristics was needed. Initial testing was done at 90°F, with 10 sec allotted for development using manual agitation.

A statistical plan, actually a fractional factorial experiment, was designed to permit the study of a number of factors and to explore the result of assigning two levels to each factor. The number of combinations was thus 2^n, where n is the number of factors. It was apparent that, where n becomes large, the experimental work would become very great. Therefore, to limit severely the number of factors, reliance was placed upon previous experience and trial-and-error testing. However, with a problem as difficult as this, there is a strong temptation to try the effect of as many compounds as possible.

Some simplification was possible. For instance, various restrainers have, in general, the same type of action—they retard development and fixation. Stabilizers and, in some cases, silver solvents, tend to reduce oxidation or to remove the exhaustion products from the reaction sites. Developing agents, however varied their character, tend to reduce silver halide to metallic silver. The limiting of the large number of candidate compounds for the developer solution to a manageably small number entailed the risk of leaving out the one material which would have been ideal. In this, the most critical step, dependence was placed on a study of the literature,[6–12] experience, trial-and-error experimentation, and good luck. The number of factors was reduced to six with some standby materials which could be included in the experiment if the opportunity arose.

To limit further the experimental effort, it was decided to employ the various materials at only two levels of concentration. The levels had to be chosen carefully, i.e., each constituent tested had to be in solution in sufficient concentration to judge its

5. R. L. Lamberts, *J. Opt. Soc. Am.*, **49:** 425 (1959).

6. J. R. Alburger, *Jour. SMPE*, **35:** 282 (1940).
7. R. Hodgson and J. Hammer, *Jour. SMPTE*, **56:** 261 (1951).
8. J. E. Duffy, *Phot. Eng.*, **6:** 127 (1955).
9. T. H. James and W. Vanselow, *Phot. Eng.*, **6:** 183 (1955).
10. L. J. Fortmiller, N. A. Exley, C. E. Ives, and T. H. James, *Phot. Eng.*, **7:** 171 (1956).
11. T. H. James and W. Vanselow, *Phot. Eng.*, **7:** 90 (1956).
12. A. Axford and J. Kendall, *Phot. Eng.*, **7:** 105 (1956).

effect. Furthermore, there had to be considerable excess of each compound to assure that the developer solution would have adequate exhaustion and keeping characteristics. In addition, the two levels selected had to be far enough apart so that a significantly different response could be measured to determine the direction the experiment should take. And, finally, the levels selected needed to be in the range of effective operation.

Having reduced the experimental factors to six, and having selected two operating levels for each factor, a one-half replicate of the combinations available was chosen.[13] Since 2^6 is 64, a one-half replicate requires 32 tests. A single test would require considerable time, but it was felt that this would be a manageable effort. Further, since it was not certain that the best materials and levels had been selected, repetition of the six-factor experiment was expected in order to find an optimum. The one-half replicate provided all main effects and all two-factor interactions.

The experiment was divided into eight blocks of four tests. Each block would thus provide an immediate estimate of the main effects. This provision greatly increased the flexibility of operation since new factors or different levels could be introduced at any time during the experiment without the need to complete all 32 tests before a new approach could be taken. It should be noted, however, that the convenience which results from dividing an experiment into blocks does reduce somewhat the certainty with which conclusions can be drawn from the data.

The matrix used in illustrating the initial experimentation is shown in Fig. 2. This matrix design explores all the factors impartially. Each factor is represented by an equal number of tests at both high and low levels. It can be noted that the diagonal symmetry is imperfect. This is because the diagonals were used to measure the interactions between factors. By making 32 tests instead of the usual 64, the information that could be extracted from the experiment was limited. It can be seen that some of the interaction information is not available on the matrix. Since the effect of interaction between three and more factors usually had little significance, the imperfect symmetry of the matrix is associated with the fact that the higher order interactions were not being explored.

Inspection of the matrix will reveal that the difference between the average response of factor A in each of its two levels is a gauge of the effect of factor A between those levels. All of the responses were thus used to measure the effect of factor A, and, when regrouped, the same responses measure factor B, and so on. The standard analysis of variance and the F test were used to measure the significance of the main effects and the two-factor interactions.

Statistical techniques provide balanced designs which have high efficiencies in the determination of responses. There must, however, be some measure of merit whereby the response can be accurately gauged. Various attempts have been made to reduce the measurement of the efficiency of an information-handling system to a single number, e.g., the "information volume" proposal.[14] It was felt wise, however, to place reliance upon the following measures: first, resolution data to provide an easily measured *feel* for the shape of the frequency response curve; and, second, comparison of D-log E curves which must provide a given minimum, maximum, and slope. In addition, merit was definitely assigned to the time of processing at the selected temperature. The resolution data and the gamma were used as the primary numerical measures of merit; the other responses were interpreted as either satisfactory or unsatisfactory. It was soon learned that, as measures of merit, gamma and maximum density were sufficient to judge the direction the investiga-

13. W. Clatworthy, W. S. Connor, L. S. Demming, M. Zelen, R. C. Burton, F. L. Miller, Jr., and H. N. Pettigrew, *Fractional Factorial Experiment Designs for Factors at Two Levels*, National Bureau of Standards Applied Math Series, No. 48, April 1957.

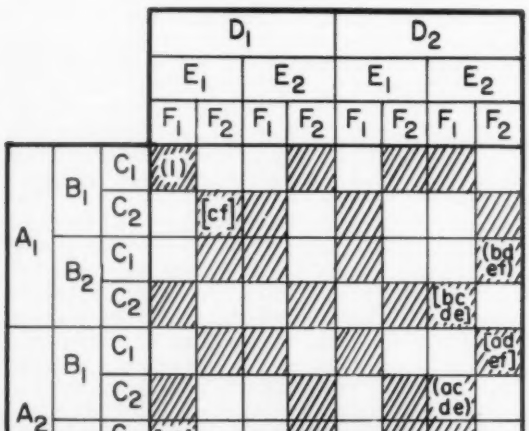

Fig. 2. Matrix representing an experimental plan for six factors. The cross-hatched squares represent tests to be performed: all factors at low level are indicated by (1) (in upper left cross-hatched square); those factors which are at high level are indicated by lower-case letters (e.g., [cf]); low level is indicated by subscript 1; high level is indicated by subscript 2; the first block of four tests is indicated by parentheses (e.g., (bdef)); the second block of tests is indicated by brackets (e.g., [adef]). The factors and concentrations were as follows:

Factor	Grams/liter	
	Low_1	$High_2$
A. Na_2SO_3	25	35
B. Hydroquinone	3	5
C. Phenidone	2	5
D. $NaBO_2 \cdot 8H_2O$	40	50
E. Sodium thiosulfate	0	10
F. Benzotriazole	0.1	0.2

14. R. S. Kardas, *Phot. Eng.*, **5**: 91 (1954).

tion should take. The first block of four tests (see Fig. 2) gave the following results:

BLOCK 1

	Gamma	Maximum density
(1) All factors in lower levels	1.38	2.1
(bdef) Factors in high concentration	1.90	2.4
(abcf) Factors in high concentration	1.14	1.8
(acde) Factors in high concentration	0.82	1.3

The estimated effect of sodium sulfite (A_1), which contained 25 grams Na_2SO_3 per liter, was computed by averaging the responses of Tests (1) and (bdef):

Gamma	Maximum density
$(1.38 + 1.90)/2 = 1.64$	$(2.1 + 2.4)/2 = 2.25$

The estimated effect of A_2, which contained 35 grams Na_2SO_3 per liter, computed from the responses of Tests (abcf) and (acde) was as follows:

Gamma	Maximum density
$(1.14 + 0.82)/2 = 0.98$	$(1.80 + 1.32)/2 = 1.56$

Thus we concluded that the higher concentration of sulfite seemed to produce a low gamma and maximum density. Hydroquinone, factor B, was associated with low gamma and maximum density at low levels and with high and medium response at high levels. The rest of the factors gave conflicting results. It was apparent that no conclusion could be drawn, so a second block of tests was run. The results follow:

BLOCK 2

	Gamma	Maximum density
(ab)	2.06	2.38
(adef)	1.88	2.30
(df)	1.32	1.85
(bcde)	1.30	2.04

Since no changes were made in the factors being tested nor in the experimental method, Blocks 1 and 2 could be grouped together. This lumping of responses from the two blocks increased the certainty with which we could draw conclusions, because the data were based on twice as many observations and on explorations of a wider area. The procedure outlined above was used, and the responses were as shown in Table I.

TABLE I

Factor	Level	Response: Gamma	Response: D_{max}	Interpretation
A. Sodium sulfite	Low A_1	1.48	2.1	Low concentration of sulfite seems to be associated with higher densities.
	High A_2	1.48	1.95	
B. Hydroquinone	Low B_1	1.35	1.90	High concentrations of hydroquinone are associated with higher gamma and higher densities.
	High B_2	1.60	2.16	
C. Phenidone	Low C_1	1.85	2.30	Low concentrations are associated with high gamma and high density.
	High C_2	1.15	1.75	
D. Sodium metaborate	Low D_1	1.48	2.03	No apparent effect; pH change is too low to cause any difference.
	High D_2	1.48	2.02	
E. Sodium thiosulfate	Low E_1	1.48	2.03	D and E are confounded since the same experiments are represented in E_1 as in D_1, as well as in E_2 and D_2.
	High E_2	1.48	2.02	
F. Benzotriazole	Low F_1	1.39	1.96	Higher concentrations are associated with higher gamma and density.
	High F_2	1.56	2.09	

Without completing the analysis of variance, more tests were indicated. For instance, the effect of the thiosulfate and the metaborate were confounded. Further, high gammas were closely tied to high maximum densities, as expected. It seemed that different variables might be explored in place of those which showed no apparent effect, and different levels might be tried. Lower and higher levels of sodium sulfite were explored. A high degree of silver solvent action was associated with sludging; hence the thiosulfate was eliminated. A much greater range of concentration of hydroquinone and Phenidone was explored, and a higher concentration of

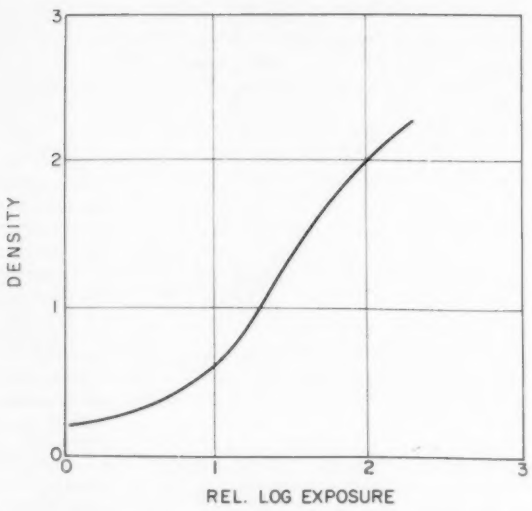

Fig. 3. Characteristic curve of rapid-processed Eastman Kodak Experimental Test Film 57-1; breadboard processor (see Ref. 3). Development time, 7 sec; temperature, 90°F. Formula: sodium sulfite, 25 grams/liter; hydroquinone, 1.0 gram/liter; Phenidone, 3.0 grams/liter; sodium metaborate, 60.0 grams/liter; plus water to make 1 liter.

hydroquinone was chosen (Fig. 3). The higher concentration of metaborate (Fig. 3) was used to improve the exhaustion characteristics of the solution, a response not sought in the initial experimental matrix. The restrainer was eliminated as unnecessary, and pH was used as a separate factor rather than various concentrations of buffering agents. The final matrix and associated computations are not shown since they are quite similar to the first.

A further technique employed was to test each experimental run in a group for gross errors. The error estimates had been established from the trial-and-error work, and by using the main effects determined by a fairly large number of experiments, the expected response from any single test run could be estimated and compared with the measured response. If the comparison was unfavorable, the test was repeated.

The main emphasis was placed on the development step, because the problem associated with it was the most difficult. Unlike development, which is terminated prior to completion, the other necessary steps—fixing, washing, and drying—go to completion. This makes the compounding of the chemical formulas for these steps easier, and it was believed that these processes could be speeded up without reticulation problems. The attainment of the fixing, washing, and drying time schedules was left to the equipment design efforts.

Results

A discussion of the effectiveness of the chemical and photometric effort would be instructive. With respect to the requirements for compatibility with 100-lines/mm photography, only rough estimates of the ultimate resolution capability or the rapid-processed film are available. However, almost no degradation of information at 150 lines/mm was observed. Some tests were made at 500 lines/mm, and it is believed that the limiting resolution of the rapid-processed film is near 1500 lines/mm.

A gamma of 1.5 was achieved, and with manipulation of development time and temperature, the gamma was adjustable through a considerable range. It was not possible to provide a constant gamma over as long a range as desired—only approximately one log-E unit was obtained (Fig. 3). When the gamma is progressively reduced, the D-log E curve tends to shoulder off at a lower maximum density, and the curved portion of the toe becomes more extensive. A total processing time of 30 sec was achieved.

	Seconds
Develop	7
Rinse	1
Fix	8
Wash	10
Dry	4
	30

Considerably shorter processing times than the above have been achieved, but mainly these were not dry-to-dry times and were certainly not for high-acuity continuous-tone reproduction

Credit for the success of this operation goes to too large a group of people for their names to be listed here. Acknowledgment is made of the assistance of H. K. Howell, who reviewed the manuscript.

PHOTOGRAPHIC SCIENCE AND ENGINEERING
Volume 5, Number 3, May-June 1961

A Design Approach to Rapid High-Acuity Processing

MALOR WRIGHT, ERNEST THOMPSON, AND IRVING SPIEGEL, *Information Technology Laboratories, Itek Corporation, Lexington, Mass.*

A breadboard processor was constructed to demonstrate the feasibility of rapidly processing single sheets of film containing both high-acuity continuous-tone images and digital information. Solutions were passed across the emulsion side of the film in the form of a thin sheet of rapidly moving liquid. Developer, rinse, fixer, wash, and drying air were sequentially programmed through the processing chamber by means of precisely timed solenoid valves. Dry-to-dry processing was achieved in 30 sec with a density uniformity of ±0.05 at a density of 1.0. High-contrast resolution of more than 500 lines/mm was achieved with a particular film and chemistry. Reasonable keeping quality was obtained with residual hypo level of 0.08 mg/sq in.

This paper discusses the development of a technique and describes the experimental equipment for the rapid processing of single film sheets containing continuous-tone information at approximately the 100-lines/mm level, together with digital data. Reproduction of this information through negative and positive generations with a minimum of degradation of the 100-lines/mm information was the prime design objective. The selection of suitable film and chemical formulation, a closely related task, is discussed in another paper.[1]

Processing Requirements

The emulsion selected (Eastman Kodak Experimental Test Film 57-1; see Ref. 1) is slow, extremely fine grained, and thin. With full development, it produces a very high gamma, in common with the Lippmann class of materials.

Detailed photometric requirements were prepared to implement the general system demands mentioned above and to guide the design phase of this effort. A gamma of 1.5 was necessary to present the input information through both negative and positive generations at a suitable contrast. The intensity of light available for viewing the output information limited the maximum density to 2.5 and required a minimum fog. The minimum dry-to-dry time believed practical was 30 sec. Since low-contrast fine-detail information must be retained, the maximum density variation over a single uniformly exposed film sheet was set at ±0.05 at a density of 1.0. The same tolerance was believed practical for sheet-to-sheet variations. It was desirable that the processor wet the emulsion side only, and that the processed film be of commercial keeping quality. The size of the film sheets selected was $2^3/_4$ by $4^1/_4$ in. Finally, the equipment would have to operate intermittently over long periods of time.

The major problems centered around (a) the short dry-to-dry time, and (b) the need to process a basically high-contrast film to a moderately low contrast, while maintaining as long a straight line as possible on the characteristic curve. Although low contrasts are achievable with single-solution developer-fixers, a conventional separate developing and fixing process was chosen to permit precise control of each step as well as to accommodate exposure and film variations. It then became part of the processing-equipment function to stop development rather abruptly at a point where the gamma was rising rapidly. Such action increased the difficulty of maintaining highly uniform and precisely reproducible results.

A nominal processing temperature of 90°F was chosen because it was believed that this temperature would be sufficiently high to permit the rapid processing desired without increasing fog unduly and without causing much film distortion. Distortion of the film is particularly undesirable because of the reproduction of fine detail and the attempt at careful mensuration.

To achieve a high degree of uniformity under these conditions, every point in the emulsion surface must be in contact with solutions of the same activity for the same short interval of time, i.e., the time, temperature, chemical concentration, and mechanical activity[2,3] of the solutions must be uniform throughout. At the interface between the emulsion and the developer, the developing solution must be renewed at such a rate that its composition is virtually unchanged by its reaction with the silver halide in the emulsion. To provide uniform processing from sheet to sheet, a replenishment solution has to be

Presented at the SPSE Rapid Processing Symposium, Washington, D.C., 15 October 1960. Received 14 November 1960; revised 28 February 1961.

1. M. Wright, R. G. Polk, and P. Fedelchak, *Phot. Sci. & Eng.*, **5:** 166 (1961).

2. J. M. Blaney, *Jour. SMPE*, **32:** 495 (1939).

3. C. E. Ives and E. W. Jenson, *Jour. SMPE*, **40:** 107 (1942).

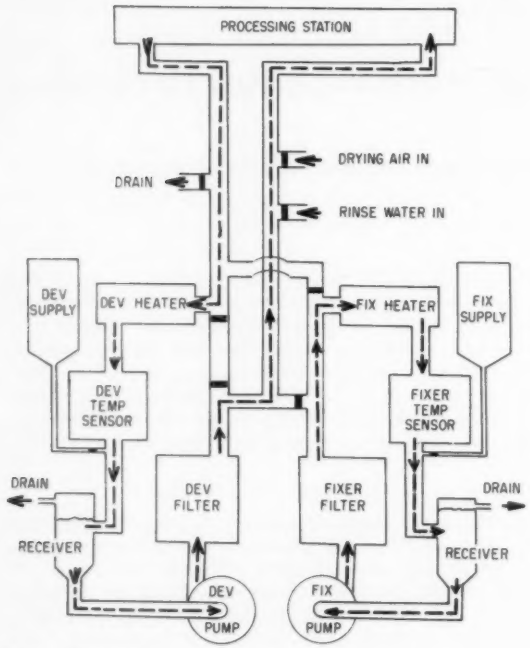

Fig. 1. Fluid system.

added in proportion to the amount of film processed.[4,5]

Approach

Several methods of application of solutions were considered. Tank processing was one method considered,[6] but a number of objections became evident. Since each processing step was to be completed in a few seconds, vigorous agitation would be required, especially during the first second or two of treatment. Further, a large transport mechanism would be required to direct the individual film sheets through the developing, fixing, washing, and drying chambers.

Roller processing similar to Russell's "X-Omat"[7] was considered, but it seemed improbable that such a technique would assure uniformity and completeness of fixing and washing in the short time proposed.

Spray processing was attempted,[8] but problems were encountered because of size, variations in aerial oxidation, and the difficulty of achieving a well-defined and measurable temperature at the film-developer interface. In addition, either the film or the spray jet would have to have been moved continuously to eliminate patterns.

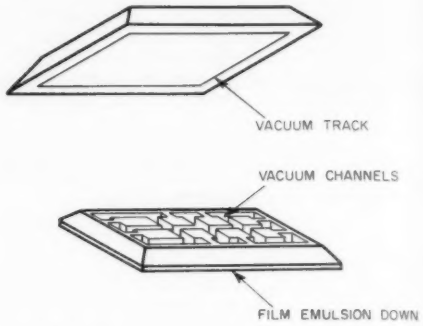

Fig. 2. Vacuum chuck.

Technique

The technique adopted, and shown to be valid in the breadboard, involves passing developer, fixer, wash water, and heated air sequentially across a stationary film surface, making it possible to adjust fluid velocities[9] independently and thus provide optimum agitation. A known volume of each of the processing solutions (i.e., developer or fixer) is retained in a separate fluid loop until required (Fig. 1). Each fluid loop consists of a receiver, pump, filter, heater, and temperature sensor, together with appropriate plumbing and valving. Each solution is thus constantly circulated within its separate loop and maintained in a state of constant readiness, regardless of whether the machine is operating. When film is being processed, precise timers open and close valves to direct solution from the loops in sequence through the processing station.

The film is held securely by the vacuum chuck (Fig. 2) in the processing station, leaving the entire emulsion surface free to be processed. The processing fluid is passed through a pipe that is in turn round, square, and then flat, fanning out to a thin rectangle slightly wider than the film. Thus the fluid is passed across the surface of the film in a thin rectangular sheet (Fig. 3). Throughout the entire processing station, the cross-sectional area of the fluid is held nearly constant to make sure that the fluid's velocity is unchanged during its passage through the applicator. Uniform cross section is necessary to maintain uniformity of fluid velocity and to eliminate the mixing of different solutions which would occur if the cross-sectional area were enlarged. With this configuration, the solutions pass across each point in the emulsion surface with the same velocity (Fig. 4).

This design is amenable to complete dry-to-dry processing in one position, which simplifies the problem of film transport; furthermore, the technique is applicable to future rapid-readout systems where exposure is made at one position, processing at the second, and viewing at the third.

---

4. H. L. Baumbach, *Jour. SMPE*, **39:** 55 (1942).
5. S. R. Goldwasser, *Jour. SMPTE*, **62:** 11(1954).
6. J. S. Goldhammer, F. J. Kelley, and C. R. DuPree, *Phot. Eng.*, **6:** 97 (1955).
7. C. J. Kunz and H. D. Russell, *Phot. Sci. & Eng.*, **3:** 27 (1959).
8. W. A. Pfaff and G. Lysle, *Phot. Eng.*, **6:** 89 (1955).
9. R. S. Kardas, *Phot. Eng.*, **4:** 169 (1953).

Film Transport

The film transport removes an individual exposed film sheet from a supply area and delivers the film sheet to the processing station, emulsion side out. A movable vacuum platen, similar to the one illustrated in Fig. 2, is used to grasp the emulsion surface of the film. The hinged cover of the processing station is then raised, the vacuum platen is moved to a position precisely in front of and against the vacuum chuck of the processing station, and vacuum is turned on at the processing station and turned off at the movable platen. The vacuum platen is then moved away and the hinged cover on the processing station is lowered to seal it. A similar mechanism is used to deliver processed and dried film sheets to a storage area.

Temperature Control

The design of the temperature control system was influenced by the requirement for intermittent operation. With each start-up of the processor, the solution must be brought quickly to the same temperature, and held at that temperature throughout the run. During the run, the film is thus processed intermittently if desired.

Sensitometric tests showed that $\pm 0.3°F$ is an adequate precision for this control. To satisfy this requirement, the temperature control system was designed to generate an error signal proportional in amplitude to the deviation of the measured temperature from a standard. An analogue of the error signal is amplified and passed through a heating element which discharges heat through an exchanger to the appropriate solution. The temperature sensor and the heat exchanger are located in the circulating loop mentioned above. With this design, close temperature control is achieved, whether film is being processed or not. Where radio noise problems are severe, this technique permits close temperature control without switching on and off electrical currents of large amperage. At start-up, this system is remarkably free from overshoot, and, during steady operation, the temperature variation is easily held to $\pm 0.3°F$. As in any servo system in which the correction is proportional to the error, some damping is necessary to accommodate the non-ideal system characteristics. In this case, these characteristics include changes in the heat capacity with temperature and, more important, in the variations in the time lag between the application of electrical energy to the resistor and its effect in heating solution. This lag is minimized by the use of highly conductive silver in the heat-exchange unit and the rapid flow of solution through the exchanger. In addition, the total volume of solution in the circulation loop is small (approximately 1 qt.).

Fig. 3. Processing station fluid path. Not drawn to scale. Processing station area is rectangular; depth of solution passing through processing station is 0.016 in.

Replenishment

Since insufficient time was available to formulate both a developing solution and a replenishment solution, the technique adopted was to circulate a small quantity of developing solution through the loop described above and to replenish this solution with a volume of developer proportional to the amount of film processed. At start-up, a small number of "dummy" film sheets are processed in the quart of solution contained in the loop. This brings the chemical activity of the "working" developer solution down to a level which can be maintained constant when reasonably small volumes of the original developer are added during each processing cycle. To accomplish this,

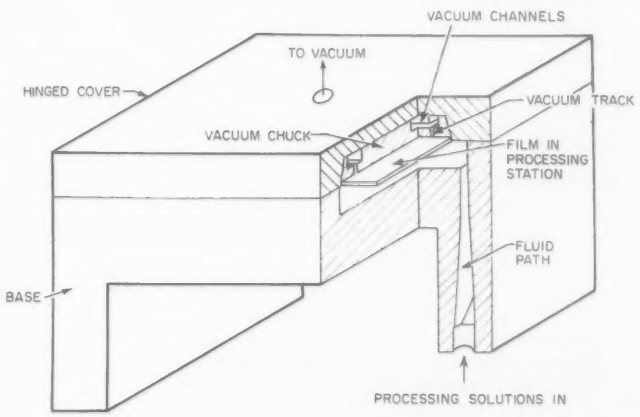

Fig. 4. Processing station assembly. Film is held by base, emulsion down, on the vacuum chuck. The passage under the film for solutions and drying air is enlarged for clarity.

a small amount of the "working" developer solution is discharged to waste and is replaced by an equal volume of fresh developer. Between the developer and fixer steps, a short (1-sec) plug of temperature-controlled rinse water is programmed. As the rinse water is discarded, a small quantity of developer and fixer goes to waste also; thus intermixing of solutions was eliminated.

The supply of developer solution is contained in a 5-gal tank, inside of which is a sealed polyethylene bag. Developer is pumped into the bag from the bottom while a pressure relief mechanism vents air from the top of the bag. As solution is withdrawn from the tank, air is admitted outside the polyethylene bag causing the bag to collapse, but contact between the developer solution and air is prevented. The developer solution is directed to the "working loop" through automatically operated solenoid valves. At the end of each cycle, when the "working loop" contains a somewhat smaller volume because of the small quantity discarded, the replenishment valve is opened, and the solution flows to the working loop until the volume is restored to its original amount. Thus constant replenishment is achieved in the loop whether the storage tank is full or nearly empty.

Drying

Filtered air at 60 lb pressure is fed through specially designed heaters to the processing station and out to waste. Drying is achieved in 4 sec[10] with air at an estimated temperature of 140°F. A special dryer design is required to provide fast heating and cooling, consistent with the need for intermittent operation. The heater reaches maximum temperature in a very few seconds, and is turned off a few seconds before the drying operation is complete. The heated mass of the dryer is small so that the cool air passing through the heater during the last 2 sec of drying will reduce the temperature of the heater to a reasonable level. The design problem was to provide a means of achieving a rapid temperature rise on start-up, and an equally rapid decrease on the termination of the drying operation. To achieve these rapid rise and decay times, the heater, which consists of spirally wound nichrome wire, is mounted in helical fashion on thin ceramic supports. The heating element is placed within a thin shell encased in a stainless-steel outer shell which contains the air pressure.

Performance

With the appropriate processing solutions, total dry-to-dry processing was achieved in 30 sec. Processing uniformity in the direction of fluid flow was ±0.05 at a density of 1.0, and in a direction transverse to the fluid direction it was ±0.02. The timing systems were accurate and repeatable to within 0.1 sec over a range of 5–20 sec. Residual hypo levels of 0.08 mg/sq in. were observed.

10. L. Katz, *Jour. SMPTE*, **56:** 264 (1951).

Back Issues Available

Photographic Engineering—1950–1956

Volumes 1 through 6 (4 issues each volume)..... $5.00 per volume..... $1.50 per issue

Volume 7 (two single issues, Nos. 1 and 2; two issues, Nos. 3 and 4, combined under one cover)..... 5.00 per volume..... 1.50 per single issue; 3.00 for combined issue

Photographic Science and Engineering—since 1957

Volume Number	Price to Members: Per single issue	Price to Members: Per volume	Price to Others: Per single issue	Price to Others: Per volume
1 and 2 (4 issues each volume)	$1.75	$6.00	$2.00	$ 8.00
3 and 4 (6 issues each volume)	1.75	$9.00	2.00	12.00
5 (current) (6 issues)	Included in annual dues	$10.00	2.00	12.00

An index appears in the final issue of each volume except Volume 6 of *Photographic Engineering*. This index was published separately and is included with the issues when Volume 6 is ordered.

Order from:

Edward S. Cobb, *Managing Secretary*
Society of Photographic Scientists and Engineers
Box 1609, Main Post Office
Washington, D.C.

PHOTOGRAPHIC SCIENCE AND ENGINEERING
Volume 5, Number 3, May-June 1961

The Printing of Underexposed Photographs by Means of "Optical Contrasters"

MICHEL CLOUPEAU, *Laboratoire de Recherches Electroniques, Institut du Radium, Paris, France*

"Optical Contrasters" are instruments which are particularly intended for the viewing or printing of very much underexposed photographic films or plates. The principle of these special photographic enlargers is that the light shall pass several times through the film, so that the contrast is approximately multiplied by the number of passages effected. In the Type A Contraster, the film is placed between two semireflecting plates, which are mounted at a very small angle to each other, and is illuminated by collimated light. The emerging light consists of beams which have passed the film one, three, five, or more times. The direction of each beam differs slightly from the others, so that it is possible to choose any one of the beams. In the Type B Contraster, the film image is re-formed on itself by means of an objective-mirror system. Several printing tests prove the efficiency of these instruments, which may lead to a systematic improvement of the performance of cameras or the utilization of accidentally underexposed negatives.

Despite the many improvements made in the manufacture of photographic emulsions, cameras, and electronic light-intensifying devices, underexposed negatives are still occasionally obtained. As the contrasts are extremely weak in the underexposed region of the characteristic curve, printing on even extra-contrast emulsions may still be incapable of making such negatives usable.

"Optical Contrasters" are special devices for making possible the viewing or the printing of greatly underexposed negatives by increasing the apparent contrast through a purely optical process.

Principle of the Apparatus

It is known that the contrast of a photographic film can be increased by placing it on a white diffusing screen; the light passes through the film twice before it reaches the observer so that the densities, and therefore the density differences, appear to be approximately doubled.

Optical Contrasters are based on this principle; however, they make it possible both to cause the light to pass through the film several times and to retain for viewing or printing only the light which has passed through the film a given number of times.

In the apparatus we have built, these multiple passages of the light through the film are obtained by two different methods,[1] which will be described in turn.

Presented at the Fifth International Congress on High-Speed Photography in Washington, D. C., 18 October 1960. Received 20 March 1961.

1. CNRS Patents: French No. 1,127,102 and No. 1,179,814; U. S. No. 2,920,527.

Type A Optical Contraster

Principle of Operation (Fig. 1)

The film F is placed between two plano-convex lenses L_1 and L_2 whose flat faces, covered with semireflecting coatings C_1 and C_2, form between them a small angle α that is less than about 30′ of arc.

The aperture in the screen D_1, where the image of a filament lamp or of a concentrated-arc lamp is formed, acts practically as a point-light source S.

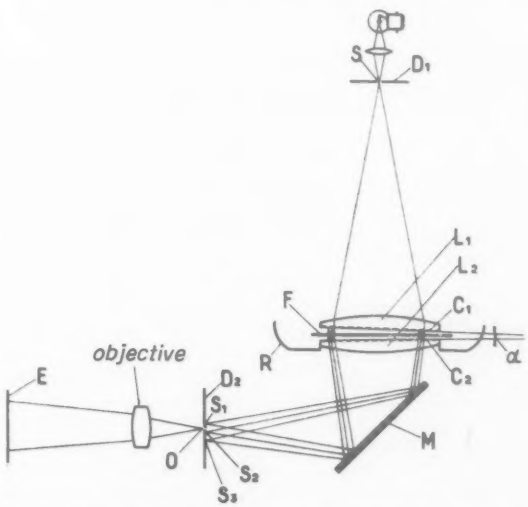

Fig. 1. Schematic diagram of Type A Optical Contraster. Semireflecting coatings are shown by broken lines. See text for identification of symbols.

The diverging beam emanating from S is made parallel by the lens L_1. Part of this beam, which passes directly through the film and the semireflecting coatings, is brought to a focus at S_1. Another part, reflected by the coatings C_2 and C_1 and then transmitted by C_2, passes through the film three times. It is brought to focus at S_2 which is separated from S_1 because the reflecting surfaces C_1 and C_2 are not parallel. Finally, there is obtained in the plane of the screen D_2 a succession of images of the source S corresponding to beams which have passed through the film once, three times, five times, etc.

An aperture O is made in the screen D_2 in such a way that, by rotating the mirror M, any of the beams converging respectively at S_1, S_2, S_3, etc., can be made to pass through O.

By placing the eye behind aperture O and by changing the orientation of the mirror M, it is possible to view the film successively, by light that has passed through it any odd number of times.

To print the film, one places behind the aperture O an objective that forms an image on the photographic emulsion E.

Contrast Gain and Adverse Effects

In view of its granular structure, a photographic film cannot be considered as an assemblage of homogeneous areas of different optical densities — that is to say, as an entire unit for which the density differences between the component areas would be exactly multiplied by the number of passages of the light.

Let us then consider the extreme case of a plate consisting of parallel strips of equal width, alternately opaque and perfectly transparent (Fig. 2).

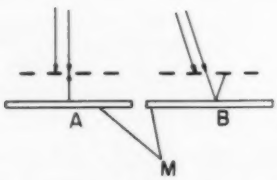

Fig. 2. Diagrammatic representation of a plate, consisting of parallel strips of equal width, alternately opaque and transparent, placed over mirror M, and illuminated by parallel light. (A) Normal incidence; (B) oblique incidence.

Let us assume that such a plate is placed over a mirror M and is illuminated by parallel light. Depending on the orientation of the beam, the light that passes through the transparent strips the first time will also pass through them the second time (Case A) or will be stopped by the absorbing strips (Case B). In Case A, an observer seeing the reflected light will see the plate just as it would appear to him as ordinarily viewed by transmission. In Case B, on the contrary, the plate will appear to be completely opaque.

Thus it can be seen that the contrast gain obtained for a photographic film through which the light has passed n times will depend both on the statistical distribution of the grains developed and on the distances (i.e., intervals) separating the successive points of passage of each light ray through the film.

But, in fact, adverse phenomena modify the gain in contrast that might be calculated from the geometrical data alone:

1. Part of the light is diffused in all directions by the gelatin during its first passage (and the following ones, too). It becomes mixed, in particular, with the beam selected for viewing, thus reducing the contrast.
2. The surface defects (unevenness), or lack of homogeneity of the gelatin and of the base, cause part of the light to be refracted outside the main beams. A "refraction image" is then superimposed on the "absorption image."
3. Partial reflections occur on both faces of the film.

It is essential to reduce these adverse effects by immersing the film in a liquid having a refractive index near that of the film. To this end, it is convenient to fill the tank R (Fig. 1) with an extra-lightweight volatile oil[2] capable of evaporating rapidly from the film without leaving a residue.

Figure 3 shows the experimental results obtained with Kodak Rayoscope Film. Curve (a) is the normal characteristic curve, and Curve (b) shows the apparent values of the optical densities of the film after seven light passages. It so happens that under the conditions of our experiments, the densities are multiplied approximately by the number n of

2. Silicone oil, Rhodorsil, 44 P., Société Rhône, Poulenc, France.

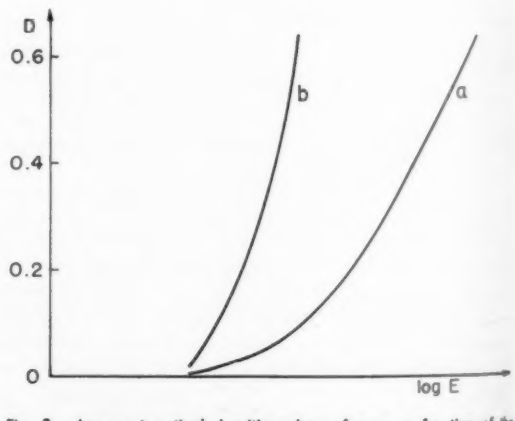

Fig. 3. Apparent optical densities above fog as a function of the logarithm of the illumination for Kodak Rayoscope Film. Curve (a), normal characteristic curve; Curve (b), apparent characteristic curve of the film viewed with seven passages of the light in the Optical Contraster.

light passages. For other emulsions, the gain may be substantially greater than n, as can be seen from Fig. 11, which relates to the printing of an electron plate.

Definition of the Images

In the Type A Optical Contraster described above, the loss of definition is caused largely by the failure of each light ray to pass through exactly the same point in successive passages through the film. This separation of the passage points through the film has two causes:

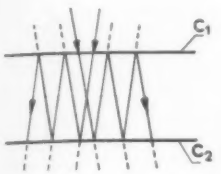

Fig. 4. Two light rays emanating from the ends of the light source S, reflected by coatings C_1 and C_2.

1. The light source S is not a perfect point; thus two light rays emanating, for instance, from the ends of the source, and illuminating the same point of the film at the time of the first passage (Fig. 4), will thereafter gradually diverge from each other.

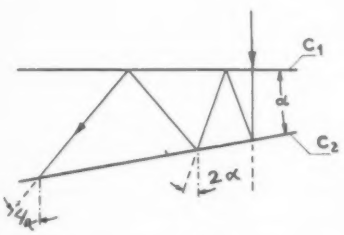

Fig. 5. Increase in the separation of successive points of passage through the film of a given light ray. C_1 and C_2 = semireflecting coatings; α = angle formed by C_1 and C_2.

2. As the semireflecting coatings form between them a certain angle α, the separation of the successive points of passage through the film of a given light ray increases rapidly with the number of passages already effected (Fig. 5). This separation of the passage points, however, can be reduced by a suitable selection of the orientation of the Lenses L_1 and L_2. Figure 6 shows the inclination that must be given to the semireflecting coatings in relation to the optical axis of the light beam in order that a ray emanating from the center of the light source S will fall on the coating C_1 at normal incidence after four passages through the film, and then retrace, in the opposite direction, the path which it has already traveled.

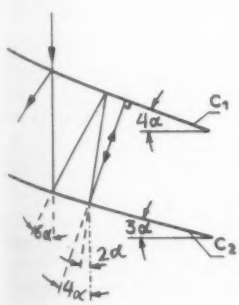

Fig. 6. Inclination of C_1 and C_2 in relation to optical axis of the light beam, in order to reduce the separation of sucessive points of passage (see Fig. 5).

In practice, the configuration of the Optical Contrasters can be arranged in such a way that a point on the film appears, after *seven passages* of the light, as a spot whose greatest dimension is less than 30 μ.

It must be pointed out that, in such a configuration, the definition of the film image formed on E would be limited by diffraction phenomena if the dimensions of the selecting hole in the screen D_2 (Fig. 1) were equal to those of the images of S. This led to the adoption, for this aperture, of a special shape (Fig. 7), which enables part of the light outside the selected beam to be received on the objective while the other beams are masked off.

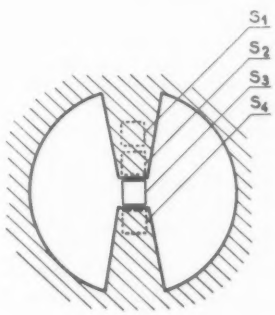

Fig. 7. Shape of aperture in selecting screen D_2 (Fig. 1) of Type A Optical Contraster.

Applications and Scope of Application

Films of low average density may benefit from a substantial contrast gain when they are viewed with the Optical Contraster. When the density is relatively high, the luminosity of the image decreases very rapidly with the number of passages made by the selected beam, while adverse effects tend to increase. Thus, for a film with tinted base having a base density of 0.3, the luminosity of the image obtained after seven passages of light would be approximately 0.01 of what it would be if the base were perfectly transparent; however, the stray light diffused at the time of the first passage into the selected beam would be, proportionally to this beam, approximately 60 times greater.

The illumination of films in parallel light causes surface defects (uneven spots) and defects of homogeneity of the gelatin and of the base to appear on

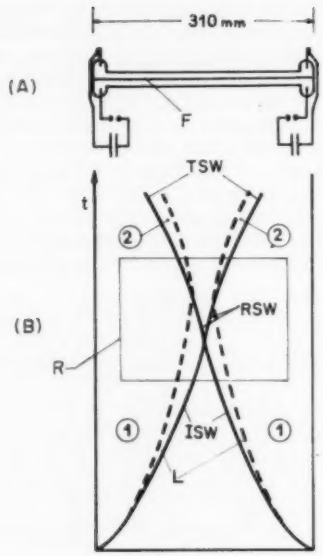

Fig. 8. (A) Magnetically-driven shock tube with two flashes. (B) Diagrammatic representation of the time evolution of phenomena occurring along slit F (Fig. 8A). 1 = luminous zones the ionization of which comes directly from the flashes; L = limit of Zones 1; *ISW* = fronts of the incident shock waves; *RSW* = fronts of the reflected shock waves; *TSW* = fronts of the reflected shock waves transmitted in the Zones 1 where they cause an increase in luminous emission (Zones 2).

the contrasted images. Such defects often become more pronounced as the negatives become older; consequently, in general, underexposed films become difficult to use a few weeks after being developed.

Most commercial films 60 mm wide give good results with the Optical Contraster. Size 24 by 36mm films with nontinted base, such as Kodak Rayoscope Film, I.R. 135 Film, Difrax Film, etc., also exhibit substantial gains in contrast.

Figures 8–11 pertain to two examples of prints made with the Type A Optical Contraster.

First example: Figure 9 relates to the magnetically-driven shock tube, shown in the diagram, Fig. 8A. The passage of two simultaneous discharges at the ends of this nitrogen-filled tube causes the sequence of phenomena shown in Fig. 8B. The Limits *L* of the luminous Zones 1, whose strong ionization comes directly from the flashes,[3] are preceded by the fronts of the shock waves *ISW*, which reflect from one another in the middle of the tube. The reflected shock waves *RSW* travel a certain distance before reaching the Zones 1, where they then propagate *TSW*, producing a substantial increase in luminous emission (Zones 2).

Figures 9A and 9B show the appearance of the prints on a film having a gamma equal to 3 from the same mirror camera streak negative (on Kodak Tri-X Film), giving the time evolution of the luminous phenomena along the slit *F* of the tube in Fig. 8A.

3. M. Cloupeau, *Compt. Rend. Acad. Sci.*, **251:** 918 (1960).

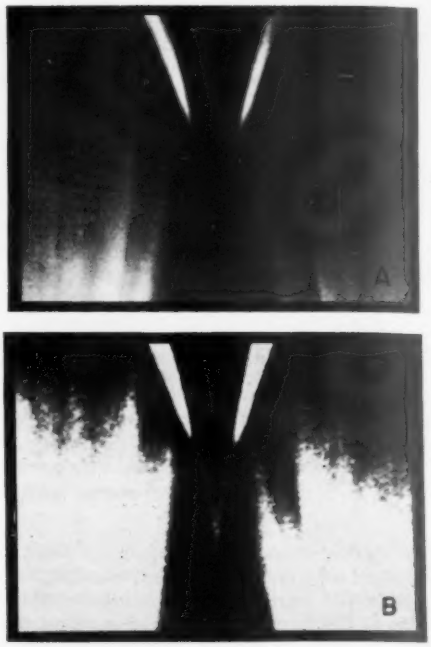

Fig. 9. Appearance of the prints on a film of a gamma of 3 from the same mirror camera negative recorded on a Kodak Tri-X Film and corresponding to the portion bounded by rectangle R in Fig. 8B. A, ordinary print; B, print made with Type A Optical Contraster and nine passages of the light. The luminous tracks of the reflected waves are clearly seen. The grain is due mostly to the irregularities of the gelatin coating of the Tri-X Film.

They correspond to the portion bounded by the rectangle *R* in Fig. 8B.

In Fig. 9B, obtained by the Optical Contraster with nine passages of the light, the path of low luminosity of the reflected shock waves is clearly visible, although it hardly appears at all on the regular print shown in Fig. 9A.

Second example: Figures 10 and 11 relate to the prints of an electron plate (Ilford G5), obtained by photographing a test object having parallel black-and-white lines by a Lallemand electronic telescope.[4] The electronic telescope is an image converter in which the photoelectrons, instead of exciting the fluorescence of a screen, fall directly on a photographic plate.

For the plate considered here,* the number of electron tracks per unit area in the most exposed regions is not sufficient to enable the lines to be seen by ordinary projection; however, it sufficiently exceeds the number of fog grains so that the "black" lines are readily distinguishable from the "white" lines in the microscope (Fig. 10).

4. A. Lallemand, M. Duchesne, and G. Wlerick, Photoelectric Image Receivers Symposium, Imperial College, London, England, 1958.

* Plate supplied through the courtesy of Messrs. Lallemand and Duchesne at the Paris Observatory.

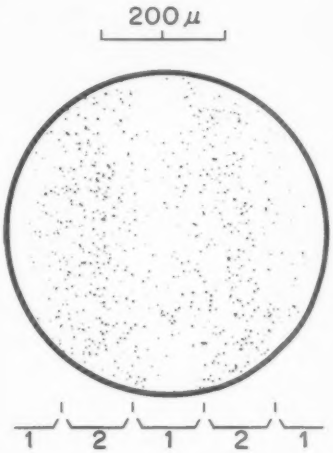

Fig. 10. Microscopic view of the distribution of electron tracks in the "white" (1) and "black" (2) lines of a test object with parallel lines, photographed with a Lallemand electronic telescope on Ilford Plate G5. (As reproduced here by line photoengraving, the points appear larger than on the original plate.)

Figure 11 shows the microphotometer traces of the prints of this test object on Kodak Micro-File Film. The lines are barely detectable in the ordinary print, Fig. 11A, but they stand out very clearly over the background in Fig. 11B, which was obtained with seven passages of light in the Optical Contraster.

Type B Optical Contraster

In the Type A Optical Contraster, the reflection coefficient of the semireflecting coatings must be relatively high (0.7 to 0.8) so that the luminosity of the various emerging beams does not decrease rapidly with the number of passages they have undergone. A large portion of the incident light is therefore reflected by semireflecting coating C_1 (Fig. 1) toward the source. Furthermore, the various beams exist simultaneously and all except one are eliminated for viewing. Thus the Type A Contraster, which is well adapted for printing on film, in practice entails exposure times that are too long for prints on papers which are slower than films. This is the reason why we have also developed another process which produces less gain in contrast, but provides brighter images than the Type A Contraster.

In this second type of contraster (Type B) (Fig. 12), the multiple passages of the light are obtained by re-forming the image of the film on itself by means of a mirror-objective system.

The film F is placed between a plane mirror M_1 and a plano-convex lens L. The image of a projection lamp (not shown) is formed on the outer face of a small prism by total reflection, and this image acts practically like a point-light source S. The beam from this source, after being reflected by the mirror M_1 and passing twice through the film, is brought to focus at S_1 which is separated from S.

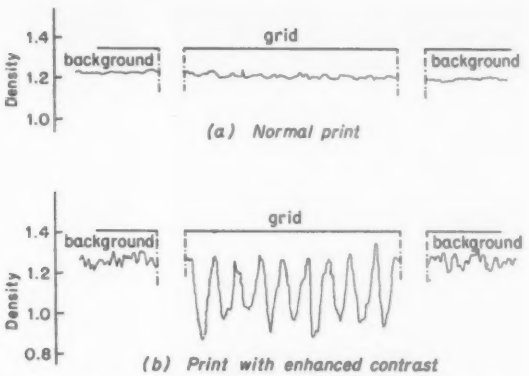

Fig. 11. Microphotometer traces of the prints, made on Kodak Micro-File Film, of the plate, part of which is shown in Fig. 10. (a), ordinary print; (b), print made with seven passages of the light in Type A Optical Contraster.

The beam then passes through the objective O_1 which forms an image of the film F in the plane of the mirror M_2. The beam reflected by M_2 is focused by the objective O_1 at S_2 and re-forms an image of the film on itself. The beam passes twice more through the film, and is then brought to focus at S_3 from whence it can be sent back to the O_1–M_2 system as before, or, as shown in Fig. 12, sent by the mirror M_3 to objective O_2. This objective forms an image of the film F in the plane of the photographic emulsion (or of the screen) E, and this image is more contrasty than the negative itself.

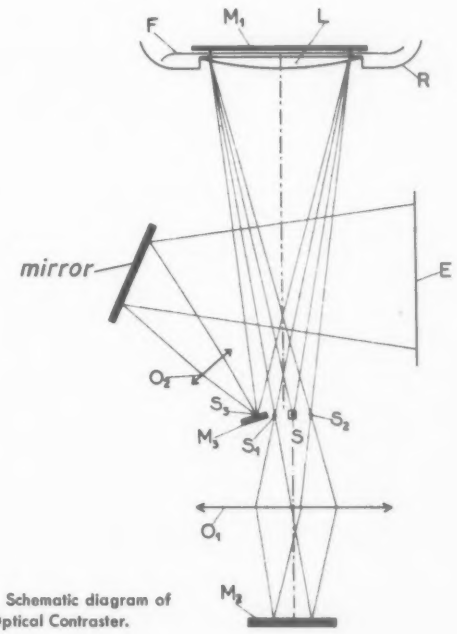

Fig. 12. Schematic diagram of Type B Optical Contraster.

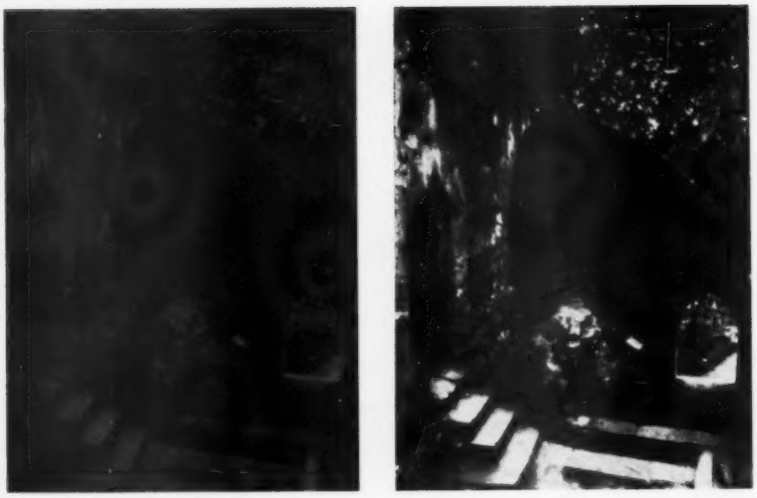

Fig. 13. *Left*, ordinary print; *right*, print made with four passages of the light in Type B Optical Contraster. Both prints were made from the same negative; and the same grade of paper was used for both prints.

In this type of apparatus, the number of passages through the film to which the light can be effectively subjected is limited, at present, to four. One reason for this limitation is stray light and another is the loss of definition in the final image resulting from multiple passages of the light beam through the objective O_1.

Figure 13 shows two prints, on paper of the same grade, of an underexposed negative made on Ferrania Film 28. Figure 13A is a print of the usual type while Fig. 13B is one obtained by the Type B Optical Contraster with four passages of the light.

Conclusion

The examples of prints which have been presented show that, in the field of photography, Optical Contrasters have numerous applications for both printing and viewing underexposed negatives. It may be expected that special studies—concerning, for instance, the behavior of emulsions in the threshold exposure region, and the effect of methods of latensification on the characteristic curve in this region—will make it possible to improve further the results already obtained with the Optical Contraster for better camera performance.

Editor's Note: The Fifth International Congress on High-Speed Photography was sponsored by the Society of Motion Picture and Television Engineers and supported in part by the Departments of Army, Navy, and Air Force through a grant administered by the Chief Signal Officer of the Army. Congress papers and related discussion will be published in the *Proceedings* of the Congress by the SMPTE.

PHOTOGRAPHIC SCIENCE AND ENGINEERING
Volume 5, Number 3, May-June 1961

• Discussion and Evaluation

Equivalent Dyes for Color Films with Incorporated Colored Couplers

ALBERT J. SANT, *Color Technology Division, Eastman Kodak Company, Rochester, N.Y.*

For color films with incorporated colored couplers, two sets of spectral density distributions are important. One set shows the spectral density distributions obtained by spectrophotometry of actual dye deposits. The second set, called the equivalent dyes, represents the contributions of the individual layers to the observed variations in spectral density obtained by varying exposures on normally manufactured and processed film. A method of determining the equivalent dyes from spectral data is described, and the results of the suggested procedure are given for a typical color negative film.

With this information the photographic engineer will be in a favorable position (1) to make more valid intercomparisons among products and among densitometries, and (2) to synthesize spectral distributions that agree with those observed by spectrophotometry of actual patches.

Since the inception of modern color photography, engineers and scientists in the field have found it important to have data available that describe the spectral properties of a given color film. For the quality control engineer this information provides a means for estimating the visual significance of densitometric measurements, the changes in sensitometric H&D curves induced by variations in densitometer filters, and the relations between integral densitometry and equivalent neutral densitometry. For the photographic engineer concerned with the design of color films these spectral data are essential to predicting the color appearance of film patches.

To be suitable for these purposes, the spectral density data supplied should provide estimates of the spectral distributions of the dyes of a film process that (a) match closely the spectral density distributions obtained by spectrophotometry of actual dye deposits and that (b) in linear combination account for the observed variations in spectral density obtained by varying exposures on normally manufactured and processed film.[1]

Once a set of spectral distributions has been determined that in linear combination accounts for the observed variations in spectral density for a given color film, any other set of spectral distributions formed by linear combination of the first set would serve to satisfy (b). Thus an infinite number of spectral distributions can, in general, be found that satisfy requirement (b) alone. When possible, a set that satisfies (b) is chosen that matches closely the spectral distributions obtained by spectrophotometry of actual dye deposits. Color films intended for direct viewing employ couplers that are colorless. For such films, requirements (a) and (b) given above may be met simultaneously by a single set of spectral distributions.

Received 24 October 1960.

1. E.g., see R. H. Morris and J. H. Morrissey, *J. Opt. Soc. Am.*, **44**: 530 (1954).

In the case of color negative films that are intended primarily for use in the preparation of color prints, it is a distinct advantage to use incorporated couplers that are colored. The nature and advantages of colored couplers are discussed at length in a paper by Hanson[2] and will not be elaborated in this discussion. Briefly, colored couplers serve to eliminate, in whole or in part, the effect upon the color print of the unwanted absorptions of the dyes in the color negative film image. The manner in which colored couplers act to accomplish this function will become more apparent in the discussion below under *Theory*.

In the past it has been customary to present the same kind of spectral distributions to characterize a color negative film employing colored couplers as the kind of spectral distributions used for color films employing colorless couplers. Customarily, these would consist of the spectral densities of a normally manufactured and processed, neutrally-exposed film patch and the spectral density contributions of the component layers. For color films employing incorporated colored couplers these distributions, while satisfying requirement (a), fail to satisfy requirement (b). To satisfy requirement (b) it is necessary to present additional spectral distributions. These additional spectral distributions would account for the observed variations in spectral density for such a film. For a number of years some advanced workers have been able to derive and to make good use of such distributions. Experience has shown more and more that, if these distributions were made available, they would provide a useful tool for any photographic engineer or scientist concerned with the design or manufacture of this type of color film. The purpose of this tutorial paper is to outline the theory underlying the determination of such distributions and to indicate some applications of these distributions to problems in color photography.

2. W. T. Hanson, Jr., *J. Opt. Soc. Am.*, **40**: 166 (1950).

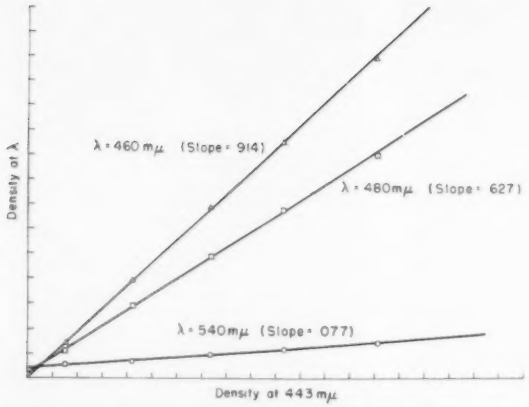

Fig. 1. Plots of the density at wavelength λ vs. the density at 443 mμ for a concentration series of a yellow dye having a peak absorption at 443 mμ.

Theory

A number of methods may be used for obtaining satisfactory estimates of the dyes in a color film. While these methods vary considerably in their complexity, they all depend upon the assumption that over a suitable range of concentrations of the dye, the ratio of the densities of the dye at any two wavelengths is constant. Dyes that satisfy this requirement are said to obey the "proportionality" rule.

For photographic dye systems that obey the proportionality rule, it is easy to obtain an estimate of the spectral density of the assumed dye from spectral density data for a series of patches containing a single dye in varying concentrations. One simply plots the density at a given wavelength for each dye patch as "*y*" against the density at the wavelength of peak absorption for the same dye patch as "*x*," as shown in Fig. 1. Sixteen such plots are required to specify the assumed dye at 20-mμ intervals from 400 through 700 mμ.

The slope of the best straight line through the points of such a plot for each given wavelength is then determined. This slope is the ratio of the density of the dye at that wavelength to the density at the wavelength of peak absorption. A plot of the *slopes* thus obtained at every wavelength gives an estimate of the spectral densities of the dye of the process normalized to a density of 1.0 at the wavelength of peak absorption. Figure 2 is an example of such a curve for the yellow dye of a typical color negative film. The spectral distributions obtained by this method satisfy requirement (b) above. The conformance to requirement (b) is readily tested by fitting the spectral distributions of the dyes to the differences among the spectral densities of a suitable number of normally manufactured and processed film patches that have been exposed to a variety of colors and light levels.

The spectral distribution used as an illustration above (Fig. 2), in addition to satisfying requirement (b), also satisfies requirement (a) since no colored coupler is involved for this dye. However, as will be shown below, in those cases where an incorporated colored coupler is involved, no single spectral distribution is possible that can satisfy (a) and (b) simultaneously. That is, separate spectral distributions are needed, one to represent the spectral density distributions obtained by spectrophotometry of actual dye deposits that include any residual colored couplers, and a second set, the "equivalent" dyes, that will satisfy requirement (b), as already indicated.

For the case of a dye layer that contains a colored coupler, colored coupler is used up in *proportion* to the amount of dye that is formed. The loss in spectral density due to loss in colored coupler is therefore proportional to the increase in the amount of the dye formed. Thus, for a series of single dye patches of varying concentration, a plot of the densities of the patches at any given wavelength against those at the wavelength of peak

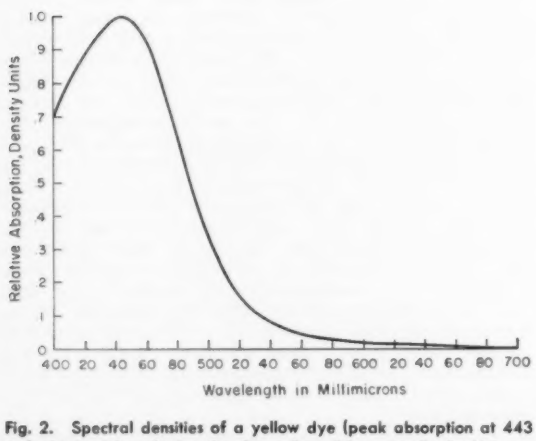

Fig. 2. Spectral densities of a yellow dye (peak absorption at 443 mμ) obtained by plotting the slopes from 16 curves, 3 of which are shown in Fig. 1, against the corresponding wavelengths λ.

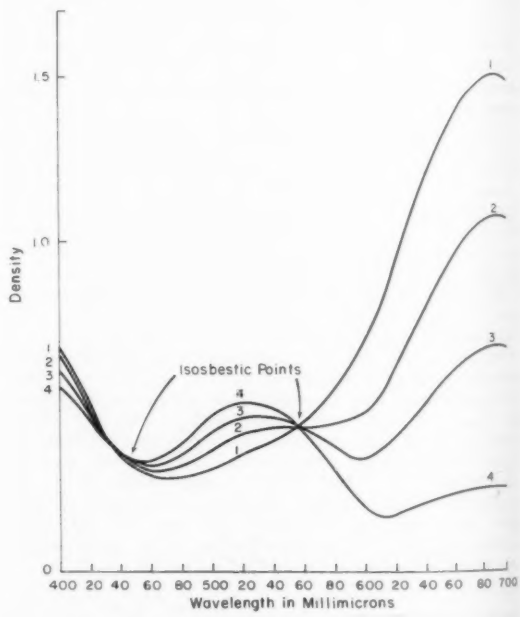

Fig. 3. Spectral densities of a cyan dye with its associated colored coupler at a series of concentrations.

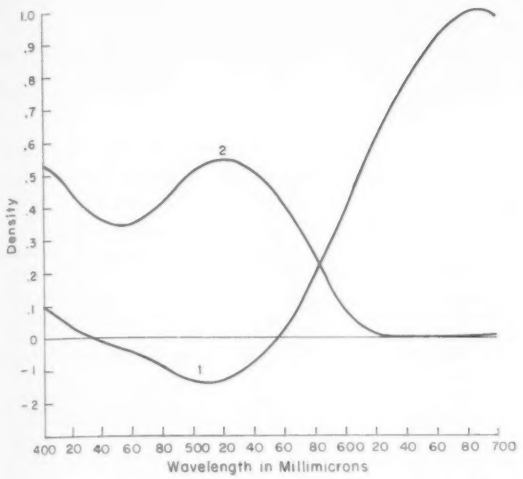

Fig. 4. Curve 1, equivalent cyan dye derived from data of Fig. 3. Curve 2, maximum density of the colored coupler in the cyan-forming layer.

absorption will again yield a straight-line relationship. In this case, however, the straight lines may have negative slopes in the regions of peak absorption of the colored coupler.

In the case of the color films that employ uncolored couplers, it is convenient to think of the slopes at each wavelength for a given dye as the spectral "densities" of the dye at a concentration for which the density at the wavelength of peak absorption is unity. Similarly, in the case of films employing colored couplers, it is useful to think of the slopes as spectral densities and to think of those regions where the slopes are zero or negative as regions of "zero" or "negative" absorption. This is in fact the manner in which the effective dye actually behaves. In what follows, therefore, this viewpoint will be adopted.

For dye layers employing colored couplers then, the equivalent dye shows the combined effect of the loss in colored coupler and the formation of dye. Thus an equivalent dye shows zero absorption at those points where the combined action of dye and coupler is such that the density of a film patch does not change with changes in the concentration of the dye. Such points, the so-called isosbestic points,[2] are the points of intersection of a family of conventional spectrophotometric curves of the dye with its associated colored coupler at a series of concentrations plotted on the same sheet (Fig. 3). In those regions where the equivalent dye has negative "absorptions," the combined action of the dye and the coupler is such that the density decreases as dye is formed. Regions where this is the case are called regions of "overcorrection" (overcorrection for the unwanted absorption of the dye). Outside the regions of principal absorption, regions in which the density increases with dye concentration are called regions of undercorrection. Figure 4 shows the equivalent cyan dye (Curve 1) and the spectral density of a patch where no cyan dye has formed (Curve 2), corresponding to maximum density of colored coupler. The equivalent dye of Fig. 4 was obtained from the data of Fig. 3 by the method described above. By close examination of the two figures, one can observe quite readily the relationship between the curves

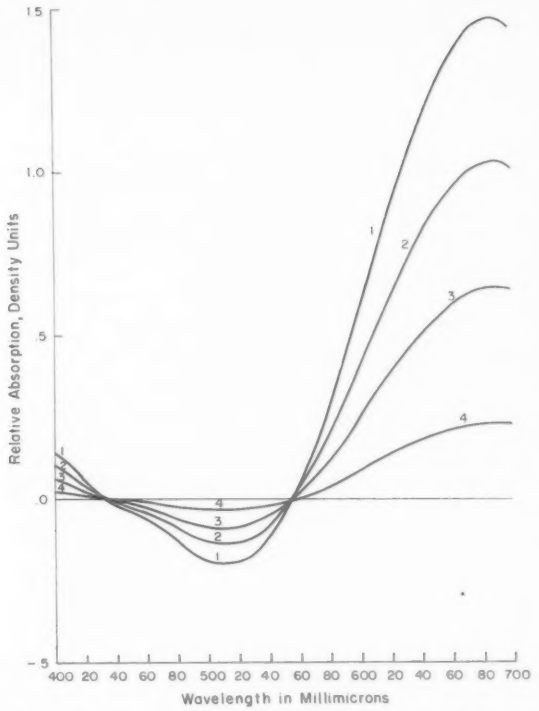

Fig. 5. Equivalent dyes for the same concentration series of the cyan dye shown in Fig. 3.

for the concentration series of the dye and the curve for the equivalent dye. Figure 5 is a plot of the spectral densities of the equivalent dye at the same concentrations as shown in Fig. 3. The individual curves of Fig. 5 are obtained from those of Fig. 3, by subtracting from the

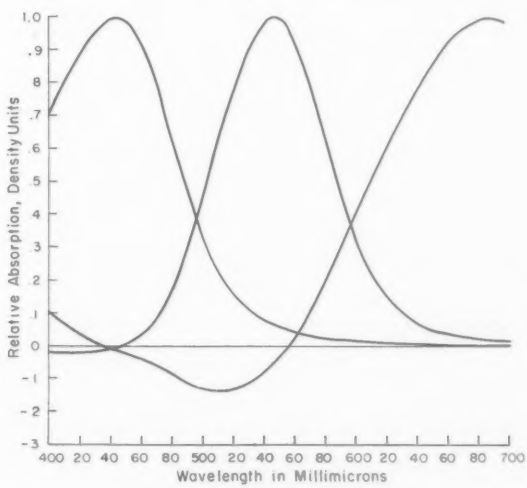

Fig. 6. Spectral densities of the equivalent dyes for a typical color negative film.

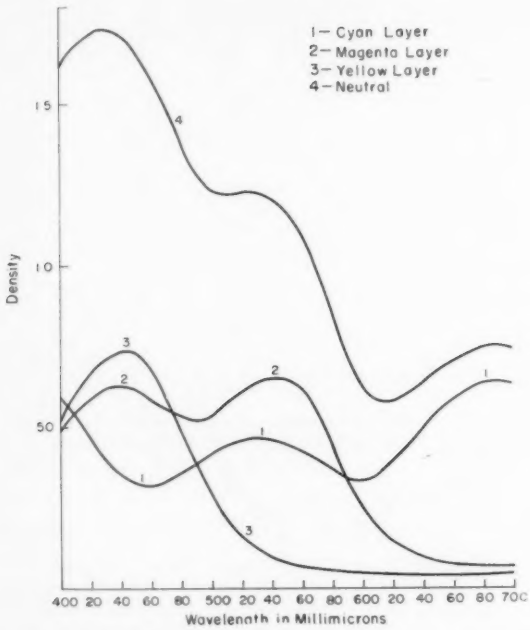

Fig. 7. Spectral densities of a typical neutrally-exposed dye patch and the spectral densities of the component layers.

curves of Fig. 3 the spectral densities of the colored coupler employed in the cyan layer of the film (Fig. 4, Curve 2).

The spectral densities of the equivalent dyes for a typical color negative film are shown in Fig. 6. The spectral densities of a typical neutrally exposed dye patch and the spectral densities of the component layers for the same film are shown in Fig. 7. Figure 8 shows spectral densities corresponding to the maximum density amounts of the colored couplers (Curves 1 and 2), the residual or stain density (Curve 3), and the composite density obtained by spectrophotometry of a typical unexposed normally processed patch (Curve 4).

In the case of a color film that uses uncolored couplers, the spectral density of a patch may be fitted by a linear combination of the cyan, magenta, and yellow dyes, plus the spectral density of the stain (or D_{min}). For color films containing colored couplers, a completely analogous situation exists. The spectral density of a patch may be fitted by a linear combination of the equivalent dyes plus the spectral density of the D_{min}. In this case, however, the minimum density corresponds to the maximum-colored coupler density, which is comprised of the density of the colored coupler at full concentration plus the process stain. Thus, the individual components of Fig. 7 are the sum of the spectral densities of the equivalent dyes in the amounts in which they are present in the neutral patch of Fig. 7 and the appropriate colored coupler densities from Fig. 8.

Plots of the equivalent dyes of a film employing colored couplers are extremely useful. (1) They permit ready

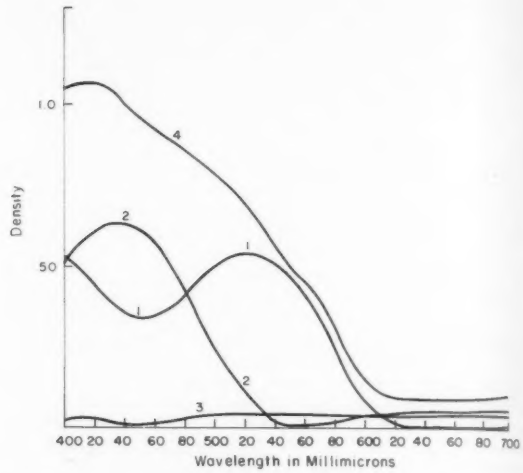

Fig. 8. Density contributions of (1) colored coupler of cyan layer, (2) colored coupler of magenta layer, and (3) residual stain to (4) density of composite unexposed patch.

observation of the properties of the dye system without resort to the use of families of spectrophotometric curves; (2) they permit easy discrimination of differences between the spectral densities of similar dye systems that would be difficult to observe from the spectral density distributions that occur in real film patches.

Summary

It has been shown that it is possible to derive spectral distributions, called the "equivalent dyes," that account for the observed variations in spectral density obtainable in a color film employing incorporated colored couplers. The equivalent dyes for a color negative film employing colored couplers are derived in a manner completely analogous to that used for determining the spectral distributions of the dyes for color films employing uncolored couplers. The spectral distributions that we call the equivalent dyes take on negative values in certain regions. For purposes of discussion, it is useful to think of the dyes as having negative "absorptions" in these regions, thus implying that increasing the amount of the dye leads to a drop in the spectral density of the dye image in these regions — which is indeed the case.

The equivalent dyes, then, show the combined effect upon a color film image due to the loss of colored coupler and the formation of dye. The equivalent dyes are therefore most useful for analytical purposes and for synthesizing the spectral density distributions that arise by varying exposure on normally manufactured and normally processed film patches. The equivalent dyes are an essential part of the description of the spectral properties of a color film employing colored couplers and, together with the spectrophotometric curves of actual film patches, normally presented, provide a more complete description of this type of color film.

• Book and Journal Reviews

The Technique of Photomicrography

DOUGLAS F. LAWSON, Macmillan, New York, 1960, xvi + 256 pp., illus., 4 color plates, 6 by 9 in., $12.75

On the front flap of the jacket, the publisher introduces *The Technique of Photomicrography* as a survey of the field. This reviewer cannot think of a better term for the category of books to which D. F. Lawson's *Photomicrography* belongs. It is not a textbook or manual outlining in detail the procedures which must be followed to obtain good photomicrographs. It gives many useful hints to this effect, but in a rather unsystematic way, scattered here and there in the text. It is also not an introduction to the optical and photographic principles and theories which are the basis of the technique. Where attempts in this direction are made, they are geared to the understanding of a technician without knowledge of the terminology of physics and chemistry.

As a survey, the book is very informative and of very wide scope. It describes a large variety of equipments, making use of over 100 good diagrams and many photographs. The majority of the 71 black-and-white and four color plates of excellent printing quality illustrate applications of photomicrography to many fields of science and technology. They also emphasize the character of the book as a survey: whereas in a textbook it would certainly be desirable to show a few samples of perfect work, relatively little can be learned about the technique from such an accumulation of pictures, even when exposure and equipment data are given, as is the case in this book.

The material is arranged in 16 chapters covering details of the following general areas: the microscope and its components; sources and special methods of illumination; the camera; special techniques of application; the photographic process; preparation of specimens. A short glossary of terms and a bibliography are also provided. A very large part of the book—more than one third—is devoted to sources and methods of illumination, and here the reader will find information not ordinarily available in books on photomicrography. The latest developments in lamps are covered very thoroughly; even circuit diagrams for special lamps such as xenon arc are shown. Under "Special Methods of Illumination," fluorescence and x-ray microscopy are mentioned, as well as application of interference (Tolansky multiple beam, etc.) and phase contrast, but the discussion of the basis and implications of these methods is not very informative. In contrast to the attention devoted to illumination, the treatment given the camera and the photographic technique is somewhat superficial. In a section on color material, only Ferraniacolor receives a broader description, including formulations for processing solutions.

The chapter on mounting and staining of specimens is very helpful. Here the book is far more than a survey; it shows in step-by-step procedures the technique of preparing material for successful examination under the microscope.

The glossary shows repeatedly the dangers of trying to explain well-defined physical concepts in popular terms. According to Mr. Lawson, the "focal length" is "the distance of the image from the nearest focal plane within the lens," and "aspheric" is "a term applied to a lens which forms an image in a parabolic surface rather than in a spherical surface." In some cases, the glossary seems to contradict the text, e.g., on phase contrast. This is, of course, a subject where any attempt at elementary explanation must fail, and the three pages of the book will not tell the reader why and how phase contrast works. Furthermore, the explanations are not even consistent. In the text, page 122, the author says that in ordinary work (i.e., not using phase contrast), we rely on differences in optical density to form an image. According to the glossary, "phase contrast enables slight differences in optical density . . . to be seen as differences of contrast."

The bibliography lists books as well as papers published in journals, and here again the author is not quite consistent. Numerous references are given by inserting name, volume, and page of the source between sentences in the body of the text. Other papers and books are listed in the bibliography at the end of the volume. The principle for selecting one or the other form of reference does not become apparent.

A typographical error may appear in any book and need not be mentioned, but when names are given incorrectly, the errors become more serious: on page 102, H. Siedentopf's name is misspelled, and on page 54, W. and L. E. Gurley Co. of Troy, N.Y., becomes Curley Troy, N.Y.

The microscopist or photographer seeking instruction in the artful technique of photomicrography is advised to turn to other sources of information. If a review of the applications, equipments, and techniques is desired, D. F. Lawson's book will prove to be reliable and up to date. — *Karl G. Leistner, U.S. Army Signal Research and Development Laboratory, Fort Monmouth, N.J.*

The Technique of Optical Instrument Design

R. J. BRACEY, English Universities Press, Ltd., London, 1960, and Macmillan, New York, 1961, xiii + 316 pp., $9.00

This volume is misnamed, in the reviewer's opinion, because it deals chiefly with the design of lenses (i.e., the removal of aberrations), rather than of instruments in their entirety. Considered as a text on lens design, it is necessarily much less detailed than Conrady's *Applied Optics and Optical Design* (300 small pages compared with 800 large ones), but for this very reason it is more synoptic and makes the interrelationships of the concepts clearer than does the larger text, to which it may serve as an introduction. The ray-tracing procedures are designed for desk calculators and thus can be followed by a lone worker.

An unimportant mistake is the accent on the *e* in Ernst Abbe's name. (Ernst's ancestors were French Huguenots but they had dropped the accent when they settled in Germany.) The author speaks of "image assessment" where he clearly means "image appraisal" ("to assess" means "to make a valuation for the purpose of taxation"). This misuse of the word is so common as to be hardly worth noting, but why use an unsuitable word when a suitable one is available? A more serious fault is the lack of bibliographical references, which is a great hindrance to a reader who wishes to pursue a particular point further.

Photography is given one brief and unhappy section. Reference to the revised edition of Mees's *The Theory of the Photographic Process* would have avoided the misleading definitions of latitude and contrast and the obsolete values of resolving power. The chapter on image appraisal is weak in not describing modern methods of measuring the spread function and sine-wave response of lenses and photographic emulsions, especially since these concepts are being increasingly used for designing photographic systems.

This book may not be of direct application in helping a photographer to choose between different brands of camera lenses, but it gives a good insight into the methods of the lens designer and the terms he uses, and it may help the instrument designer or user to select a suitable type of lens for an unusual job. — *F. H. Perrin, Eastman Kodak Company, Rochester, N.Y.*

Zhurnal Nauchnoĭ i Prikladnoĭ Fotografii i Kinematografii

Vol. 5, No. 5, September–October 1960 (in Russian)

Résumés by S. C. Goddard

The Influence of Silver Sulfide Impurities on the Spectral Absorption of Silver Halide Emulsions Photochemically Colored at Low Temperatures

T. Ya Sera and A. G. Gumenyuk, pp. 321–26

Spectral absorption curves of a fine-grain silver bromide emulsion were obtained at temperatures ranging from 20° to −163° C. At 20° the absorption curves showed peaks at about 270, 405, and 530 mμ, with a number of more or less well defined secondary peaks. As the temperature was lowered, the peaks at 405 and 530 mμ became smaller and disappeared completely at −163°. A similar emulsion containing 0.02 mole % silver sulfide showed no fine structure but was otherwise similar to the first emulsion. Similar results were obtained with 0.2 mole % silver sulfide, but as the temperature was lowered the intensity of the peak at 530 mμ fell sharply and had almost disappeared at −163°. The peak at about 405 mμ behaved similarly. Further increase in the silver sulfide content smoothed out the curves still more so that at 5 mole % silver sulfide the peaks had practically disappeared. However, lowering the temperature caused a fall in absorption over most of the wavelength range. This concentration of silver sulfide would be beyond the limits of the solubility of silver sulfide in a silver bromide emulsion and the excess would be expected to act as a desensitizer. Up to 1 mole % of silver sulfide had no significant effect on the absorption curve. A photochemically-colored silver chloride emulsion gave a spectral absorption curve also with three distinct bands with peaks at about 275, 385, and 530 mμ. The absorption spectrum of a silver chloride emulsion with the addition of 0.02 mole % silver sulfide hardly differed from the absorption of the pure emulsion. Lowering the temperature at the time of exposure produced a nonuniform lowering of absorption, the effect being greatest at the longer wavelengths. When 5 mole % silver sulfide was present, the three bands still remained visible at low temperatures but had practically disappeared at −163°. The interpretation of the long-wave band in these spectra is difficult, but the band disappears when an emulsion containing silver sulfide is oxidized with a dichromate solution. This implies that the centers causing the absorption are mainly on the surface of the grains. Protracted exposures at the lowest temperature (−163°) give rise to absorption spectra which are taken to support the view that silver sulfide plays only a minor role in the nature of the sensitivity to light and the formation of the latent image.

The Applicability of Bouguer's Law to the Absorption of Light by Silver Bromide Crystals

S. G. Grenishin, L. S. Nikolaevskiĭ, and A. A. Solodovnikov, pp. 327–30

Bouguer's (Lambert's) law has been frequently used in studies on the absorption of light by silver bromide crystals, but doubts have been expressed on its applicability when the optical density is high. The absorption of large silver bromide crystals grown from the melt between glass plates has been studied over the region $\lambda = 405$ to $\lambda = 470$ mμ, the optical densities being of the order of 5–6. Values of the absorption coefficient for different wavelengths and different thicknesses of crystal are tabulated, and it is concluded that within this range of wavelengths and densities the absorption coefficient does not alter with thickness of the material; hence Bouguer's law is applicable to silver bromide crystals in this range.

A Study of the Temperature Dependence of Photographic Development—VI. Reduction of Silver Bromide Sols and of the Silver Salts of Benzotriazole and 5-Methyl-7-Hydroxy-2,3,4-Triazaindolizine

V. I. Sheberstov, M. S. Borodkina and V. P. Donatova, pp. 331–33

It has been suggested that an antifogging agent added to an emulsion or developer forms an adsorbed layer of its silver salt on the surface of a silver bromide grain, the silver salt of the stabilizer having a higher activation energy of reduction than that of silver bromide. This has been tested experimentally by studying the reduction by a photographic developer of silver bromide, the silver salt of benzotriazole, and the silver salt of 5-methyl-7-hydroxy-2,3,4-triazaindolizine. The reduction of the silver benzotriazole salt proceeds much more slowly than that of the silver bromide, while the silver salt of the triazaindolizine compound is reduced more rapidly. From this it is concluded that the activation energy of the benzotriazole salt is higher than that of the silver bromide, which in turn is higher than that of the triazaindolizine salt. This agrees well with the fact that benzotriazole has marked antifogging powers in a developer while the triazaindolizine compound has no antifogging action in the developer. The stabilizing action of the latter compound in digestion and keeping of an emulsion must therefore be explained by some other mechanism.

The Influence of the Concentration of Developing Agents on Rapid Development: III—A Study of Different Developing Agents

P. I. Levina and V. A. Veĭdenbakh, pp. 334–42 (for Part I, see p. 20 (*P S & E*, **4**: 306) and for Part II, see p. 241 (*P S & E*, **5**: 118)

The effect of concentration on developing action was studied for three groups of developing agents at high pH:

Group 1, Phenidone and Metol; Group 2, *p*-aminophenol, pyrocatechol and *p*-phenylenediamine; Group 3, hydroquinone and *p*-hydroxyphenylglycine. The concentrations used ran up to 0.5 mole/l except in the case of Phenidone, the concentration of which was limited by its poor solubility. The first group showed no induction period at any concentration, and potassium bromide over a wide range of concentration showed no effect on the developed density. The second and third groups showed increasing induction periods, which decreased as the concentration of developing agent was raised. Potassium bromide has a noticeable influence on the rate of development of substances in the third group at all concentrations and on those in the second at small concentrations. Fogging action of the developers decreases in the order Group 1 > Group 2 > Group 3. *p*-Phenylenediamine is an exception in Group 2, having fogging properties similar to those of Group 3. All the results can be explained by the effect of the charged groups of the developer ions on their ability to overcome the charge barrier on the silver halide grains, and the difference between the rates of reduction and solution of the exposed silver halides. Additivity and superadditivity in Metol-hydroquinone, Phenidone-hydroquinone, and Phenidone-pyrocatechol developers were also studied.

The Basis of a Power Source for Rapid Between-Lens Photographic Shutters

I. I. KATKOV, pp. 343–51

A mathematical analysis is made of the mechanics of the between-lens iris shutter, and of the action of a spring used as a source of energy for driving the shutter mechanism.

The Problem of the Reproduction of Intermediate Tones in Electrophotography

YU. A. ZIBUTS AND L. J. NYUN'KO, pp. 352–55

The voltage drop on exposure of a charged zinc oxide semiconducting surface varies with the initial voltage. The curve of voltage drop against initial voltage consists of two parts at lower intensities, but becomes a straight line as the intensity is raised. Log voltage-drop against log E curves show an initial straight-line portion turning over into another section with a much smaller slope. In the reproduction of a range of tones, therefore, the potential drop on a zinc oxide electrophotographic plate will be independent of the initial voltage with a high intensity of illumination but will vary with initial voltage for intermediate tones. In such cases, the voltage drop will not depend linearly on the exposure. Correct tonal rendering in the potential relief image can only be obtained at low intensities and short exposure times. Sensitization with eosin cuts down the working range still more. Other variations in the image may, of course, be introduced in the development of the image.

High-Speed Stereoscopic Cinematography and Projection

V. V. GARNOV AND A. S. DUBOVIK, pp. 356–60

A brief description is given of the stereoscopic attachment which has been devised in the Institute of Chemical Physics of the Academy of Sciences, U.S.S.R., for use with the SFR high-speed camera. The picture so obtained can be used for stereoscopic projection. A frame frequency of 1,250,000/sec is claimed.

The Conversion of Impurity Centers in Accelerated Aging of a Photographic Emulsion

R. A. LEVITSKAYA, ZH. L. BROUN, AND K. V. CHIBISOV (Letters to the Editors), pp. 361–63

The spectral absorption due to impurity centers has been studied as a function of aging for Lippmann-type emulsions of silver bromide and silver chloride. Aging appears to be analogous to digestion. The spectral absorption curves show maxima corresponding to the keeping time at which speed reaches a maximum, in the case of silver bromide, or the time in which fog reaches a maximum, in the case of silver chloride. The results confirm the contention that the changes taking place during the aging of photographic material are similar to those taking place during the digestion of the emulsion.

Silver Chlorobromide Emulsions with Grains with a Layered Structure

YU. M. PROKHOTSKIĬ AND YU. B. VILENSKIĬ (Letters to the Editors), pp. 363–64

Chlorobromide emulsions were prepared with grains with a silver bromide core and silver chloride envelope (**I**), grains with a silver chloride core and silver bromide envelope (**II**), and grains with a solid solution structure (**III**). Grain counts in emulsions of types (**I**) and (**II**) show that no further crystal centers are formed when the second halide is added and that the new halide is deposited entirely as an envelope on the grains present. Curves showing equilibrium pAg against silver bromide content confirm the layered structure of the grains. Curves of the wavelength of the longwave edge of spectral sensitivity against content of silver bromide show that this wavelength is an additive function of composition in case (**III**) but is more complicated in the other two cases.

A Study of the Mechanism of Sensitization of a Photographic Emulsion by Gold Salts

I. M. RATNER (Letters to the Editors), pp. 365–67

The growth of the fog level of an emulsion containing gold ions as a function of the time of digestion has been studied. With a pBr of 2.6, pH 6.0, and a temperature of digestion of 65°C, the presence of gold ions caused a suppression of fog, while at 45° the gold ions caused an initial acceleration of fog formation followed by its suppression. The results are interpreted as the outcome of two processes proceeding simultaneously. In one, the gold ions oxidize or otherwise inactivate the metallic silver centers, while in the other they form fogging compounds, presumably by interaction with gelatin or its impurities. The mechanism of gold sensitization is considered to be the destruction of the largest silver specks (fog centers) by the gold ions under suitable conditions, thus allowing the remaining silver specks to grow to the optimum size during digestion.

The Problem of the Kinetics of Development of the Latent Electrophotographic Image

I. V. ANFILOV AND V. M. FRIDKIN, pp. 367–68

Corrections are made to the mathematics in two earlier papers (*Zhur. Nauch. i Priklad. Fotografii i Kinematografii*, **4**: 32, 155 (1959)).

The Relation Between the Photometric Equivalent and the Average Size of Undeveloped Emulsion Grains

O. V. Pyasetskaya and K. V. Vendrovskiĭ (Letters to the Editors), pp. 368–69

The photometric equivalent and average projective grain area were determined for 17 photographic materials at a density of 1. The relation between the two quantities was linear, and was given by the equation $P = 2.28\bar{a} \pm 0.95$, where P is the photometric equivalent in grams per square meter, and a is the average projective area in square microns.

The Use of Fiber Optics in Photography

V. B. Veĭnberg, pp. 370–76

The theory of fiber optics is briefly given and applications described in the literature are reviewed.

The Mechanism of the Sensitivity of a Photographic Emulsion to the Action of Light and Ionizing Radiations

K. S. Bogomolov, pp. 376–79

Thirty-one publications are reviewed.

The Graininess of the Photographic Image: II—The Application of the Theory of Stationary Functions to the Problem of Graininess

W. Romer, pp. 380–95 (for Part I, see pp. 225–30 (*P S & E*, **4**:364))

The Second All-Union Conference on High-Speed Photography and Cinematography

E. M. Goldovskiĭ, p. 396

The above conference, organized by the Commission for Scientific Photography and Cinematography of the Academy of Sciences, U.S.S.R., the Moscow State University, and NIKFI, was held in Moscow, 22–26 May 1960. Seven hundred delegates took part and about sixty papers were read. Brief notes on some of the outstanding contributions are presented.

The Work of the Camera Section at the Second All-Union Conference on High-Speed Photography and Cinematography

A. S. Dubovik and A. B. Granigg, pp. 396–400

The papers presented to the section are reviewed.

Zhurnal Nauchnoĭ i Prikladnoĭ Fotografii i Kinematografii

Vol. 5, No. 6, November-December 1960 (in Russian)

Résumés by S. C. Goddard

The Hardening of Photographic Materials

Yu. B. Vilenskiĭ, T. N. Veretenova, N. N. Budarina, and L. F. Patrikeeva, pp. 401–402

Gelatin solutions and emulsions containing chromium acetate as a hardener show a progressive increase in viscosity on keeping prior to coating. It is shown that the extent of this hardening depends upon the concentration of gelatin and is negligible at concentrations of 1.5% and below. At these low gelatin concentrations, glycerin added to enhance the hardening action causes no change in viscosity. A gelatin solution containing 0.5–1.5% gelatin and a large excess of hardener, applied as a protective coating to a multilayer coating of unhardened emulsions, provides satisfactory hardening owing to diffusion of the hardener into the emulsion layers and also improves the adhesion between them.

The Mechanism of the Action of Hardeners on Photographic Emulsions

V. L. Zelikman, pp. 403–405

In experiments on the effect of formaldehyde in the presence of phloroglucinol on gelatins, it was found that the viscosity of a gelatin with a low initial viscosity reached a sharp maximum immediately after the addition of the hardener, followed by a slow drop on standing at 40°, while a gelatin with a high initial viscosity was much less affected by the hardener. A similar difference between the gelatins was shown when the viscosity was measured after repeated setting and melting, instead of standing, following the addition of the hardener. These phenomena, and those of the "after-hardening" of an air-dry gelatin or emulsion layer are explained on the basis of the formation by the hardener of both intermolecular and intramolecular bonds with the gelatin. The former produce a three-dimensional network of gelatin molecules and so increase the visocity and hardness, while the latter have no such effect, but are capable of hydrolysis which liberates hardening molecules able to form further intermolecular bonds.

Accelerated Testing for Stability of Photographic Materials by Storage in an Oxygen Atmosphere

S. M. Solov'ev, pp. 406–412

For the type of aging associated with optically sensitized films (an uninterrupted fall in speed with very little increase of fog), storage in oxygen at 20 atmospheres and room temperature is a reliable form of accelerated aging test. It may not be suitable for other types of aging.

The AKP-2 Additive Printer for the Contact Printing of Color Aerial Photographs

A. N. Uspenskiĭ, pp. 413–418

A description is given of an additive printer made by the Central Research Institute for Geodesy, Aerial Photography, and Cartography of the Soviet Union. It is intended for accurate and reproducible contact printing of aerial color photographs taken for surveying purposes.

The Law of the Change of Rate of Color Development with Change in the Properties and Increase in the Concentration of Nondiffusing Color Couplers in a Photographic Material: II—The Change of Contrast Coefficient with Small Concentrations of Coupler

V. I. Uspenskiĭ and N. I. Rodionova, pp. 419–423

Part I (see *P S & E*, **4**:60 (1960)) confirmed a linear relationship between gamma of a developed color image and log concentration for a number of color couplers over a concentration range of 2–16 grams/liter of emulsion. However, the experimental points did not lie well on the straight lines at low concentrations. Experiments now carried out by developing emulsion

coatings containing low concentrations of the same couplers (derivatives of benzoylacetic acid, of pyrazol-5-one, and of 1,2-hydroxynaphthoic acid) have shown that at low concentrations (up to ~ 4 grams/liter) the relation is not logarithmic, gamma being directly proportional to the concentration of coupler. Because of the differences in behavior of couplers with a high activity compared with those with medium and low activities it is necessary to take care in choosing the concentrations for comparative tests.

Cinematography of Motion of a Body in Two Media

V. I. RŸBAKOV, A. G. NIKOLAENKO, AND O. A. SOKOLOV, pp. 424–432

The high-speed cinematography of a body passing from one medium into another (e.g., from air into water or *vice versa*), or moving along the boundary, presents particular difficulties in lighting because of the differences in the absorbing and scattering properties of the two media and differences of scale caused by differences in refractive index. These points are discussed in some detail and lighting schemes for some special cases are described.

The Spectral Sensitivity of Electrophotographic Materials

S. G. GRENISHIN AND YU. A. CHERKASOV, pp. 433–438

Spectral sensitivities of electrophotographic layers have been obtained by measuring the fall in potential of a charged electrophotographic layer after constant exposure to light of a selected wavelength. The important region for selenium layers lies between $\lambda = 300$ mμ and something less than 600 mμ. Peaks are observed in the region of $\lambda = 440$ mμ and in the ultraviolet at $\lambda = 365 - 370$ mμ. The metal of the support has some influence on the absolute value of the spectral sensitivity, coatings on tin plate, brass, and copper showing the highest sensitivities. Storing the plates with a "latent image" at 60°C showed a progressive loss in sensitivity when the plates were positively charged and an increase in sensitivity when negatively charged. The addition of tellurium to the selenium increased the sensitivity of the layer to the visible region of the spectrum, and at the same time produced a certain amount of sensitivity at longer wavelengths up to 900 mμ.

Pure zinc oxide layers showed maximum sensitivity at λ 360–370 mμ, but sensitizing with erythrosin introduced a peak corresponding to the absorption of that dye. The results for cadmium sulfide layers depended upon the method of preparation of the material and its heat treatment before use.

Objective Distortions of Motion-Picture Images with Vertical and Horizontal Projection Angles: I—The Plane Ciné Screen

E. M. GOLDOVSKIĬ AND S. S. RŸSHKOV, pp. 439–445

Objective distortions of motion-picture images are those introduced by the geometry of projection, as distinct from subjective distortions which are due to the position of the viewer. A mathematical analysis is made of the dependence of such distortions on the angle of projection in relation to a flat screen.

A Comparative Characteristic of the Color-Separating Properties of "Fototsvet" Photographic Papers

V. M. BAKHVALOV (Letter to the Editors), pp. 446–447

A method of determining the color-separating properties of a three-layer film by measuring the densities of each of the three dyes with red, green, and blue light has been adapted for measuring the color-separating properties of a multilayer paper. The results are tabulated for the two Soviet-produced color papers F-1 and F-2. The differences between the two papers are discussed.

A Sensitometric Light Source for Testing Graphic Arts Films

B. S. SHASHLOV AND YU. S. ANDREEV, (Letter to the Editors), pp. 448–449

The spectral energy distribution of carbon-arc lamps used in graphic-arts photography has been plotted, and on the basis of the data obtained a filter has been designed for use with a tungsten lamp operating at 2850°K so as to provide lighting equivalent to the "mean arc lamp" as a light source for the sensitometry of graphic-arts materials.

An ISO Speed Criterion Suitable for Graphic Arts Films

V. I. SHEBERSTOV AND Z. I. ADAMSKIĬ (Letter to the Editors), pp. 450–451

The ISO recommendation for the determination of film speeds is based on a density of 0.1 above fog and the density obtained with an exposure of 1.3 log units above that required to give 0.1 above fog. However, high-contrast graphic arts materials developed in their appropriate developers give densities of the order of 3.5 with an exposure difference of 1.3. This is too high for accurate measurement and therefore it is suggested that such films should be tested with an exposure difference of 1.0 log units which would correspond to an upper density of 2.5.

The Photochemical Activity of Polymethine Dyes in the Mono- and Polymolecular States

S. B. NATANSON AND E. F. KLIMZO (Letter to the Editors), pp. 452–453

Dyes in the H-state show different photochemical activities, depending on the position of the absorption maximum in relation to the M-band, ranging from an activity equal to that of the dye in the molecular state to practically zero. As the absorption maximum of the dye in such a state passes further into the shortwave region, in comparison with the M-band, the dye becomes less effective. This is especially well shown by the N-methyl derivatives of many thiacarbocyanines with a strong tendency to pass into the H-stage, and also in the case, e.g., of 2-carbocyanines.

The Determination of the Activation Energy of Photographic Development

I. B. BLYUMBERG, p. 454

Attention is drawn to the fact that the usual expression for the determination of the energy of activation of

development is only valid when the process is a purely chemical one. Under circumstances where diffusion is in part or wholly the rate-determining factor the energy of activation cannot be determined in this way. The kinetics of development are purely chemical only in the least exposed portions of an image and it is only for such portions that the energy of activation can be determined.

The note is intended to arouse discussion on these points.

Suggestions on Testing Photographic Materials for Micro-Photocopying

B. K. BERZIN, pp. 455–456

Photographic materials used in microphotography are often called on to record documents with very pale writing, but the usual methods of testing photographic materials are not particularly suitable to show the properties of the materials under these conditions. The author therefore proposes a series of tests in which speed, resolving power, and latitude are determined for exposures giving a density level much closer to that required in practice. The author nevertheless agrees that testing by the usual standards is still necessary in order to be able to compare the properties of micro-photographic materials with others.

Photographing the Cavities of the Human Body

E. G. SHAER, pp. 457–462

The literature of endoscopic photography is reviewed (59 refs.).

The Graininess of the Photographic Image

W. ROMER, pp. 463–472 (see also, *Zhur. Nauch. i. Priklad. Fotografii i Kinematografii*, **5**:225–230 and 380–395)

Since the appearance of the author's monograph on graininess and resolving power (Warsaw, 1953), there have been considerable developments in the subject, particularly from the point of view of the application of information theory. These developments are reviewed in some detail (72 refs.).

New National Standards for Metol, Hydroquinone, and Sodium Sulfite

V. I. SHEBERSTOV, F. P. KANTOR, AND N. A. NOVIKOVSKAYA, pp. 473–476

The main provisions of three new Soviet standards for photographic chemicals are summarized and commented upon. They are GOST 5644–59 (replacing GOST 5644–51) for sodium sulfite, GOST 2549–60 (replacing GOST 2549–44) for hydroquinone, and GOST 24–60 (replacing GOST 24–40) for Metol.

• New Products and Developments

FRANK SMITH

• Cameras and Accessories

Perkin-Elmer Telescope-Camera for Project Stratoscope II

A 4500-lb, 36-in. telescope-camera system, which will be flown to high altitude by balloon to photograph planets, nebulae, and other celestial objects, is being constructed for Project Stratoscope II by the Perkin-Elmer Corp., Norwalk, Conn.

The purpose of Project Stratoscope is to loft high-performance systems by unmanned balloon above nearly all of the atmospheric turbulence and dust that distorts or obscures ground-based observations. This permits much better resolution than possible from the ground.

The telescope's fused silica primary mirror will be a 36-in., $f/4$ parabaloid. It will have a theoretical resolving power of 1/10 sec of arc—equivalent to the ability to distinguish two objects 15 in. apart 500 miles away. The secondary optical system, which relays and magnifies the image onto 70mm film, will provide an effective focal length of 300 ft.

The telescope will be controlled and roughly pointed by command signals from observers on the ground, with final precise pointing accomplished automatically by sensing and control equipment in the telescope. When the telescope is precisely pointed, ground command will activate the associated camera.

STL Image-Converter Camera

Space Technology Laboratories, Inc., 8929 S. Sepulveda Blvd., Los Angeles, Calif., has developed an image-converter camera which is capable of taking framed photographs at exposure times varying from 3 mμsec to 200 mμsec. Three-picture series can be made at rates of half a million to 20,000,000 exposures/sec. Streak photographs may be taken at writing speeds of four to 1,000 mm/sec.

The unusual performance of the camera is made possible by converting the optical image to an electron image which allows electronic shuttering, light amplification, and image deflection. Conversion of the light image into an electron image is accomplished by using an image-converter tube. The electrons carrying the picture information are focused on a fluorescent screen at the end of the tube. The optical image is thus recreated at an amplified intensity, and can be photographed by conventional means. A gating grid, placed in the path of the electrons flowing toward the anode, serves as an electronic shutter by permitting or preventing the flow of electrons. Advanced circuit design

Although the information contained in this section is compiled from sources believed to be reliable, the author cannot assume responsibility for its accuracy. Publication of the information here is not to be construed as an endorsement or recommendation of the product or equipment described.

provides a fast-rising voltage pulse to the gating grid, and thus the shutter speed is limited only by the parameters of the pulse-forming circuitry. Varying the duration of the pulse provides a range of exposure times.

Tektronix Type C-12 Oscilloscope Camera

Tektronix, Inc., P. O. Box 500, Beaverton, Ore., has developed a binocular-viewing direct-recording oscilloscope camera. The camera is equipped with a sliding back which is adjustable horizontally or vertically. On this back, one can interchange the par-focal film holders, lock them securely in any one of five positions, or rotate them through 90° increments (with the long axis of the film horizontal or vertical). The camera is equipped with an *f*/1.9 lens (with 1:0.9 object-to-image ratio), cable release, focusing back, and Polaroid back. Other lenses and accessories are available.

Birns and Sawyer Underwater Camera Blimp

Birns and Sawyer Cine Equipment Co., 6424 Santa Monica Blvd., Hollywood 38, Calif., has designed a rugged streamlined underwater camera blimp of half-inch welded marine aluminum girder plate, which will accept either 16 or 35mm Arriflex Cameras. The base is standard for both cameras, but different top housings are used.

The blimp operates at 300-ft depth without pressurization, and includes a stainless-steel viewfinder for through-the-lens viewing, and a sports finder. The cameraman uses the same optical axis for both finders. Parallax correction is adjustable and is normally set for 10 ft. An aperture scale indicator is available for various lenses. Offset gun-grip handles are provided.

• Illumination

Navy Self-Shuttering High-Intensity Electronic Flash

A self-shuttering electronic flash of high intensity, developed at the Naval Ordnance Laboratory, Silver Spring, Md., consists of a gaseous discharge tube coupled with an artificial transmission line made up of a number of capacitors. When the flash unit is used in a missile test, its charged capacitors are discharged, allowing alternating current to race first back and then forth through the transmission line. This keeps the arc burning evenly for 0.003 sec. At the end of this time, the voltage across the discharge tube abruptly drops to zero, causing the light output to suddenly drop to zero. The self-shuttering light source thus solves a major lighting problem in the photographing of high-speed motion which lasts only a split second.

Sylvania Motion-Picture Projection Lamps

Motion-picture projection lamps that reduce by 50% the heat reaching the film have been introduced by Sylvania Lighting Products Division. To separate the infrared from the visible light, the Sylvania Dichroic Super Tru-Flector Projection Lamps use a "sagged" glass reflector with a dichroic coating, instead of the conventional metal reflector with a metal coating. The sagging process accurately curves the bowl of the reflector and insures a smooth, uniform reflecting surface. The dichroic coating, developed in cooperation with Bausch & Lomb, Inc., causes the infrared to be transmitted through the rear of the reflector. The relatively cool visible light is reflected forward.

• Processing

In-Camera Rapid Photographic Processor

U.S. Patent 2,971,445, Photographic Method and Apparatus, issued to Carl Orlando, New Shrewsbury, N. J., Feb. 14, 1961. Negative and positive materials, together with a monobath processing solution, are contained within a camera housing, and so disposed as to develop the exposed negative and to move it into position with the print material, which is exposed by suitable printing lights, also contained within the camera, and developed by a film of processing fluid between them. After processing is completed, the negative and print are withdrawn from the camera and separated to provide a finished print and a reusable negative.

• Projection

Geotechnical Corp. Wide-Screen Film Viewer

A wide-screen 16mm film viewer, Model 6585, featuring a motorized film drive, a remote operator control, and data magnified 20 times on a large screen, has been developed by The Geotechnical Corp., 3401 Shiloh Rd., Garland, Tex.

The operator can locate data of interest quickly by using a push button to traverse the film in either direction at 120 cm/sec. The self-protecting film drive uses magnetic clutches to provide positive control and to enable film direction to be reversed without stopping the drive. The operator can study data in detail by varying the film speed continuously from 1.3 to 0 cm/sec. Controls are also provided for changing the direction of film travel, varying the light intensity, varying magnification between 19× and 21×, and maintaining a continuous sharp focus. An optional remote control unit permits operation up to 10 ft from the screen. A film area of 14.5 by 35mm is projected on the 27.5 by 11.5-in. screen. The cast-aluminum cabinet weighs 125 lb and measures 31 by 27 by 23 in.

• Sensitive Materials

Negative and Print from Polaroid 4×5 Film Packet

A 4 by 5-in. film packet that produces both a print and a negative completely developed outside the darkroom in 15 sec has been announced by the Polaroid Corp., Cambridge 39, Mass. Known as Type 55 Positive/Negative (P/N) Polaroid Land 4×5 Film packet, the new film is panchromatic and has a daylight speed rating of 100 (ASA daylight equivalent exposure index). Each packet contains a paper sheet for the positive print, a film-base sheet for a negative, and a foil pod carrying the developer. The packet can be exposed in a wide variety of conventional cameras which accept the Polaroid 4×5 Film Holder introduced in October 1958.

Because the process uses all the silver halide in the negative, no additional fixing is required. Before use, and within a day or two after development, the negative is washed to remove the developing chemicals and antihalation dye. The preferred washing method uses an acid hardener bath which simultaneously hardens the emulsion and removes the developer chemicals and antihalation dye in 2 to 3 min. When the acid hardener bath is not available, the negative may be washed in running water, but care must be exercised to avoid damaging the unhardened emulsion.

• Miscellaneous

Recordak DACOM System

The Recordak Corp., 415 Madison Ave., New York 17, N.Y., has developed high-speed computer print-out equipment known as the DACOM (Datascope Computer Output Microfilmer) System, which will convert information from magnetic tape into plain language on microfilm at speeds up to 20,000 characters/sec. The DACOM System complements modern computer equipment, providing print-out speeds which will match computer output speeds. A complete page of data, containing as many as 8,064 characters, can be exposed in approximately 0.5 sec, on a single 16mm microfilm frame. Any desired background format, such as statement, bill, or accounting forms, may be optically combined with the magnetic tape information so that the data can be reproduced in final finished form. Peripheral equipment for on-the-spot high-speed film processing and for continuous or selective hard-copy facsimile production from the film will be available, in addition to visual film reference work stations.

Point plotting can also be accomplished with the DACOM System. No overlays or descriptive labeling are required. Descriptions are automatically recorded by the DACOM System, which can alternate between point plotting and alpha-numeric character recording at a sustained speed of 15,000 characters/sec.

Microcopy Resolution Test Chart Revision

One of the more unusual standard materials issued by the National Bureau of Standards, Washington, D.C., is the Microcopy Resolution Test Chart prepared there by the Photographic Research Laboratory. About 12,000 of these charts, which are used to test the performance of lenses, are sold each year to the microfilm industry.

The charts consist of line patterns with lines and spaces of equal widths. Each pattern contains 2 sets of lines, one situated at right angles to the other.

Instruction for the use of the chart, which are furnished with each order, have recently been revised. The charts are available from the Standard Samples Clerk, National Bureau of Standards, Washington 25, D.C. (twenty cents per chart). Minimum order is for five charts.

Engineering Drawings Direct from Computer Output

General Dynamics Electronics Div., San Diego, Calif., has developed a method for using its S-C 4020 High-Speed Microfilm Recorder to make detailed multi-view drawings in a fraction of a second. A computer can be programmed with the contours and specifications of the part to be designed, and the output, in the form of the drawing, will be displayed on the Charactron Shaped-Beam Tube, which is the output of the microfilm printer. The image on the tube face is then photographed on 35mm film. Prints can be made from the film as needed, while an accessory unit permits processing and projection of the film on a 2 by 2-ft screen within 8 sec.

Resolution Targets

To fulfill needs for an 8mm resolution target for camera and projector lens tests and evaluation, Wollensak has designed a target in which the patterns are located in center, corners, sides, top, and bottom of a 0.125 by 0.1875-in. area in the middle of a 11/32 by 15/32-in.

glass plate (see illustration). Each pattern consists of parallel black lines $2.5/x$ mm long and $0.5/x$ mm wide, with a clear space $0.5/x$ mm wide, where x = number of lines per millimeter. A limited number of the resolution targets is available at $50.00 each from D. C. Gilkeson, Wollensak Optical Co., Rochester 21, N.Y.

1961

eeded,
ection

amera
k has
ted in
25 by
32-in.

sts of
wide,
ber of
lution
esun,

The Society of Photographic Scientists and Engineers

Box 1609 • Main Post Office • Washington D.C

OFFICERS

President	STEVEN LEVINOS, Ansco-Ozalid, Binghamton, New York
First Vice-President	C. E. IVES, Research Laboratories, Eastman Kodak Company, Rochester 4, N.Y.
Western Area Vice-President	JACK C. URBAN, Urban Engineering Co., 6717 Melrose Ave., Hollywood 38, Calif.
Eastern Area Vice-President	WILLIAM S. SHOEMAKER, Rochester Institute of Technology, 65 Plymouth Ave. South, Rochester 8, N.Y.
Conference Vice-President	IRA R. KOHLMAN, LogElectronics Inc., 500 East Monroe Ave., Alexandria, Va.
Engineering Vice-President	FORDYCE M. BROWN, Photomechanisms, Inc., Huntington Station, L.I., N.Y.
Editorial Vice-President	R. CLARK JONES, Polaroid Corporation, 730 Main Street, Cambridge 39, Mass.
Financial Vice-President	ROBERT S. QUACKENBUSH, JR., R.Adm., 2412 North Quincy St., Arlington, Va.
Secretary-Treasurer	FRANCIS J. HEYDEN, S.J., Georgetown College Observatory, Washington 7, D.C.
Executive Secretary	EDWARD S. COBB, Box 1609, Main Post Office, Washington, D.C.

CHAPTERS *and* CHAPTER OFFICERS

Binghamton, New York	*President*	HARRY G. MORSE, 326 Riverside Drive, Binghamton, New York
	Secretary	E. SCUDDER MACKEY, Stone Road, MR-98, Binghamton, New York
Boston, Massachusetts	*President*	JOHN B. TAYLOR, 290 Davis Road, Bedford, Massachusetts
	Secretary	ROBERT J. KOHLER, Itek Corp., 10 Maguire Rd., Lexington, Mass.
Chicago, Illinois	*President*	ROBERT J. MAZOR, Standard Studios, Inc., 540 North Michigan Avenue, Chicago 11, Illinois
	Secretary	NELSON W. RODELIUS, 2749 Reese Avenue, Evanston, Illinois
Cleveland, Ohio	*President*	HARRY L. FICHTER, JR., 1256 Overlook Road, Lakewood 7, Ohio
	Secretary	JOHN N. PIKE, 1480 Belle Avenue, Lakewood 7, Ohio
Monmouth, New Jersey	*President*	D. L. CASTELLINI, 98 Leland Terrace, New Shrewsbury, New Jersey
	Secretary	MISS MARILYN LEVY, 100 McLaren Street, Red Bank, New Jersey
New York, New York	*President*	HENRY CROIX, Industrial Photo Products, Inc., 86 Worth Street, New York 13, New York
	Secretary	JAMES W. HOWARD, Interchemical Corporation, 432 West 45th Street, New York 36, New York
Northern California	*President*	J. KENNETH CORNELL, 2331 Ross Rd., Palo Alto, Calif.
	Secretary	PETER L. CICCARELLO, Ansco, 640 Second Street, San Francisco 8, California
Rochester, New York	*President*	JOHN D. HAYES, Bausch & Lomb, Inc., St. Paul St., Rochester 2, N.Y.
	Secretary	WOODLIEF THOMAS, JR., Color Technology Division, Eastman Kodak Company, Rochester 4, New York
Southern California	*President*	GEORGE W. BOEMLER, 22632 Collins Street, Woodland Hills, California
	Secretary	GEORGE FUKASAWA, 18809 Citrus Edge, Azusa, California
Washington, D.C.	*President*	CALVIN S. McCAMY, 5004 Bangor Dr., Kensington, Md.
	Secretary	WALTER E. SHEA, Eastman Kodak Company, 1000 Connecticut Ave., N.W., Washington 6, D.C.

Sustaining Members / Society of Photographic Scientists and Engineers

Abrams Instrument Corporation
Lansing 1, Michigan

Aero Service Corporation
Philadelphia 20, Pennsylvania

Ansco Division, General Aniline & Film Corporation
Binghamton, New York

Atkinson Laboratory, Incorporated
Hollywood 38, California

Atlantic Gelatin, Div. General Foods Corporation
Woburn, Massachusetts

Bausch & Lomb Incorporated
Rochester 2, New York

Bell & Howell Company
Chicago 45, Illinois

Charles Beseler Company
East Orange, New Jersey

Bulova Watch Company, Inc., Photographic Division
Woodside 77, New York

Burke & James, Incorporated
Chicago 4, Illinois

Byron Motion Pictures, Incorporated
Washington 7, D.C.

Chicago Aerial Industries, Incorporated
Barrington, Illinois

Consolidated Film Industries
Hollywood 38, California

DeJur-Amsco Corporation
Long Island City 1, New York

E. I. du Pont de Nemours & Company
Parlin, New Jersey

Eastman Kodak Company
Rochester 4, New York

Edgerton, Germeshausen & Grier, Incorporated
Boston 15, Massachusetts

Elgeet Optical Company, Incorporated
Rochester 6, New York

Fairchild Camera & Instrument Corporation
Syosset, Long Island, New York

Farrand Optical Company, Incorporated
New York 70, New York

Oscar Fisher Company, Incorporated
P.O. Box 426, Newburgh, New York

FMA, Incorporated
El Segundo, California

The FR Corporation
New York 51, New York

General Electric Company
Schenectady, New York

General Film Laboratories
Hollywood 28, California

Graflex, Incorporated
Rochester 3, New York

W. & L. E. Gurley
Troy, New York

Hardale Associates
New York 22, New York

Hi-Speed Equipment, Incorporated
Waltham 54, Massachusetts

Houston Fearless Corporation
Los Angeles 64, California

Charles A. Hulcher Company, Incorporated
Hampton, Virginia

Philip A. Hunt Company
Palisades Park, New Jersey

Hycon Manufacturing Company
Pasadena, California

Itek Corporation
Waltham 54, Massachusetts

The Kalart Company, Incorporated
Plainville, Connecticut

Kollmorgen Corporation
Northampton, Massachusetts

LogEtronics Incorporated
Alexandria, Virginia

J. A. Maurer, Incorporated
Long Island City 1, New York

The Morse Instrument Company
Hudson, Ohio

North American Aviation, Incorporated
Los Angeles 45, California

Pako Corporation
Minneapolis 40, Minnesota

Photogrammetry, Incorporated
Silver Spring, Maryland

Photomechanisms, Incorporated
Huntington Station, Long Island, New York

Polaroid Corporation
Cambridge 39, Massachusetts

Rolor Industrial Corporation
New York 17, New York

Simmon Brothers, Incorporated
Long Island City 1, New York

Technicolor New York Corporation
New York 19, New York

Viewlex, Incorporated
Holbrook, Long Island, New York

Wollensak Optical Company
Rochester 21, New York

Xerox Corporation
Rochester 3, New York

Zoomar, Incorporated
Glen Cove, New York